Investigation of homeostatic calcium fluxes in hippocampal neurons by means of targeted-esterase induced dye loading (TED)

Untersuchung von homöostatischen Kalziumströmen in hippokampalen Neuronen mittels “targeted-esterase induced dye loading (TED)”

Doctoral thesis for a doctoral degree
at the Institute for Clinical Neurobiology,
University Hospital Würzburg
and Graduate School of Life Sciences,
Julius-Maximilians-Universität Würzburg
Section: Neuroscience

Submitted by

Samira Samtleben

from Recklinghausen

Würzburg, 2014

Submitted on:……..

Members of the *Promotionskomitee:*

Chairperson:	Prof. Dr. Thomas Hünig
Primary Supervisor:	PD Dr. Robert Blum
Supervisor (Second):	Prof. Dr. Carsten Hoffmann
Supervisor (Third):	Prof. Dr. Manfred Heckmann

Date of Public Defence:……..

Date of receipt of Certificates:……

Table of contents

List of figures

List of tables

Abbreviations

a.u.	arbitrary units
ACSF	cerebrospinal fluid
ALS	amyotrophic lateral sclerosis
AM	acetoxymethyl ester
Ara C	Cytosine β-D-arabinofuranoside
BES	N, N-Bis(2-hydroxyethyl)-2-aminoethanesulfonic acid
Ca^{2+}	free calcium ions = calcium
CA	Cornu ammonis
CamK(II)	Ca^{2+}/Calmodulin dependent protein kinase(typeII)
Ca_v	voltage-gated calcium channel
CFP	cyan fluorescent protein
CiCR	calcium-induced calcium release
CNQX	6-Cyano-7-nitroquinoxaline-2,3-dione
Cy 3/5	cyanine 3/5; dye labels of secondary antibodies
Dapi	4,6-diamidino-2-phenylindol
DHPG	Dihydroxyphenylglycine
DIV	days in vitro, days after seeding of cells
(D)MEM	(Dulbeccos`s) modiefied eagle medium
EGTA	ethyleneglycol-bis(ß-amino-ethylether)-N,N,N,N-tetra-acetic acid tetrasodium
ER	endoplasmic reticulum
F5N, (AM)	Fluo5N, AM
GECI	genetically-encoded calcium indicator
GFAP	glial fibrillary acidic protein
GFP	green fluorescent protein
GPcR	G (TPase)-protein coupled receptor
HBSS	Hank`s balanced salt solution
HRP	horseradish peroxoidase
ICC	immunocytochemistry
ICRAC	calcium release activated calcium current
IHC	immunohistochemistry
IiCR	IP_3-induced calcium release
IP_3	inositol-1,4,5-triphosphate
IP_3R	inositol-1,4,5-triphosphate receptor channel
IRES	internal ribosomal entry site
mACHR	metabotropic acetylcholine receptor

Map2	microtubule associated protein 2; marker for neurons/dendrites
mCES2	mouse Carboxylesterase 2
MF2, (AM)	Mag-Fura-2, AM
MF4, (AM)	Mag-Fluo-4, AM
NB(A)	neurobasal (A) medium
NG2	NG2 proteoglycan; marker for glia/oligodendrocyte precursor cells
OGB1, (AM)	Oregon Green 488 BAPTA-1, AM
O.N.	over night
PBS	phosphate buffered saline
PCR	polymerase chain reaction
Pen/Strep	Penicillin/Streptomycin
PLC	phospholipase C
PORN	poly-DL-ornithine hydrobromide
PVDF	polyvinylidene fluoride
RedCES2	optimized mouse Carboxylesterase 2 core fused to TagRFP-T
RFP	red fluorescent protein
ROI	region of interest
rpm	revolutions per minute
RYR	ryanodine receptor
R.T.	room temperature
SDS	sodiumdodecylsulfate
SEM	standard error of the mean
SERCA	sarco-/endoplasmic reticulum calcium ATPase
SOCE	store-operated cacium entry
STIM1/2	stromal interaction molecule type 1 /type 2
TBS(-T)	tris buffered saline (with tween)
TED	targeted-esterase induced dye loading
Thy 1.2	promoter of the thymocyte differentiation antigen 1 gen
TrpC	transient receptor potential channel
TTX	tetrodotoxin
UBQ	promoter of the ubiquitin gen
vGat	vesicular GABA transporter; marker for GABAergic presynapses
vGlut	vesicular gutamate transporter; marker for glutamatergic presynapses
WB	western blot

Zusammenfassung

Kalzium kann intrazelluläre Signalkaskaden aktivieren und somit Schlüsselfunktionen in allen Typen von Neuronen kontrollieren. Diese Schlüsselfunktionen umfassen Zellmigration, Freisetzung von Neurotransmittern, synaptische Plastizität, Transkription von Genen und Apoptose. Der wichtigste Speicher für Kalzium in Neuronen ist das endoplasmatische Retikulum (ER); ein kontinuierliches, membranumschlossenes Zellorganell, das sich in alle Teile von Neuronen erstreckt, von Axonen bis zu Dendriten. Im ER ist die Kalziumkonzentration ca. eintausendmal höher als im Zytosol. Dieser Kalziumgradient wird von der sogenannten SERCA, der *sarco-/endoplasmic reticulum calcium ATPase,* Kalziumpumpe aufrechterhalten, die Kalziumionen aktiv vom Zytosol in das Innere des ER pumpt.

Obwohl die einzelnen induzierten Kalziumsignalwege in Neuronen gut untersucht sind, war es lange nicht bekannt wie es Neuronen gelingt die hohe Kalziumkonzentration des ERs in Ruhe aufrechtzuerhalten. Um diese Frage zu klären wurde die sogenannte *targeted-esterase induced dye loading* (TED) Technik verbessert. TED ermöglicht es ER Kalzium direkt, in intakten Neuronen und in Gegenwart von extrazellulärem Kalzium sichtbar zu machen. Dadurch wird es möglich den Kalziumstrom des ERs direkt zu beobachten. TED beruht darauf, dass eine für das ER bestimmte Carboxylesterase der Maus überexprimiert wird, die sich im ER ansammelt. Im Inneren des ERs wandelt dieses Enzym den synthetischen Kalziumfarbstoff Fluo5N, AM um, der zur Gruppe der Acetoxymethyl-ester gehört. Dadurch wird aus diesem Farbstoff ein kalzium-sensitiver, niedrig-affiner Kalziumindikator, der nicht mehr permeabel für biologische Membranen ist und daher im ER verbleibt. In seiner Kalzium-gebunden Form erhöht sich die Fluoreszenz dieses Indikators einhundertfach im Vergleich zur Kalzium-ungebunden Form, wenn er durch Fluoreszenzlicht angeregt wird.

Es wurde beobachtet, dass der Entzug von extrazellulärem Kalzium zu Verlust von Kalzium im ER und Zytosol von Neuronen führt. Bei Rückgabe des Kalziums erholt sich die Kalziumkonzentration wieder. Daraus wurde gefolgert, dass es bei Neuronen in Ruhe einen starken Einstrom und Ausstrom von Kalzium geben muss. Diese Ströme halten den Kalziumgehalt der Neurone konstant. Wenn SKF-96365, ein Inhibitor des sogenannten *store-operated calcium entry* (SOCE), akut auf die Neurone appliziert wurde, wurde sofort ein Abfall der ER Kalziumkonzentration beobachtet, wohingegen die Kalziumkonzentration des Zytosols gleich blieb. Aufgrund dieser Ergebnisse kann ein neues Kalziumhomöostase-Modell für Neurone vorgeschlagen werden: In ruhenden Neuronen halten ein starker SOCE-ähnlicher Kalziumeinstrom und ein entsprechender Kalziumausstrom den Kalziumgehalt des

ERs aufrecht. Diese Ströme werden an Störungen angepasst um eine konstante Kalziumkonzentration zu erreichen.

In dieser Studie wird zum ersten Mal der Ruhestrom von Kalzium in das ER sichtbar gemacht. Kalzium gelangt über einen *store-operated calcium entry* -ähnlichen Mechanismus in die Neurone. Bisher dachte man, dass diese Art von Kalziumeinstrom nur nach Aktivierung von Signalen stattfindet.

Abstract

Calcium ions can activate intracellular signalling cascades that control key functions in all types of neurons. These functions include neuronal excitability and excitation, synaptic plasticity, cell migration, transmitter release, gene transcription, and apoptosis. The major intracellular neuronal store for calcium is the endoplasmic reticulum (ER), a continuous and dynamic, membranous organelle that extends through all parts of neurons, from axons to dendrites. The calcium concentration in the ER is appr. one thousand fold higher than in the cytosol and this calcium gradient is built up by the sarco-/endoplasmic reticulum calcium ATPase (SERCA) pump that pumps calcium from the cytosol into the ER.

Despite detailed knowledge about various induced calcium signals within neurons, it was still elusive, how resting neurons maintain their ER calcium content at rest. In order to shed light on the calcium homeostasis at rest, the targeted-esterase induced dye loading (TED) technique was improved. TED allows the direct and non-disruptive visualization of ER calcium in presence of extracellular calcium, thus enabling to visualize the dynamic flow of ER calcium. TED is based on the overexpression of an ER-targeted mouse carboxylesterase. Inside the ER the carboxylesterase cleaves the acetoxymethyl ester calcium dye Fluo5N, AM, thereby converting this dye into a calcium sensitive, low-affinity, cell membrane impermeable calcium indicator that is trapped in the ER. When bound to calcium ions and excited by fluorescent light, its fluorescence intensity increases one hundredfold compared to the calcium-free state.

It was observed that calcium withdrawal from resting neurons led to a rapid loss of calcium from both the ER and the cytosol, which recovered upon calcium re-addition. It was concluded that a strong calcium influx and efflux must exist under resting conditions that maintain a constant calcium concentration in neurons at rest. TED calcium imaging could visualize this resting calcium influx event. When the inhibitor of store-operated calcium entry (SOCE), SKF-96365, was acutely added to neurons an immediate decline in ER calcium levels was observed, whereas cytosolic calcium levels remained constant. Based on these findings, a novel calcium homeostasis model is proposed in which a strong SOCE-like calcium influx and a corresponding calcium efflux maintain the ER calcium levels at rest. These fluxes are adapted to disturbances in order to maintain a constant calcium level in resting neurons.

This study visualizes for the first time the resting calcium flow into the ER. The calcium enters the neurons via a store-operated calcium entry-like mechanism, a form of calcium influx that was thought to be induced by signalling events.

1 Introduction

1.1 Calcium signals and calcium distribution in neurons

Role of Ca^{2+} in eukaryotic cells: In eukaryotic cells free calcium ions (calcium, Ca^{2+}) are used as a ubiquitous messenger or signalling molecules that are involved in a multitude of functions. Calcium exerts its effect mostly by binding to proteins which are thereby activated or inhibited in their function. In this way calcium can regulate protein synthesis, cell proliferation, cell death, exocytosis and the cell metabolism (Berridge et al., 2000; Carafoli et al., 2001). Because the regulated processes have profound impact on the cells, calcium signals need to be tightly regulated and cells possess a variety of tools to control their calcium content. These tools are the endoplasmic/sarcoplasmic reticulum acting as the major intracellular calcium store, mitochondria, calcium buffering proteins, pumps, and channels and receptors that conduct the calcium fluxes between the stores, the cytosol and the extracellular environment. The best known example of a calcium function is its role in activating muscle contraction by binding to troponin-tropomyosin molecules after it is released from its store, the sarcoplasmic reticulum.

Ca^{2+} in neurons: In neurons calcium is involved in regulation of the above mentioned functions but in addition it influences functions characteristic to neurons, i.e. regulation of neuronal excitation, synaptic transmission and plasticity (Berridge et al., 2003; Berridge et al., 2000; Verkhratsky, 2005). In neurons, Ca^{2+} influx into the cytosol has a strong excitatory action and acts as a fast messenger of multiple neuronal signalling cascades (Berridge, 1998; Berridge, 2002; Park et al., 2008; Verkhratsky, 2005).

Calcium signalling: A common feature of calcium signalling is the regulated flow of calcium between the extracellular space, the cytosol and intracellular membranous organelles, mainly the mitochondria and the endoplasmic reticulum (ER) (figure 1) (Berridge et al., 2003; Berridge et al., 2000; Jaepel and Blum, 2011; Verkhratsky, 2005). The mechanisms of regulating calcium influx into the cytosol are well established (Berridge et al., 2003; Soboloff et al., 2012); however, the homeostatic flow of free ER calcium is barely understood. At rest, neurons show a quite stable level of 40 – 100 nM of free cytosolic calcium (Berridge et al., 2000; Garaschuk et al., 1997b; Grienberger and Konnerth, 2012; Schmidt and Eilers, 2009). This constant resting level is maintained by a complex interplay of ion pumps and ion channels that compensate for steady-state calcium influx events (Verkhratsky, 2005).

Ca^{2+} influx into the cytosol: One of two prominent calcium influx routes into the cytosol is from the extracellular space and it is generally thought to depend on neuronal activation

processes, either through voltage-gated calcium channels (Ca_Vs) or calcium permeable ionotropic receptors. After stimulation of neurons, these channels open and calcium ions flow into the cytosol following the concentration gradient and neuronal depolarization is a rapid consequence.

The other prominent influx of calcium to the cytosol is passive and driven by the high calcium concentration in the ER lumen and mediated through so called ER calcium "leak channels" (Lang et al., 2011a; Schäuble et al., 2012; Verkhratsky, 2005). Recent studies provided compelling evidence that the dynamic protein-conducting channel, the Sec61 complex, provides a pore for ubiquitous ER calcium leakage, a process regulated by calcium via cytosolic calmodulin action or luminal BIP (Lang et al., 2011a; Schäuble et al., 2012). Other candidates for neuronal ER leakage are the proteins Presenilin, a protein linked with early-onset Alzheimer's disease in humans (Tu et al., 2006), or truncated versions of the sarco-/endoplasmic reticulum calcium ATPase (SERCA, see below) (Guerrero-Hernandez et al., 2010).

The neuronal ER as Ca^{2+}-store: Conceptually, the neuronal ER acts as source and sink for calcium and drives and shapes cytosolic calcium signals (Berridge, 1998; Miller, 1991; Verkhratsky, 2005). The calcium concentration in the neuronal ER lumen has not yet been clearly determined, but seems to be in the range of 60 – 800 µM, at least for sensory neurons (Burdakov et al., 2005; Solovyova and Verkhratsky, 2003; Solovyova et al., 2002). The maintenance of the calcium concentration gradient between the cytosol and the ER lumen is the primary function of the SERCA which uses ATP to pump calcium from the cytosol into the ER. (Burdakov et al., 2005; Jaepel and Blum, 2011).

Neuronal ER Ca^{2+} signals: Multiple signalling cascades integrate the ER calcium into the fluxes between extracellular environment and cytosol (figure 1): the classical IP_3-induced calcium release (IICR), the fast calcium-induced calcium release (CiCR) and the store-operated calcium entry (SOCE).

IICR was discovered in 1983 and is initiated by activation of G-protein coupled receptors (GPcRs) in the plasma membrane. The activated G-proteins in turn activate phospholipase C which synthesizes inositol-1,4,5, triphosphate (IP_3). IP_3 then binds to and opens calcium permeable IP_3 receptors (IP_3Rs) in the ER membrane. (Streb et al., 1983; Verkhratsky, 2005). Several types of these GPcRs are found in neurons, e.g. metabotropic glutamate receptors, serotonin receptors and metabotropic acetylcholine receptors.

CiCR describes the opening of ryanodine receptors (RyRs) in the ER membrane. (Berridge, 2002; Lanner et al., 2010).RyRs are opened by either cytosolic calcium itself or by ryanodine.

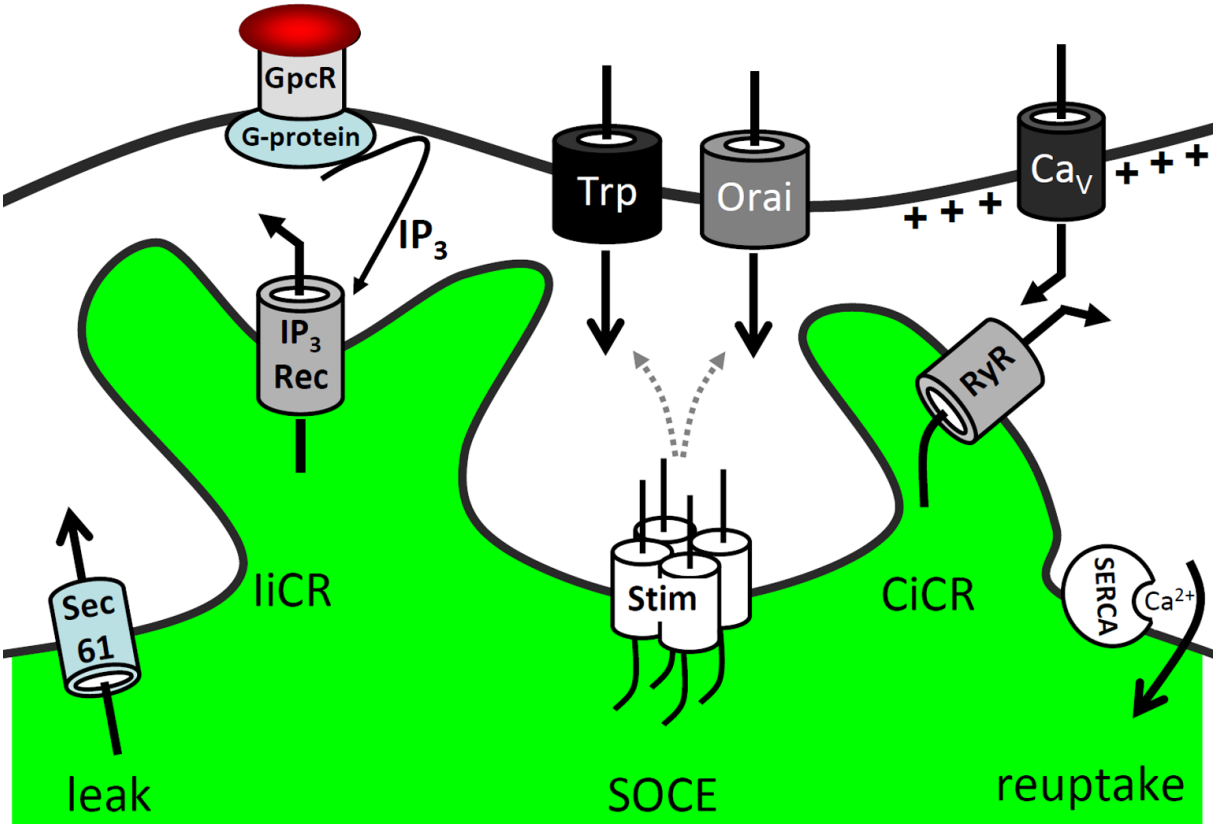

Figure 1: Main calcium signals in neurons
Calcium can enter neurons from the extracellular environment either via voltage-gated calcium channels (Ca_V) or store-operated calcium entry (SOCE) mediated by a plasmalemmal pore comprised of Orai proteins and possibly transient receptor potential channels (Trp) in combination with the ER membrane proteins of the stromal interaction protein family (STIM). From the cytosol, calcium is pumped into the ER calcium store by the Sarco-/endoplasmic reticulum calcium ATPase (SERCA).Calcium release from the ER takes place via 3 routes: 1. G-protein coupled receptors (GpcR) stimulate IP_3 production, which then causes IP_3-induced calcium release (IiCR). 2. Cytosolic calcium activates ryanodine receptors (RyR) thereby inducing calcium induced calcium release (CiCR). 3. Following its concentration gradient calcium "leaks" out of the ER in a process involving Sec 61 pore complexes. Figure from Samtleben *et al*., 2013. Further molecules involved in calcium signalling are not depicted here, but mentioned in the text body.

Store-operated calcium entry: Finally, SOCE (figure 2) or capacitative calcium entry (CCE) is a ubiquitous cellular mechanism. Neuronal activation by stimulation of cells and subsequent release of Ca^{2+} from the ER is an initiation signal that stimulates Ca^{2+} entry from the extracellular site (Berridge et al., 2003; Putney, 1986; Putney, 2007). The molecules responsible for SOCE involve the stromal interaction molecule (STIM) family that senses and coordinates regulated Ca^{2+} release from the ER and triggers SOCE or similar calcium entry signals for maintaining cellular Ca^{2+} homeostasis (Berna-Erro et al., 2009; Feske et al., 2006; Putney, 1986; Putney, 2007; Roos et al., 2005; Varnai et al., 2009; Zhang et al., 2005). In response to ER calcium store depletion STIMs interact directly or functionally with calcium permeable ion channels in the plasma membrane. These channels comprise Orai channels (Feske et al., 2006; Vig et al., 2006; Zhang et al., 2006) and canonical transient receptor potential channels (TrpC) (Huang et al., 2006; Jardin et al., 2008; Liao et al., 2009). Upon

calcium release from the ER, STIM proteins form local ER-plasma membrane junctions, interact with Orai and/or TrpC channels and stimulate calcium entry and the refilling of the ER calcium store (Huang et al., 2006; Luik et al., 2006; Wu et al., 2006; Zhang et al., 2005). Although SOCE has been known for decades, its mechanism in neurons was only described over the last five years (Berna-Erro et al., 2009; Gruszczynska-Biegala and Kuznicki, 2013; Gruszczynska-Biegala et al., 2011; Stathopulos et al., 2013; Wang et al., 2010a). SOCE is thought to be responsible for local exchange of calcium between extracellular sites and the ER (Cahalan, 2009; Shen et al., 2011; Soboloff et al., 2012). Interestingly, within the same microdomain STIMs can control a reciprocal function on voltage-dependent signalling by inhibiting the L-type calcium channel $Ca_V1.2$ (Wang et al., 2010b).

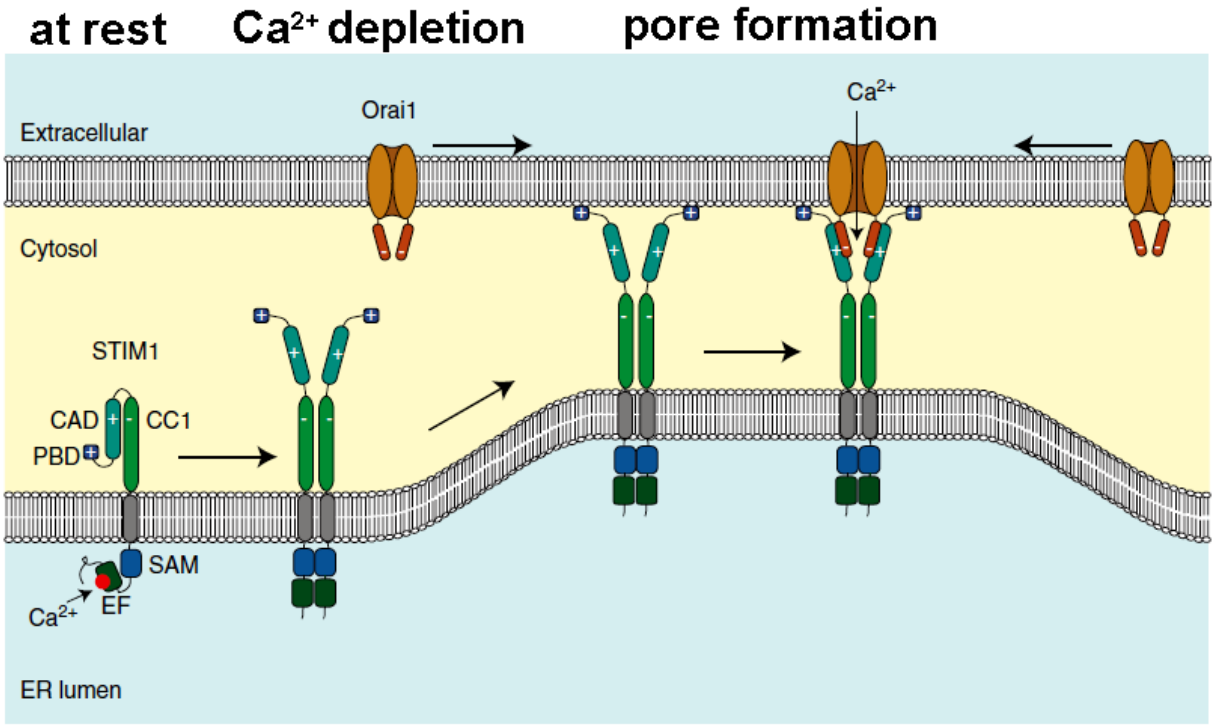

Figure 2: Current model of Store-operated calcium entry
At rest Ca^{2+} (red dot) is bound to the EF-hand motif of STIM which prevents the interaction of the CRAC activation domain (CAD) with Orai. Upon calcium release STIM molecules oligomerize and diffuse to ER membrane-plasma membrane junctions. At the junctions the CAD of STIM oligomers interact with the coiled coil 1 (CC1) region of Orai proteins via electrostatic interactions forming a calcium permeable pore. EF = canonical EF hand; SAM = sterile α -motif; PBD= polybasic domain. Figure from Lewis, 2011.

Calcium binding proteins: It is also important to note that the majority of a cells` calcium is normally bound to calcium binding proteins (CBP), which act as calcium buffers, and therefore these calcium ions are not available as messengers. The most abundant calcium buffers of the ER are Calreticulin, which has 20-50 calcium binding sites and calsequestrin (Krause and Michalak, 1997; Verkhratsky, 2005). Important cytosolic calcium buffers are Calretinin, Parvalbumin and Calbindin. By binding the calcium ions CBPs modulate and alter

calcium signals and are in this way involved in the regulation of neuronal excitability (Berridge et al., 2003; Gall et al., 2003; Roussel et al., 2006). It was even suggested that CBPs can exclude calcium ions from some, but not other signalling events and thereby form a so called “concealed calcium pool” (Guerrero-Hernandez et al., 2010).

Ca^{2+} in neurodegenerative diseases: As a consequence of its ubiquitous actions and tight regulation, disturbance of calcium homeostasis is a frequent cause of early-stage key processes in the pathogenesis of neurodegenerative diseases (figure 3).This finding is termed ”calcium hypothesis of neurodegenerative diseases”. Mutations or other defects that lead to an increased calcium level of neurons can cause a calcium overload, and can, either directly or by way of mitochondrial calcium overload, cause cell death. Parkinson’s disease and Alzheimer’s disease are the best known examples of such processes (Cali et al., 2014; Supnet and Bezprozvanny, 2011), but in Huntington’s disease, amyotrophic lateral sclerosis and other diseases calcium signalling is also disturbed. (Bezprozvanny, 2010).

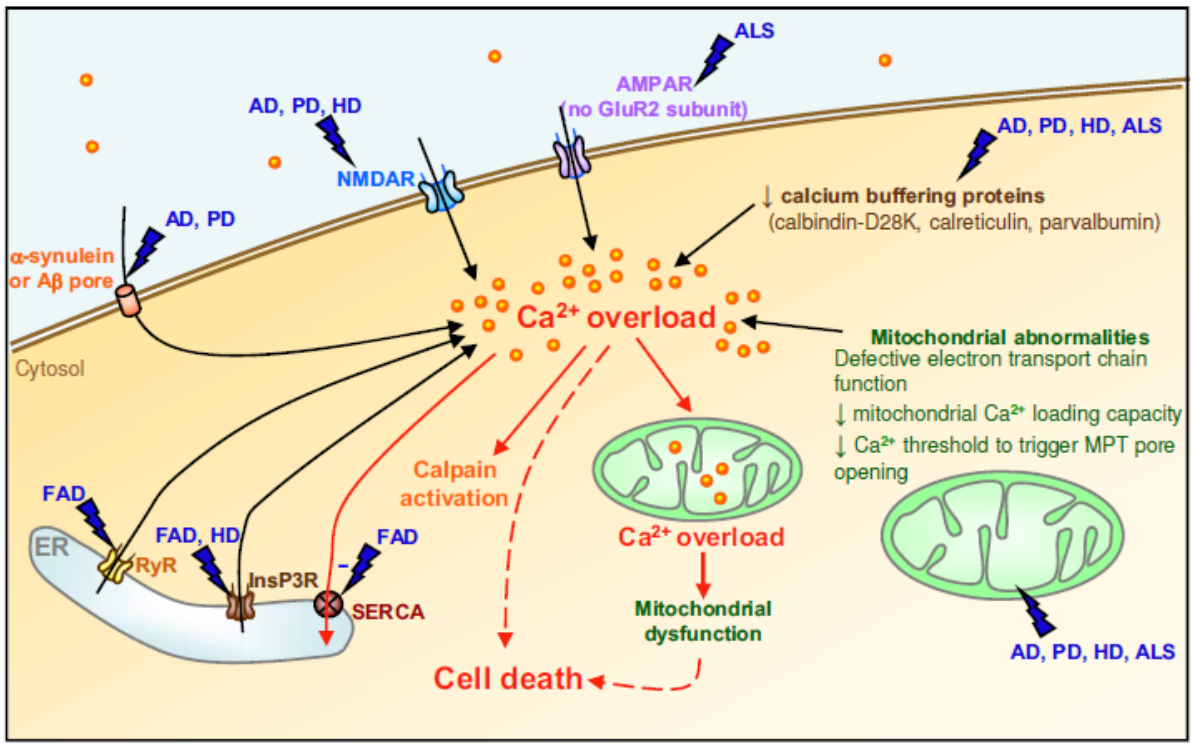

Figure 3: Disturbed calcium homeostasis in neurodegenerative diseases
Cytosolic calcium levels are affected in (familial) Alzheimer’s disease ((F)AD), Parkinson’s disease (PD), Huntington’s disease (HD), and amyotrophic lateral sclerosis (ALS). The underlying defective proteins are mostly part of the normal calcium signalling machinery, but it was also shown that the protein plaques of AD and PD can built calcium permeable pores. Figure from Marambaud *et al*., 2009.

1.2 Role of the endoplasmic reticulum in calcium homeostasis

Overall structure and function of the neuronal ER: The endoplasmic reticulum is the major calcium store of eukaryotic cells. It is a continuous cellular organelle that consists of membranous cisternae and tubules that extent into every part of a neuron; from spines via the dendrites into the cell soma and into the axons (Cooney et al., 2002; Spacek and Harris, 1997). Figure 4 depicts this currently prevailing opinion. The ER has the dual role of a calcium sink and calcium source because the molecules conducting release (IP_3R and RyR) and uptake (SERCA) were detected in all parts of the ER. Because of its distribution within neurons, it was suggested to act as “a neuron within a neuron” (Berridge, 1998). In this concept the ER takes up calcium at different localizations of a neuron, e.g. in different spines, and this information about activity is then conveyed towards the soma. In this way several smaller calcium signalling events are summed up by the cell into one larger signal. The summed up signal may then exert an effect on the neuron, it could, for example, increase its excitability or enhance protein synthesis in the soma. This means that the ER may act like a coincidence detector that conveys information about local events like the neuronal plasma membrane and that it could therefore integrate several calcium signals (Berridge, 1998). Although this idea appears to be generally well accepted, scientific proof still remains poor.

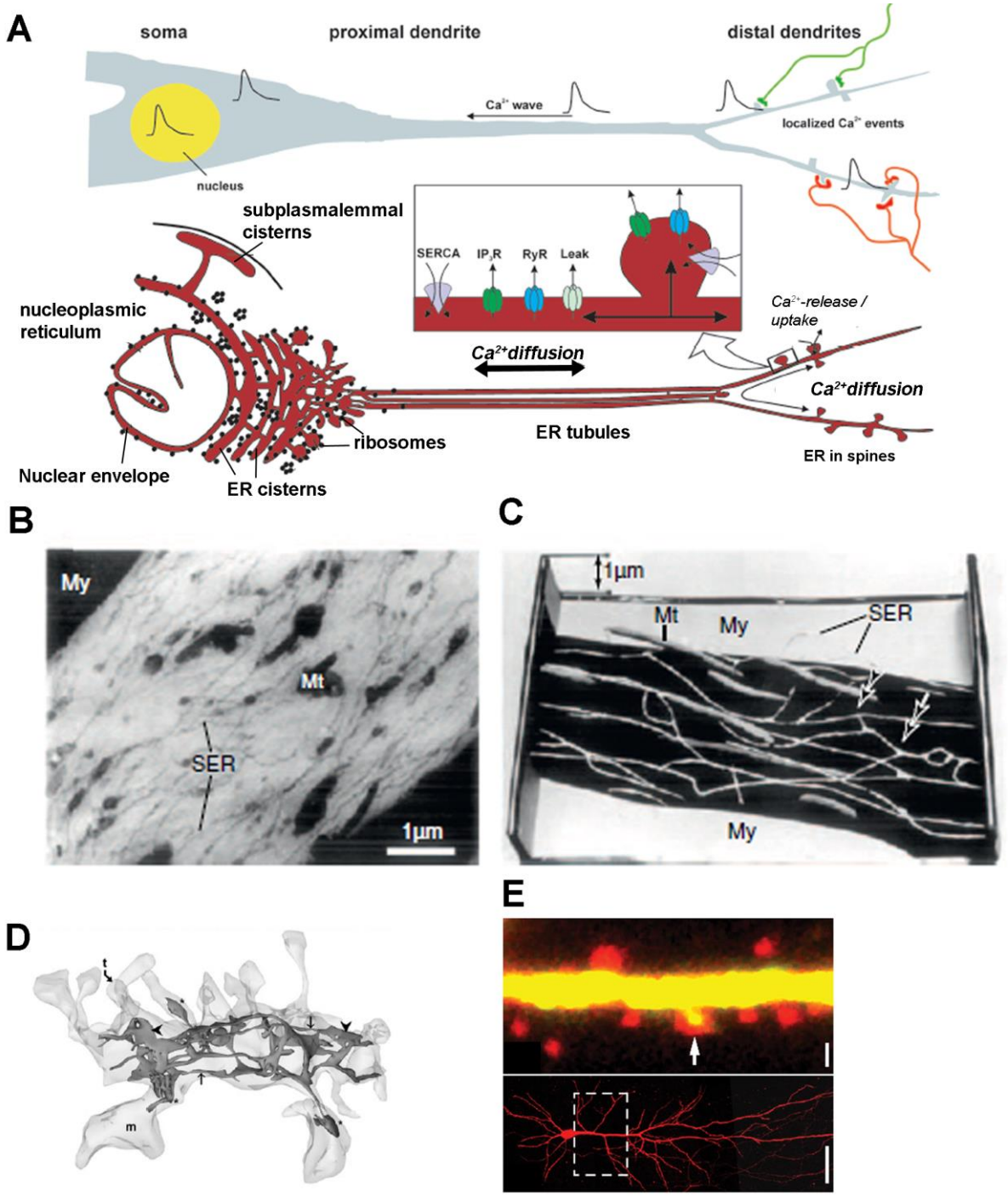

Figure 4: ER structure and function in neurons
The endoplasmic reticulum is a tubular organelle that spreads into all parts of neurons. **A**) The ER is present in the somas and dendrites of neurons and exerts an integrative function by conveying calcium waves. Image modified from Park *et al*., 2008. **B) and C**) The smooth ER (sER) was detected in axons in form of tubules. **B)** is an electron microscopic picture of an axon and **C)** a three dimensional reconstruction. Mt = mitochondria; My=myelin; Figure from Ramirez and Couve, 2011. **D)** A three-dimensional reconstruction of dendrites from Cooney *et al*., 2002 shows ER tubules and cisternae in the dendrite and spine necks and shafts. **E)** An ER targeted EGFP (Holbro et al., 2009) demonstrates the presence of ER stretched over the dendritic arbour and into dendritic spines (arrowheads). Scale bars represent 50 µm and 1 µm.

Dendritic and axonal Ca^{2+}: Many reports describe the function of the ER calcium store in specific neuronal signalling events. Calcium signals in spines of hippocampal CA1 neurons and cerebellar Purkinje neurons are involved in the regulation of synaptic plasticity (Rose and Konnerth, 2001). It was also reported that the spine apparatus, the ER sub compartment within spines, is required for long term potentiation.(Jedlicka et al., 2008). At the other pole of neurons, the axon, calcium is a key regulator of the turning and guidance of growth cones towards guidance cues and the importance of ER calcium in this processes was demonstrated (Gomez and Zheng, 2006; Mitchell et al., 2012). In line with this, ER calcium release was shown to result in calcium overload of axons which led to axonal degeneration in neurons of the sciatic nerve (Villegas et al., 2014).

Somatic Ca^{2+} regulates gene expression: In the soma and nucleus of neurons calcium is involved in most major functions of neurons by regulating gene expression. Calcium binds to a multitude of regulatory proteins that in turn can then regulate transcriptions factors causing specific effects, or chromatin modifying enzymes causing global changes. For example, calcium binds to Calmodulin thereby activating the Ca^{2+}/Calmodulin dependent protein kinases (CamK) which in turn activates the transcription factors CREB, CBP and ETF-1. The DREAM/KChip family of transcriptional repressors are directly regulated by calcium. Furthermore, the COX2 gene coding for Cyclooxygenase 2, is involved in pain and its expression is regulated by DREAM and CREB in a calcium dependent manner (Bading, 2013; Mellstrom et al., 2008).

Generally, regulation of gene expression by calcium and its effects is a complex network of events rather than single, straightforward signalling cascades because calcium- as mentioned before- is a ubiquitous signalling molecule.

Neuronal calcium homeostasis: Although detailed knowledge of single calcium signals and their function exists, the understanding of the regulation of calcium levels at rest or the regulation of global calcium levels remains poor. In 1997 it was suggested by the group of Konnerth that the intracellular calcium stores are loaded at rest because caffeine induced calcium peaks in the cytosol were reduced in amplitude after repetitive caffeine stimulations. After resting for some time, caffeine peaks showed their original amplitude. This effect was dependent on extracellular calcium, remained constant when neurons were kept close to their resting potential and was blocked by SERCA blockade with cyclopiazonic acid (CPA) and by ryanodine (Garaschuk et al., 1997).

1.3 Methods to investigate free calcium ions in living cells- Introduction to TED

Generally, **three different ways to investigate free calcium ions** in cells exist. The most indirect variant is the patch clamp technique: This technique measures the electric currents that flow through the plasma membrane via ion channels. By inhibiting all other but calcium channels it is possible to conclude on calcium fluxes through the plasma membrane. However, one cannot distinguish between the source or sink of the calcium i.e. whether calcium flows into or from the ER or into or from the cytosol. Second, protein-based calcium indicators can be used. The simplest variant is the protein Aequorin which was isolated from the jellyfish *Aequoria victoria.* Upon binding of calcium ions, this protein undergoes an irreversible conformational change and emits a photon of 470 nm. Because of the irreversibility, its application is limited. (Solovyova and Verkhratsky, 2002). More sophisticated are the genetically encoded calcium indicators (GECIs). GECIs are designed fusion proteins consisting of at least one calcium sensitive protein and one fluorescent protein. Upon binding of calcium a conformational change in the fusion protein is induced that either leads to an increase in the fluorescence of the fluorescent protein moiety (named single fluorophore GECIs) or the fluorescence of one fluorescence protein is reduced and the fluorescence of its partner fluorescent protein increases (named FRET based GECIs) (Grienberger and Konnerth, 2012). The best known variants of GECIs are named cameleons and consist of the cyan fluorescent protein (CFP) fused to the calcium sensitive calmodulin, the calmodulin binding protein M13 and a green fluorescent protein (GFP) (Miyawaki et al., 1997). Older, and more recent studies presented new GECIs with increasingly improved properties (see also discussion 4.1): Cameleon YC2.1, YC 3.3 and YC4.3 (Griesbeck et al., 2001; Miyawaki et al., 1997), redesigned cameleons D2, D3, D4 cpV (Palmer et al., 2006), the circularly permuted GFP named Pericam (Nagai et al., 2001), ER-D1 (Palmer et al., 2004), gCaMP (Nakai et al., 2001), GAPs (Rodriguez-Garcia et al., 2014) and finally a group of calcium sensors targeted to the ER and mitochondria named CEPIAs (Suzuki et al., 2014).

Most frequently, free calcium ions in cells are monitored with synthetic calcium indicators: They exist in form of salts, dextrans and acetoxymethyl esters (AM) (Tsien, 1981). (Paredes et al., 2008).

AM calcium indicators (Tsien, 1981) are low molecular weight molecules that, upon binding of calcium, emit fluorescent light of a particular wavelength when excited by fluorescent light of a different wavelength. Various forms exist that differ in their excitation and emission spectra, affinity for calcium, and subcellular localization. (Paredes et al., 2008; Thomas et al., 2000). AM dyes *per se* are cell membrane permeable and insensitive to calcium. During incubation with living cells they diffuse into the cells and are then cleaved by intracellular

esterases and thereby converted into their cell-membrane impermeable and calcium sensitive form.

Therefore AM dyes have the disadvantage that they cannot be targeted to a specific subcellular compartment. In addition, cleavage of the ester group also releases formaldehyde which is toxic for cells. Their advantage is a wide range of wavelength and calcium affinities and a high photon emission rate. Contrasting to this, GECIs can be targeted to subcellular organelles and are less toxic. On the other hand, GECIs have to be expressed, sorted and folded properly in the cells and these processes vary between cell types and can hardly be controlled by the experimenter. In addition, the calcium affinity, which determines the detection range, depends on the protein properties and can therefore not be altered easily.

Calcium imaging in cellular organelles: In order to investigate specific calcium signals, it is necessary to detect only the calcium in specific subcellular compartments, e.g. to resolve the role of mitochondrial calcium overload in Parkinson's disease or, as in this study, to investigate the role of the ER calcium in calcium homeostasis.

In order to visualize calcium ions in these subcellular organelles, three different strategies can be applied.

First, GECIs can be modified. Localization signals like the ER signal peptide and ER retention motif or the mitochondrial targeting sequence are added to the sequences encoding the calcium sensor and fluorescent protein (Filippin et al., 2005; Palmer and Tsien, 2006; Rizzuto et al., 1992; Suzuki et al., 2014). After expression in the cells of interest, the proteins are then sorted into the respective subcellular compartment by the cells protein trafficking machinery.

Second, AM dyes can be used in combination with clearance of the cytosol. AM dyes diffuse through all cellular membranes and are therefore also present in the ER and other subcellular organelles. In order to visualize ER calcium with synthetic calcium indicators, the cells can be incubated with the AM-indicator. Afterwards the plasma membrane is permeabilized with a mild detergent and the dye is washed out of the cytosol. (Hofer and Machen, 1993). Alternatively, a whole cell patch pipette can be used to clear out the cytosolic dye (Samtleben et al., 2013; Solovyova and Verkhratsky, 2002).

Third, cytosolic calcium ions can be monitored with chemical calcium indicators. Then conclusions are drawn for ER calcium signals based on observations made in the cytosol. It is assumed that in absence of extracellular calcium (by usage of calcium-free buffer solution) any calcium occurring in the cytosol originates from intracellular stores, i.e. the ER.

Targeted-esterase induced dye loading to visualize ER calcium: In order to visualize ER calcium dynamics under physiological conditions, with a high temporal and spatial resolution a new strategy, named targeted-esterase induced dye loading (TED) was developed

(Rehberg et al., 2008). TED combines the advantages of genetic targetability from GECIs and the biochemical properties from synthetic calcium indicators. The strategy is based on targeting of a recombinant carboxylesterase activity to the ER lumen.

Earlier experiments revealed that TED works best using the mouse Carboxylesterase 2 (mCES2) (Rehberg et al., 2008). mCES2 is naturally equipped with an ER translocation signal peptide and an ER retention and retrieval motif and is therefore transported to and hold in the ER of cells (Rehberg et al., 2008; Satoh and Hosokawa, 2006;Blum et al., 2010; Medda and Proia, 1992). For TED imaging, cells are transduced with lentiviral particles to express high amounts of mCES2 in the ER (figure 5B1).The cells are then incubated in extracellular solution containing the calcium indicator Fluo5N (F5N), AM which diffuses through the plasma-membrane and ER membrane (figure 5B2). In the ER, F5N, AM is converted by the CES2 activity to its calcium-sensitive, fluorescent and membrane-impermeable form (figure5B3). F5N is therefore trapped inside the ER and F5N/Ca^{2+}-complexes are built in presence of calcium ions (figure 5B3). When the F5N/Ca^{2+} complexes are excited by fluorescent light of 470-480 nm, a strong fluorescence signal is emitted, indicative of a high calcium concentration. Upon release of calcium from the ER, the F5N/Ca^{2+} complexes disintegrate, the concentration of F5N/Ca^{2+} declines, and the fluorescence signal declines accordingly (figure 5B4). This process of complex building and disintegration is reversible.

For ER calcium imaging, TED can best be used with the AM dye Fluo5N, AM because F5N has a very low affinity for calcium ions (K_D =90µM) Therefore, the high amounts of F5N released in the ER detect the rather high calcium concentration of 100-800 µM in the ER. The F5N that is released in the cytosol by endogenous esterases is not able to detect cytosolic calcium because cytosolic calcium concentrations are below the detection range of F5N (figure 5A).

Therefore TED allows the direct visualization of free calcium ions in the ER of intact, non-disrupted cells in the presence of extracellular calcium.

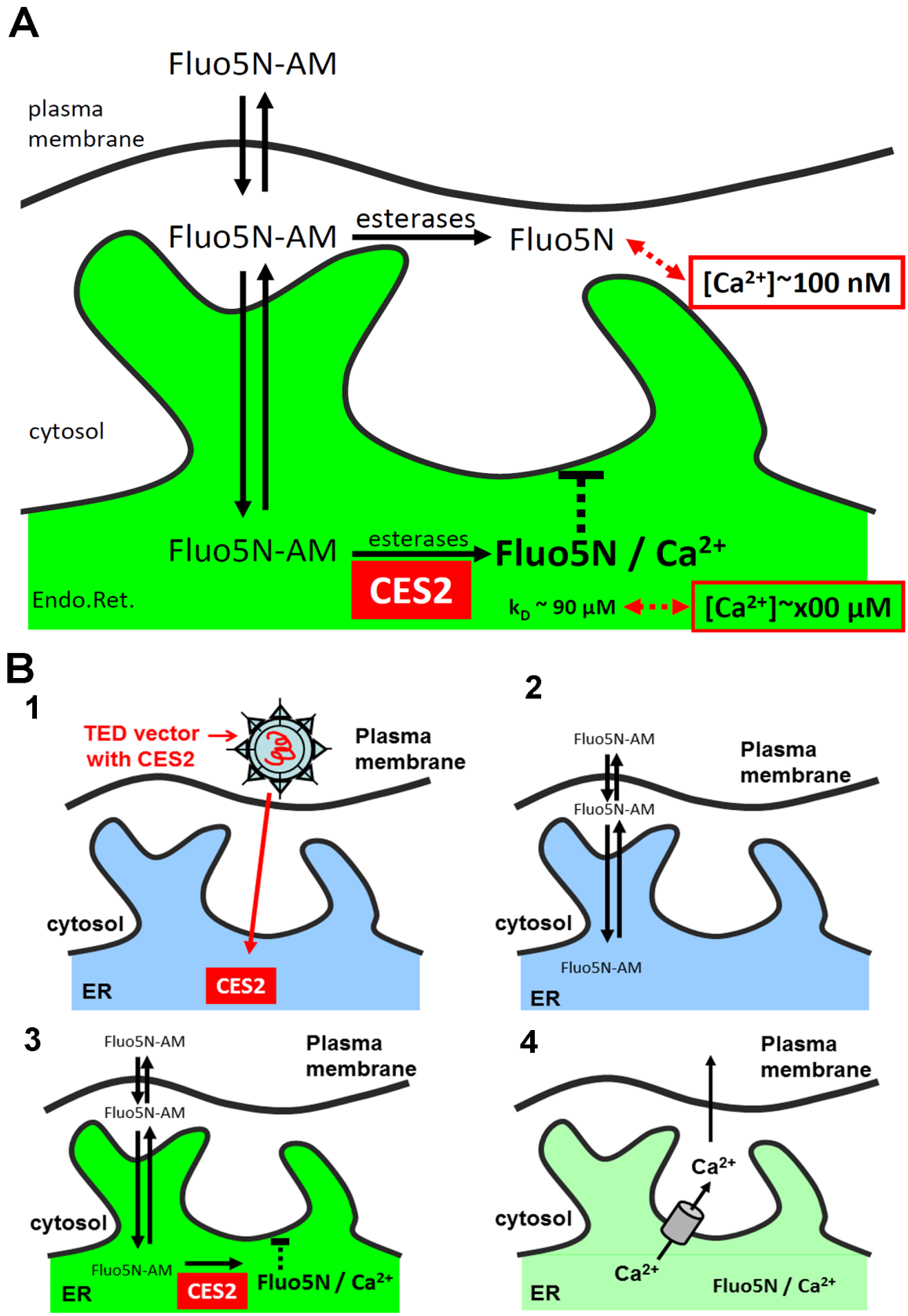

Figure 5: Basic principle of targeted-esterase induced dye loading
A) Overexpression of an ER targeted carboxylesterase (CES2) leads to high esterase activity in the ER. The esterase converts the Fluo5N, AM dye to a calcium-sensitive, fluorescent dye that is trapped in the ER. Under resting conditions, fluorescent F5N/Ca^{2+} complexes are preferentially formed in the

ER because F5N has a very low calcium affinity and the calcium concentration is appr. 1000-fold higher in the ER than in the cytosol. **B)** For TED calcium imaging cells are transduced by a lentivirus leading to overexpression of CES2 in the ER**.** During incubation in extracellular solution containing Fluo5N, AM, the dye diffuses through the cellular membranes. Inside the cell F5N, AM is preferentially converted to its calcium sensitive form in the ER. Upon calcium release from the ER, the amount of F5N/Ca^{2+}-complexes and the fluorescence decline. Pictures from Samtleben *et al*., 2013.

1.4 Aim of the thesis

In neurons Calcium is a ubiquitous messenger molecule that mediates and regulates functions ranging from survival to gene expression to synaptic plasticity. The main store of free calcium ions is the endoplasmic reticulum. Over the last decades multiple effects of ER calcium and the calcium toolkit were unravelled. Contrasting to this, the regulation of calcium homeostasis in resting neurons remained elusive. The aim of this work was to improve the temporal and spatial monitoring of the dynamics of free calcium ions in the ER with the help of the TED technique and to use this improved method to investigate the regulation of calcium homeostasis in neurons. The central question was: How is the basic, resting calcium level maintained in neuronal ER calcium stores?

2 Material and methods

2.1 Material

2.1.1 Buffers and solutions

Table 1: Buffers and solutions for live cell imaging
All buffers and solutions were made with ddH_2O

artificial cerebrospinal fluid (ACSF)	
Chemical	**concentration in mM**
NaCl	127
KCl	3
$MgCl_2 \times 2H_2O$	1
$CaCl_2 \times 2H_2O$	2
$NaH_2PO4 \times H_2O$	2.5
$NaHCO_3$	23
D-Glucose monohydrate	25
mOSm 315-325 , pH= 7.4, carbogen aeration	

calcium-free ACSF	
Chemical	**concentration in mM**
NaCl	127
KCl	3
$MgCl_2 \times 2H_2O$	3
$CaCl_2 \times 2H_2O$	0
$NaH_2PO_4 \times H_2O$	2.5
$NaHCO_3$	23
D-Glucose monohydrate	25
EGTA	0.1
mOSm 315-325, pH= 7.4, carbogen aeration	

HEPES ACSF	
Chemical	**concentration in mM**
NaCl	120
KCl	2.5
$MgCl_2 \times 2H_2O$	1.2
$CaCl_2 \times 2H_2O$	2.4
$NaH_2PO_4 \times H_2O$	1.2
$NaHCO_3$	26
D-Glucose monohydrate	10
HEPES	10
pH = 7.4	

calcium-free HEPES ACSF	
Chemical	**concentration in mM**
NaCl	120
KCl	2.5
$MgCl_2 \times 2H_2O$	2.4
$CaCl_2 \times 2H_2O$	0
$NaH_2PO_4 \times H_2O$	1.2
$NaHCO_3$	26
D-Glucose monohydrat	10
HEPES	10
EGTA	0.1
pH = 7.4	

caffeine ACSF	
Chemical	**concentration in mM**
Caffeine	40
NaCl	107
$NaH_2PO_4 \times H_2O$	2.5
$NaHCO_3$	23
D-Glucose monohydrate	25
$MgCl_2$	1
KCl	3
$CaCl_2$	2
mOsm 320-330 and pH = 7.4	

calcium-free caffeine ACSF	
Chemical	**concentration in mM**
Caffeine	40
NaCl	107
$NaH_2PO_4 \times H_2O$	2.5
$NaHCO_3$	23
D-Glucose monohydrate	25
$MgCl_2$	3
KCl	3
$CaCl_2$	0
EGTA	0.1
mOsm 320-330 and pH = 7.4	

HEPES Ringer	
Chemical	**concentration in mM**
NaCl	125
KCl	3
HEPES	25
$MgCl_2 \times 2H_2O$	2
$CaCl_2 \times 2H_2O$	1
$NaH_2PO_4 \times H_2O$	1.25
D-Glucose monohydrate	10
pH = 7.4	

calcium-free HEPES Ringer	
Chemical	**concentration in mM**
NaCl	127
KCl	3
HEPES	25
$MgCl_2 \times 2H_2O$	2
$CaCl_2 \times 2H_2O$	0
$NaH_2PO_4 \times H_2O$	1.25
D-Glucose monohydrate	10
EGTA	0.1
pH = 7,4	

Table 2: Other buffers and solutions
All buffers and solutions were made with ddH_2O unless otherwise noted.

solution	concentration and ingredients
1xPBS	137 mM NaCl 2.7 mM KCl 1.5 mM KH_2PO_4 8.2 mM Na_2HPO_4
Blocking solution for ICC	10 % Bovine serum albumin 0.3 % Triton X100 0.1 % Tween 20 In 1x PBS
Blocking solution for IHC	10 % Horse serum 0.3 % Triton X100 0.1 % Tween 20 In 1x PBS
Washing solution for ICC	0.3 % Triton X100 0.1 % Tween 20 In 1x PBS
Washing solution for IHC	0.1 % Triton X100 0.1 % Tween 20 In 1x PBS
50x TAE stock solution (1x for agarose gels)	2 M Trisbase (from stock solution) 1 M EDTA (from stock solution) pH 8.5
Trypsin solution (for HeLa cells)	Tryple Express diluted in PBS 2:3
1xTBS	150 mM NaCl 10 mM Trisbase pH =8
TBS-T	0.2% Tween in 1xTBS
Electrophoresis buffer (for SDS-Page gel)	25 mM Trisbase 190 mM Glycine 3.5 mM SDS (= 0.1 % w/V) pH = 8.45
Transferbuffer for western blot	20 % Methanol 80 % Electrophoresis buffer
Protein lysis buffer	50 mM HEPES, pH 7.5 150 mM NaCl 10 % Glycerol ½ Tablet complete mini (w/0)EDTA per 5 ml 1 % Nonidet P40

	1 mM NaF
Protein sample buffer (Laemmli)	200 mM TrisCl 8 % SDS 25 % Glycerol 3 % β-Mercaptoethanol 0.2% (w/v) Bromphenolblue
Blocking solution for western blot	5 % Milk powder 10% Goat serum in TBS-T
Culture medium for primary hippocampal cells	1x B27 supplement 0.5 % Pen/Strep 1 % Glutamax 1x N2 supplement In neurobasal medium, equilibrated in cell culture incubator over night
Wash medium for primary hippocampal cells	1x B27 supplement in neurobasal medium, equilibrated in cell culture incubator overnight
Wash medium for primary glial cells	10 %FCS 5% Horse serum 1% Pen/strep 0.45 % Glucose In a 1:1 mix of DMEM:F12
Culture medium for primary glial cells	10 %FCS 5 % Horse serum 1% Pen/strep 0.45 % Glucose 10 ng/ml EGF 1x B27 supplement In a 1:1 mix of DMEM:F12
2x BBS	50 mM BES 280 mM NaCl 1.5 mM Na_2HPO_4 pH 7.05 (with NaOH)
HBSS and NBA for transfection	commercial HBSS and neurobasal A, each brought to mOsm 320-330 with mannitol, sterile filtrated
Liquid LB medium	1 % (w/V) Bacto-tryptone 0.5 % (w/V) bacto yeast extract In ddH_2O, then autoclaved; Add 50 µg/ml kanamycin or 100 µg/ml ampicillin
LB Agar plates	1 % (w/V) Bacto-Tryptone 0.5 % (w/V) Bacto Yeast 1.5 % (w/V) select Agar

	In ddH_2O, then autoclaved, add 50 µg/ml kanamycin or 100 µg/ml Ampicillin
TBS-5 for lentiviral particles	50 mMTris-HCl, pH 7.8, 130 mM NaCl 10 mM KCl, 5 mM $MgCl_2$
Cryoprotection solution	30% Ethyleneglycol 25% Glycerine 0.4 M Phosphate buffer
TE buffer (for DNA)	10 mM Tris 1 mM EDTA pH 8.5
Injection buffer	49.5 ml embryo certified water 500 µl 1 M Tris-Cl, pH 7 10 µl 0.5 M EDTA sterilize desired amount with a 0.45 µm Millex-HV syringe-driven filter unit before use

2.1.2 Material for cell culture

Table 3: Material for cell culture

chemical / material	**company**
10 mm microscope cover glasses	Marienfeld
B-27 supplement, 50x	Invitrogen, life technologies
BES (N,N-Bis (2-hydroxyethyl)-2-aminoethanesulfonic acid)	Sigma Aldrich
Cytosine-ß-D-arabinose-furanoside (=Ara C)	Sigma Aldrich
DMEM with Glutamax	Gibco, life technologies
Dulbecco's PBS without Ca/Mg 1x	PAA
Fetal calf serum	Gibco, life technologies
Glutamax	Invitrogen, life technologies
Ham`s F12 nutrients mixture	Gibco, life technologies
Hank`s BSS(1x) without Ca, without Mg, with Phenol Red, (HBSS)	PAA Laboratories
Horse serum	Linaris

Ibitreat µ-Dish 35 mm, high	IBIDI
Murine EGF	PreproTech
N2 supplement 100x	Invitrogen, life technologies
Neurobasal medium	Gibco, life technologies
OPTI-MEM	Gibco, life technologies
Penicillin/Streptomycin (both 5000 U/ml)	Gibco, life technologies
Poly-DL-ornithine hydrobromide (PORN)	Sigma Aldrich
Poly-D-lysine hydrobromide	Sigma Aldrich
Poly-L-Lysin	Sigma Aldrich
TrypLE Express	Invitrogen, life technologies
Trypsin	Worthington
Trypsin inhibitor from Glycine MAX (soybean)	Sigma Aldrich

2.1.3 Material for molecular biology methods

Table 4: Material for molecular biology methods

chemical / material	**company**
Accu-prime PFX polymerase	Invitrogen
Agarose	Biozym
Ampicillin	Sigma Aldrich
Bacto tryptone	BD bioscience
Bacto Yeast	BD bioscience
Centrifugal filter units-Ultrafree-MC-HV PVDF-0,45µm Durapore (centrifugal filter unit)	Millipore
Dark reader transilluminator	Clare chemical research
dNTPs	Fermentas
EndoFree plasmid Maxi kit	Qiagen
Gelstar nucleic acid gel stain (for cloning)	Lonza
Generuler 100bp /1kb ladder (100 bp/1 kb DNA	Fermentas

ladder)	
Kanamycin	Sigma Aldrich
Midori Green advanced DNA stain	Nippon Genetics Europe GmbH
Minipräp -Plasmid-Kit	Seqlab
PCR purification kit	Qiagen
Qiaquick Gel extraction kit	Qiagen
Quick Blunting kit	New England Biolabs
Restriction buffers	New England Biolabs
Restriction enzymes	New England Biolabs
Select agar	Sigma Aldrich
T4 DNA Ligase buffer	New England Biolabs
T4 DNA-Ligase	New England Biolabs

Table 5: Plasmids
SP = signalling peptide; CMV = cytomegalovirus promoter; UBQ = promoter of the human ubiquitin2 gene; CamKII = promoter of the Ca^{2+}/Calmodulin dependent protein kinase II gene; HA = influenza haemagglutinin epitope protein tag ; His = polyhistidine protein tag; CES2short = core sequence of the mouse carboxylesterase2; myc = sequence for the c-Myc protein tag; TagRFPT = red fluorescent protein designed as a protein tag; (E)GFP = (enhanced) green fluorescent protein; KDEL= ER retention motif; Thy1.2 = promoter of the thymocyte differentiation antigen 1 gen; LV = lentiviral, the plasmid contains genes necessary for lentiviral production; numbers are according to AG Blum plasmid library; the name states by which name the plasmid is referred to in this work; features only lists the features of the insert, but not of the total plasmid ,e.g. genes for antibiotic resistance are not listed; in bold are the distinct features

number	**name**	**features**	**comment/origin**
433	mCES2	CMV-native mCES2	(Rehberg et al., 2008)
434	mCES2	UBQ-native mCES2	(Rehberg et al., 2008)
593	$mCES2^{OPT}$	CMV-SP-CES2short-myc-KDEL	AG Blum, Munich
603	RedCES2	**CMV**-SP-TagRFPT-CES2short-myc-KDEL	(Jaepel and Blum, 2011)
706	FUVal	UBQ-EGFP (LV)	(Lois et al., 2002)
712	RedCES2	**UBQ**-SP-TagRFPT-CES2short-myc-KDEL (LV)	AG Blum, Würzburg by Thomas Andreska
768	$Red^{LNK}CES2$	CMV-SP-TagRFPT-**LNK**-CES2short-myc-KDEL (LV)	this study

772	RedCES2	**CamKII**-SP-TagRFPT-CES2short-myc-KDEL (LV)	this study
775	pcDNA-CMV-His-P2Y1-HA	CMV-**His-P2Y1-HA**	Prof. Carsten Hoffmann, Inst. of Pharmacology, Würzburg
786	RedCES2-IRES2-P2Y1	**UBQ**-SP-TagRFPT--CES2short-myc-KDEL-**IRES2-HA-P2Y1-His** (LV)	this study
787		CMV-IRES2 HA–P2Y1-His	this study
802	FCK	FUCamKII-GFP (LV)	(Dittgen et al., 2004)
803	CamKII-RedCES2-IRES2-P2Y1	**CamKII**-SP-TagRFPT-CES2short-myc-KDEL-**IRES2-HA-P2Y1-His** (LV)	this study
804	UBQ-Red^{LNK}CES2	**UBQ**-SP-TagRFPT-**LNK**-CES2short-myc-KDEL (LV)	this study
819		hGFAP-mRFP1	Dr. Anja Scheller, Inst. for Physiology, University of Saarland
825		Thy1.2-GFP for transgene expression	P.Caroni lab,Friedrich Miescher Institute, Basel
827	Thy1.2-RedCES2	**Thy1.2**-SP-TagRFPT-CES2short-myc-KDEL	this study
839		**GFAP**- SP-TagRFPT-CES2short-myc-KDEL	this study

Table 6: Sequencing and PCR Primers

primer name	**sequence**	**usage**
BamHI-EcoRI-IRES2 for	5`TCGGATCCTAGAATTCCCGCTACGTAAATTCC3`	cloning of $P2Y_1$ construct
IRES2-BamHI rev	5`ATGGATCCGGTTGTGGCCATATTATCATCG 3`	
Sal-TagRFP-for	5` GTAAGTCGACGTGTCTAAGGGCGAAGAGCT 3`	cloning of linker construct
Xho-TagRFP-link-rev	5`TACTCGAGGCCTCCGCCTCCGC-CAGATCCGCCCTTGTACAGCTCGTCCATGC 3	
TagRFPT2 for	5`AAGACCACATACAGATCCAA 3`	Genotyping

TagRFPT2 rev	5 `TCGTCCATGCCATTAAGT 3`	
CamKII for	5`CCACAGTGCCCTGCTCAGAA 3`	Sequencing
TagRFP rev	5`TTGTTCACGGTGCCCTCCAT 3`	
UBQ for	5`ACCAAAGAAACTGACGCCT 3`	
5`TagRFPT2 for	5`GTACGGCAGCAGAACCTT 3`	
5`CES2 for	5`AACCCCATCAGAAACACAC 3`	
3`CES2 for	5`GTCTTTGCGTCCTTCTTCT 3`	
mid CES2 for	5`ATGTTGTGTCCCCCATGTC 3`	
3`CES2 rev	5`GTGTCCCCCATGTACTCTTC 3`	
5`CES2 rev	5`GCAGACTCGCCAAAAATAG 3`	

2.1.4 Material for live cell imaging

Table 7: Chemicals and material for live cell imaging

material/chemical	**company**
4-Chloro-3-methylphenol (= cresol)	Sigma Aldrich
6-Cyano-7-nitroquinoxaline-2,3-dione (=CNQX)	Sigma Aldrich
(S)-3,5-Dihydroxyphenylglycine(DHPG)	Tocris
5′-ATP-Na_2, ATP disodium salt hydrate	Sigma Aldrich
Caffeine	Sigma Aldrich
Carbamoylcholine chloride (Charbachol)	Sigma Aldrich
Cyclopiazonic acid (CPA)	Ascent scientific
Dimethylsulfoxide (DMSO)	Sigma Aldrich
DL-2Amino-5-Phosphovaleric acid (=AP5)	Sigma Aldrich
DMSO	Sigma Aldrich
Ethyleneglycol-bis(ß-amino-ethylether)-N,N,N,N-tetra-acetic acid tetrasodium (=EGTA)	Sigma Aldrich
Fluo5N, AM, 10 x 50µg	Molecular probes, life technologies

L-Glutamate	Ascent scientific
Ionomycin Ca^{2+} salt	Ascent scientific
Kainic acid (=Kainate)	Sigma Aldrich
Mag-Fluo-4, AM	Molecular probes, life technologies
Mag-Fura-2, AM	Molecular probes, life technologies
Oregon Green 488 BAPTA-1, AM	Molecular probes, life technologies
Pluronic F127, low UV absorbance, 2 g	Invitrogen, life technologies
Ryanodine	Ascent scientific
S-AMPA	Abcam
SKF96365	Abcam
Tetrodotoxin	Abcam
Thapsigargin	Calbiochem

2.1.5 Other materials

Table 8: Other chemicals and material

chemical/material	**company**
4',6-diamidino-2-phenylindol (=DAPI)	Sigma Aldrich
Bovine serum albumin (=BSA)	Sigma Aldrich
Aqua-Poly/Mount	Polyscience, Inc.
Clarity western ECL substrate	Biorad
ECL Prime Western Blotting Detection Reagent	GE Healthcare
Extra thick blot paper	Biorad
Ethanol	Sigma Aldrich
Glycerol	Merck
Glycine (western blot)	Sigma Aldrich
Goat serum (western)	Linaris
Immuno-Blot PVDF membrane	BioRad
Methanol	Sigma Aldrich

Milk powder	Roth
Nonidet P40 Substitute	Fluka Analytical;
Page ruler prestained protein ladder	Thermo scientific
Paraformaldehyde	Alfa Aesar
Pierce BCA Protein Assay Kit	Thermo scientific
Polyacrylamide	BioRad
Sodium dodecyl ulphate (=SDS)	BioRad
Super RX x-ray film	Fujifilm
Tablet of complete Mini EDTA-free	Roche
Trisbase	Sigma Aldrich
Triton X 100	Carl Roth GmbH
Tween 20	Sigma Aldrich

Table 9: Software

software	**company**
ApE- A plasmid Editor v2.0.36	2003-2009 by M. Wayne Davis
GraphPad Prism 4.02	1992-2004 GraphPad Software, Inc., San Diego, California, USA
ImageJ	Rasband, W.S., ImageJ, U. S. National Institutes of Health, Bethesda, Maryland, USA, http://imagej.nih.gov/ij/, 1997-2014
LAS AF Lite 2.2.1 build 4842	2005-2009 Leica Microsystems CMS GmbH
Olympus	Olympus Fluoview Ver 4.0-4.1a
OriginPro 9.0.OG	1991-2012 OriginLab Corporation, One Roundhouse, Plaza Northampton, MA 01060 USA
Photoshop CS5	Adobe Systems, San Jose, CA, USA
StreamPix 4	NORPIX Digital Video Recording

	Software

2.1.6 Microscopic equipment for live cell calcium imaging

Table 10: Microscopic equipment for live cell imaging

equipment	**company**
confocal live cell imaging setup No.1	
TCS SP5 microscope	Leica
Minipuls 3 Peristaltic Pump	Gilson
Inline solution heater	Warner Instruments
Tygon tubing	VWR
LAS AF Lite 2.2.1 build 4842	2005-2009 Leica Microsystems CMS GmbH
20x Objective HC PL APO 20x/0.7 IMM (used with H_2O)	Leica
confocal live cell imaging setup No.2	
IX81 microscope	Olympus
confocal FV1000 laser scanning system	Olympus
FVD10 SPD spectral detector	Olympus
Minipuls 3 peristaltic pump	Gilson
Inline solution heater SH-27B	Warner Instruments
Dual automatic temperature controller	Warner Instruments
Plexiglas chamber	custom-made
Microscope stage No. 48-22-427-0000	Märzhäuser Wetzlar GmbH
Heating insert P	Leica
Heating microscope stage DM IL Fluo/Bio Leica	Leica
Temperature controller 37-2 digital	PenCon. Germany
Tygon tubing	VWR
60x H_2O Objective LUMPLAN Fl/IR, N.A. 0,9	Olympus
20 x air objective UPlanSapo 20/0.75 ∞/0.17/FN26.5	Olympus

60 x Oil objective 1.35 UPlanSApo ∞/0.17/F26.5	Olympus
non-confocal live cell imaging setup	
BX51WI upright microscope	Olympus
Epifluorescent light source CoolLED	Visitron systems
Rolera XR Mono fast 1394 CCD camera	Qimaging
Inline solution heater SH-27B	Warner Instruments
Badcontroller V	Luigs &Neumann
Tygon tubing	VWR
Shutter driver uniblitz VCM-D1	Vincent Accosiates
Software streamPix 4	NORPIX Digital Video Recording Software
Ceramic imaging chamber	Luigs&Neumann
40 x Objective Lumplan Fl/IR 0.80W	Olympus

2.2 Cell culture and live cell imaging methods

2.2.1 Animal rights approvement

All experiments were performed in accordance with European Union guidelines, as approved by our institutional animal care and utilization committee.

2.2.2 HeLa cell culture

The HeLa cell line was derived from “Leibniz-Institut Deutsche Sammlung von Mikroorganismen und Zellkulturen GmbH”. Cells were kept in DMEM including glutamax, supplemented with 5% fetal bovine serum (FBS) and 1 % penicillin/streptomycin (pen/strep) in a cell culture incubator with 5% CO_2 at 37°C in T25 cell culture flasks. On every third or fourth day (see below) the cells were split.

Splitting of cells:

After aspiration of all cell culture medium, 1 ml Trypsin solution was given to the cells and used to wash the cell layer for 10-20 s. The Trypsin was aspirated and another 1 ml Trypsin was given to the cells. The flask was panned for 1 min and 5 ml HeLa medium was added to stop the trypsinisation reaction. The cell solution was triturated 2-3 times using a serological

10 ml pipette tip and transferred to a 15 ml falcon tube. After centrifugation for 3 min at 14.000 rpm, the supernatant was removed and cells were washed again in 5 ml HeLa medium. 250.000 or 300.000 cells, respectively, were seeded in a T25 flask in 10 ml HeLa medium.

For live cell calcium imaging 150.000 or 200.000 cells in a total of 2 ml were seeded in 3.5 cm 4 well-dishes containing glass cover slips. Two or one days later, respectively, the coverslips were used for calcium imaging.

2.2.3 Transient transfection of HeLa and glial cells

One day after seeding, HeLa cells were transfected using the following reaction batch for each 3.5 cm dish. The cell number was dependent on the experiment but was generally between 150.000- 200.000 cells in 2 ml medium per 3.5 cm dish. In order to transfect primary glial cells, 10.000 glial cells were seeded on PDL coated 10 mm glass coverslips in 4-well dishes and incubated overnight. Then the same procedure as for HeLa cells was performed using glia medium instead of HeLa medium. Transfection batches for each dish were composed of:

Transfection mix: 400 µl opti-MEM
4 µl lipofectamine 2000
2 µg plasmid DNA or no DNA for controls

The transfection mix was incubated for 30 min at room temperature and then transferred onto the cells. Cells were incubated with the transfection mix for 4h in an incubator and then the medium was exchanged for fresh HeLa or glial medium.

2.2.4 Primary glial cell culture

One day before glial cells were seeded a T75 cell culture flask was coated with PORN over-night in a cell culture incubator. Before cells were seeded the bottom of the flask was washed twice with HBSS and once with glial wash medium. All media were prewarmed to 37°C before usage and glial culture medium was prepared fresh for each usage from a stock of wash medium by adding EGF and B27 from frozen stocks.

One 5-day-old mouse of the CD1 strain was decapitated according to animal rights guidelines. Subsequently, the skin and skull were removed and the total brain was isolated and placed in PBS. The olfactory bulb, all meninges, and the hippocampus were removed bilaterally and the frontal cortex was isolated. The cortical tissue was cut into several smaller pieces which were kept in HBSS on ice during the dissection procedure. All subsequent steps were performed under a sterile laminar flow hood. The tissue was transferred to a 15 ml falcon tube, 5 ml of glia wash medium was added, and cells were triturated with a fire-

polished glass pipette. Trituration was repeated twice using a fire polished glass pipette with a slightly smaller diameter. Between trituration steps cells were centrifuged and resuspended in fresh glial wash medium. After the last trituration step, cells were resuspended in glial culture medium and plated in a total of 20 ml glial culture medium in the PORN coated T75 cell culture flask. Cells were incubated in a cell culture incubator at 37°C and 5% CO_2 for 3-4 days. Cells were then washed with 10 ml PBS and the culture medium was exchanged for fresh medium. Seven to ten days after seeding, when a confluent layer of prospective astrocytes was observed, cells were split. For this, the cells were washed with PBS twice and subsequently incubated in 5 ml TrypleExpress for 30 s to 1 min. Addition of 10 ml wash medium stopped the reaction. To remove the trypsin, the cell solution was transferred to a 15 ml falcon tube, centrifuged for 3 min at 1200 rpm and resuspended in 5 ml wash medium. Centrifugation and resuspension was repeated, this time resuspending the cells in 5 ml of glial culture medium. Next, the respective number of cells needed for live cell imaging (10. 000 cells per cover-slip) was transferred to a 1.5 ml Eppendorf tube in a volume of less than 300 µl and 2 µl of lentiviral particles mediating UBQ RedCES2 expression were added and incubated for 10 min at room temperature. The volume of the medium was then filled up to the respective amount (100 µl per one 10 mm coverslip) and cells were seeded on pre-treated 10 mm coverslips placed into 4-Well cell culture dishes (coating: incubation in 20 µg/ml PDL in PBS overnight followed by three steps of washing with HBSS and one washing step with wash medium). Two hours after seeding, the cell culture dishes were filled up with culture medium to a final volume of 2 ml for each 3.5 cm 4-well dish. For live cell calcium imaging, cells were grown for 2-5 days in a cell culture incubator.

2.2.5 Primary hippocampal neuron culture

All experiments were performed in accordance with European Union guidelines, as approved by our institutional animal care and utilization committee.

Hippocampal cells were prepared as described elsewhere (Samtleben et al., 2013) using CD1 mice. Briefly, hippocampi from P0 mice (born at the day of dissection) were removed bilaterally and stored in tubes containing Hank's buffered saline solution (HBSS). Trypsin was added to a final concentration of 0.1 % and the tissue was incubated for 15 min at 37°C shaking the tubes for 30 sec at 600 rpm every 30 sec. Trypsinization was stopped in 0.1 % Trypsin inhibitor. The tissue was collected in 15 ml falcon tubes and triturated and washed 4 times in total (1x with fire polished glass pipette, 2x with a 1000 µl plastic pipette tip and finally 1x using a 200 µl plastic pipette tip). Centrifugation was performed at 1400 rpm for 3 min and fresh washing medium was used for each step; only for the last trituration culture medium was used. For TED imaging, neurons were transduced with lentiviral TED vectors at this point by incubating the respective number of cells in presence of 2-4 µl Virus in a cell

suspension of 100 µl in total for 10 min at RT. Next 25.000-40.000 cells were plated on poly-L-lysine-coated glass coverslips in a total of 100 µl culture medium. After the cells were attached to the bottom of the wells, the 4-well dishes were filled with additional 1.6 ml culture medium. 50 % of the culture medium was exchanged for fresh culture medium every week. For some cultures 10 µM cytosine β-D-arabinofuranoside (AraC) was added on DIV 2. Twenty-four hours later, all medium was removed and replaced by a 1:1 mixture of fresh culture medium and glial cell conditioned culture medium. Neurons were used for live cell imaging at DIV 6-21 and for immunocytochemical analysis at DIV 3-37 as stated in the results section.

2.2.6 Transfection of cultured hippocampal neurons

Hippocampal neurons were cultured as described above (see 2.2.5) and transfected on DIV 2. For this the growth medium was carefully aspirated and replaced by prewarmed neurobasal A (NBA) to equilibrate the cells for the transfection procedure. The original medium and the cells were stored in the cell culture incubator. Next the transfection batch was prepared, mixed and incubated at RT for 30 min

Transfection batch for a for a 3.5 cm cell culture dish:
2.5 µg DNA
Ad sterile H_2O to 23 µl
+ 2.5 µl 2.5 M $CaCl_2$ (final conc. 12.5 mM)
Mix
+ 25 µl 2x BBS

Incubate at RT 30 min, then mix with 450 µl NBA medium.
Subsequently, the NBA medium was aspirated from the neurons, replaced by the transfection batch, and the neurons were incubated in the incubator for 30 min. Finally, the neurons were washed twice with prewamed HBSS and the original culture medium was brought onto the cells.

2.2.7 Production of lentiviral particles

Lentiviral particles were produced in the viral facility of the Institute of Clinical Neurobiology as described earlier (Rehberg et al., 2008). For this, HEK293T cells (derived from “Leibniz-Institut Deutsche Sammlung von Mikroorganismen und Zellkulturen GmbH”) were grown in a 175 cm^2 cell culture dish in cell growth medium, so that they were 90% confluent 3 days later. The transfection mixture was prepared by setting up 2 separate tubes containing:

1	2
9 ml OPTI-MEM without FCS	9 ml OPTI-MEM without FCS
45 µg packaging vector Δ 8.9	214 µl Lipofectamine 2000
30 µg pseudo typing vector VSVG	
18 µg expression plasmid	

The pCMVΔR8.91 (Δ8.91) vector originates from (Zufferey et al., 1998) and the pCMV-VSV-G (VSVG) vector from (Lois et al., 2002). Both tubes were first incubated at RT separately, and then their content was combined and gently mixed and again incubated at RT for 30 min. During the incubation Hek293T cells were harvested from the 175 cm flask and suspended in 42 ml OPTI-Mem with 10% FCS.

Next, the cells were mixed with the transfection mix, incubated at RT for 10 min, and 10 ml of the mixture was plated into each well of a 6x 10 cm cell culture dish. Cells were then incubated overnight in a cell incubator. On the next day, cells were washed once and then further incubated in NB medium with 2 % FCS. Cells were then allowed to grow for another 2 days. Then the lentiviral particles were harvested.

For this the complete cell medium was aspirated from the cells and centrifuged at 3.600 rpm 15 min at RT to remove remaining cells. The supernatant was then sterilized with a Millex HV 0.45 µm filter and lentiviral particles were enriched by ultracentrifugation; The supernatant was placed on a 20% sucrose solution and centrifuged for 2 hrs at 25.000 rpm at 4°C. Afterwards the supernatant was aspirated and the pellet was covered with cold TBS-5 buffer and stored at 4°C for 3 hrs to overnight. Finally, the lentiviral pellet was resuspended by gentle pipetting, aliquoted and stored at -80°C until used for infection. The viral titer was roughly at 10^6 to 10^8 clone forming units per ml, when determined on HEK293T cells.

2.2.8 Live cell imaging

Depending on experimental needs, three different live cell imaging setups were used. Each setup consisted of a perfusion system, the microscope and the imaging chamber.

The first setup was built at a confocal Leica TCS SP5 microscope, which was used at a 12-bit setting. The Perfusion system was set up as described for the Olympus Fluoview system (see below).

The second setup was built at an inverted Olympus IX81 microscope with an Olympus confocal FV1000 laser scanning system, a FVD10 SPD spectral detector, and diode lasers of 405 nm, 473 nm, 559 nm, and 635 nm. To detect Fluo5N signals and Oregon Green signals the 473 nm laser was used at 0.3-1 % of its maximal power to avoid bleaching and phototoxicity, the detection range was set to 507-545 nm and 12-bit images were acquired.

The confocal pinhole was set to 700-800 µm, the current of the photomultiplier detector power (HV) was 600-900 and no amplification of the PMT signal was used. A 60x H_2O objective was used. The perfusion unit consisted of a Minipuls 3 peristaltic pump, an inline solution heater operated by a dual automatic temperature controller set to 37°C. The neurons, grown on a 10 mm cover slip, were held by a custom made, plexiglas imaging chamber with a chamber volume of 200-300 µl which was mounted into a stage adapter heated to 37 °C by a temperature controller 37-2 digital (Samtleben et al., 2013).
In addition, a non-confocal setup was used, composed of an Olympus BX51WI upright microscope setup equipped with a coolLED epifluorescent light source for 470 nm and 550nm a Rolera XR Mono fast 1394 CCD camera (8-bit). Here, image sequences were continuously acquired with help of the streaming software Streampix 4.0. The perfusion system was built up as described above. The image chamber contained a volume of about 1.5 ml. The bath controller was kept at 33 °C by a Badcontroller V, while the inline heater was kept at room temperature. To ensure that any agonist or antagonist solution reached the cells, the cover slip was always placed next to the suction tube.
All tubing consisted of Tygon tubing (VWR), diameters 10.2 to 1.75 mm.
To enable an estimation of the time point when an agonist/antagonist met the cells, the flow was examined with the help of ACSF solution containing fluorescent antibodies (Alexa 488). Using the conditions for the experiment to follow, the solution was perfused into the system and the fluorescence was recorded for the complete visual field. The time point of the peak fluorescence of all three trials was determined and the mean value was used to determine the time point of the respective experiment. Because the tubing changed between experiments (due to wear out of the material) this procedure was repeated at each experimental day.

2.2.9 Quantification and statistical analysis of fluorescence curves

To obtain the $\Delta F/F_0$ curves from the calcium time laps imaging movies fluorescence values were extracted using the ImageJ software (Rasband, W.S., ImageJ, U. S. National Institutes of Health, Bethesda, Maryland, USA, http://imagej.nih.gov/ij/, 1997-2014). Regions of interests (ROIs) were drawn either around somatic regions (including nuclear region for Oregon Green movies and without nuclear region in ER F5N movies) or dendritic regions. In addition 3 ROIs were placed on a cell free region to determine the background noise. Using the ImageJ plugin time series analyser v2.0 the average pixel intensityof a ROI representing the mean fluorescence intensities for each ROI were determined from time-lapse image series. Next, the mean background fluorescence was subtracted from single fluorescence values resulting in the F_{ROI} values.

Using the formula $\frac{(F_{roi} - F_0)}{F_0} = \Delta F / F_0$ the fluorescence values were normalized. Here, F_0 is the mean fluorescence of the first ten time points for each ROI, i.e., the basal fluorescence. In order to analyse these curves, fluorescence curves were generated using the origin9 software. $\Delta F/F_0$ values were plotted against time and the resulting curves were corrected for bleaching, if necessary: The Savitzky-Golay Filter (set to window size 1, threshold 0.05, polynominell order 2) with 8 points were applied to determine the curves baselines, i.e. to straighten the curve. The bases before and after a reaction were used as reference points in this process. Then all values were determined as depicted in figure 6. The time from calcium withdrawal until a new fluorescence minimum was reached was determined (termed "initial-depleted"). These values were determined for every single ROI and then statistically analysed using the Graphpad Prism 4.0 software. To test for significant changes the non-parametric, unpaired, two-tailed Mann-Whitney test was used to calculate the p-value. Confidence intervals were set to 95% and results were defined as follows: $p < 0.001$ extremely significant (***), $0.001 < p < 0.01$ very significant (**), $0.01 < p < 0.05$, significant (*) and $p > 0.05$ not significant (ns).

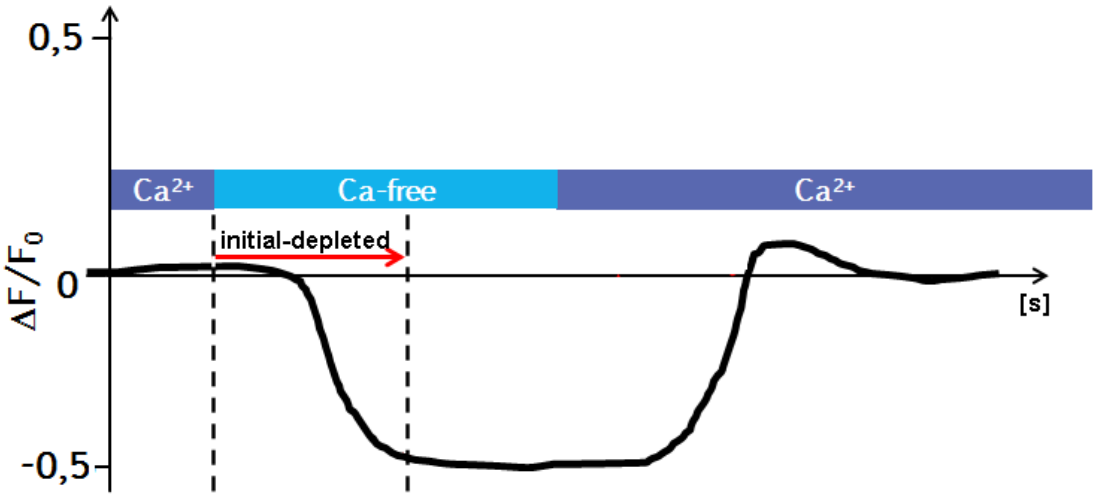

Figure 6: Idealized fluorescence curve exemplifying quantification
This idealized fluorescence curve depicts the values that were determined for quantification.

2.3 Molecular biology methods

2.3.1 Agarose gel electrophoresis

Depending on the experiment 0.8 - 2 % agarose was dissolved in 1x TAE buffer in a microwave. To visualize DNA molecules Midori (final dilution 1:20000) was added. After polymerisation of the gels, electrophoresis was performed at 50 - 120 V submerged in 1x

TAE buffer for 30-50 min. Pictures were taken in a dark chamber using a UV light and exposure times according to experimental needs.

2.3.2 Cloning procedures: Restriction digestion, ligation, PCR amplification, blunting and phosphorylation of DNA, and DNA isolation

Generally, all procedures for cloning were performed according to the manufacturers` instructions for the respective reaction.

Restriction digestion

The amount of DNA used varied between 1 - 5 µg. Generally, per 1 µg DNA 10 µl of reaction volume was used and the reaction was performed according to manufacturer's instructions.

Cloning

To improve cloning performance, DNA was cleaned up using a PCR purification kit or Gel extraction kit after each procedure, i.e. restriction and isolation of insert fragments from gels. Furthermore the DNA was dissolved in 10 mM Tris HCl, buffer (pH 8.5). All DNA fragments that were involved in cloning were visualized by the use of agarose gels with Gelstar Gel stain and a Dark reader transilluminator with pure visible blue light to avoid mutagenic effects by ultraviolet light.

Ligation

Ligation was always performed in a 10 µl reaction volume at 16 °C overnight. The molar ratio of insert to backbone DNA was 10:1.

DNA isolation from *E. coli*

DNA was isolated with a commercial Miniprep kit for cloning or the Endofree plasmid Maxi kit to gain plasmid DNA for lentiviral packaging.

2.3.3 Transformation and culture of competent *E. coli*

To amplify and select plasmid DNA, selfmade chemically competent *E. coli* from the Top10 strain were used. The cells were stored at -80°C and thawn on ice. Then, 5 µl of each ligation reaction (or 10 pg of existing plasmid for a retransformation) were added, the tubes were swirled to mix, and incubated on ice for 30 minutes. Subsequently, the *E.coli* were heat shocked by emerging the tubes in a water bath at 42 °C for 45 s and a subsequent incubation on ice for 3 min.Then, 500 µl of liquid LB medium was added and the tubes were incubated at 37 °C at 400-600 rpm for 45-60 min to expand the cell number. For each ligation 100 µl of this suspension was seeded on LB Agar plates containing 100 µg/ml of ampicillin or 50 µg/ml kanamycin. To ensure a sufficient amount of bacterial colonies, the remaining cells

were centrifuged for 5 min at 1300 rpm, the pellet was resuspended in 100 µl LB medium, which were then seeded on a separate LB agar plate with antibiotics. After incubation at 37 °C overnight bacterial colonies were picked using a sterilized toothpick and transferred to liquid LB medium containing the respective antibiotic. The culture was incubated at 37°C at 180 rpm for 4-12 h and then plasmid DNA was isolated.

2.3.4 Preparation of DNA for pronucleus injection

In order to generate a transgenic mouse line it was necessary to remove the gene from its plasmid, sterilize the DNA and dilute it in a buffer suitable for pronucleus injections. This procedure started by performing a restriction digestion containing 10 µg Thy1. RedCES2 (827) plasmid DNA, 20 units PvuI,40 units EcoRI, 5 µL 10 x NEB3 buffer and 5 µl 10x BSA in a total volume of 50 µl. The reaction was incubated at 37°C for 2h and the complete reaction mix was separated on a 0.8 % agarose gel, stained with Midori, at 100V for 30 min. The uppermost band of ca. 9 kb was removed from this gel and the DNA was isolated using a Qiagen Gel extraction kit and the following modified protocol. All steps were performed at RT unless otherwise noted and a table top centrifuge was used. Three volumes (volumes of the weight, i.e. 600 µl for a 200 mg gel slice) of buffer QG were added and the tube was incubated at 50°C at 600 rpm for 10 min to dissolve the gel. Next, one volume of isopropanol was added to the tube and two Qiagen columns were loaded with one half of the mixture each. After centrifugation for 1 min at 4500 rpm the flow-through was discarded and 500 µl buffer QG was added to each column. The columns were incubated for 5 min at this point; centrifuged as before and the flow-through was discarded. This washing was repeated once more, incubating the columns for three minutes. Next, 750 µl of buffer PE was added, incubated for 3 min and removed by centrifugation at 4500 rpm for 1 min. This washing was repeated once and 750 µl PE was added for a third time. Centrifugation at 4500 rpm for 1 min followed and then all remaining flow-through was carefully discarded. To dry the columns, they were next centrifuged at full speed for 5 min. Afterwards 50 µl injection buffer was applied onto the membrane of one of the columns and incubated for 1 min. The DNA was collected in a sterile reaction tube by centrifugation at 13.000 rpm for 2 min. The same 50 µl elution buffer was then transferred to the other column and the elution procedure was repeated. As a result a concentration of 54 ng/µl DNA was obtained.

Following isolation, the DNA was cleaned from all debris and contaminations. To achieve this, only filtered pipette tips were used which were rinsed in sterile injection buffer before handling the DNA. In the same way the tubes for the DNA were rinsed.

A centrifugal filter unit with a pore size of 0.45 µm was prepared by addition of 50 µl sterile injection buffer and centrifugation for 4 min at 12.000 rpm. The flow-through was discarded

and the isolated DNA was applied to the filter. The centrifugation was repeated as before resulting in 54 ng/µl DNA.

2.3.5 Genotyping of transgenic mouse DNA

In order to identify transgenic mice carrying the Thy1 RedCES2 expression cassette a Polymerase chain reaction (PCR) was established. Mouse tail DNA was used as a template and the primers were complementary to the TagRFP-T sequence since both the Thy 1.2 promoter and the CES2 sequence are present in wildtypic mouse genomes. The primers used were TagRFPT2forw 5`aagaccacatacagatccaa 3` and TagRFPT2rev 5`tcgtccatgccattaagt 3`. The ingredients of each PCR reaction and the thermocycler program are given in table 11 below:

Table 11: Genotyping of Thy1::RedCES2 transgenic mice

substance	**Volume in µl**	**PCR program:**	
Selfmade Pfu polymerase	0.3	**Temperature** [°C]	**Duration [s]**
10xbuffer	3	95	120
dNTP 2 mM	3	95	15
DNA template	50-100 ng tail DNA	60	30
TagRFPT2 for 20 µM	3	72	60
TagRFPT2 rev 20 µM	3	Repeat steps 2-4 30 times	
H_2O	ad 30 µl	72	300

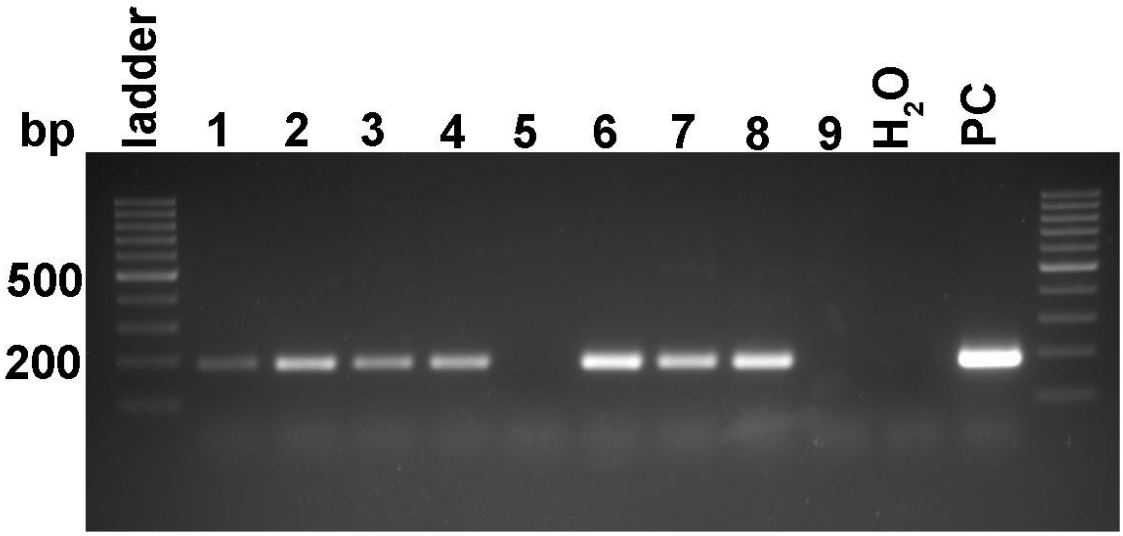

Figure 7: Genotyping of transgenic Thy1::RedCES2 mice
Genomic mouse tail DNA was used as a template for a PCR reaction to detect the transgene. DNA containing the transgene resulted in bands at the expected size of ca. 200 bps .PC = Positive control DNA. Samples 5 and 9 did not carry the transgene. Gel 2 % agarose, Midori staining.

The PCR reaction was then analysed on a 2 % agarose gel in 1x TAE which was run for 30 min at 120 V. The expected band size was 188 bp for DNA containing the TagRFP-T sequence. Figure 7 shows the result of DNA samples received from the transgenic unit.

2.4 Immunocytochemical stainings

2.4.1 Immunocytochemical stainings

Hippocampal neurons grown on coverslips (as described above) were washed once with PBS, then fixed with prewarmed 4% paraformaldehyde (PFA) for 15 min, and subsequently incubated in blocking solution for 30 - 60min at RT. Cells were then incubated in blocking solution containing primary antibodies diluted as listed in table 12 for 2-3 h. Then, the coverslips were washed in washing solution eight times and incubated in secondary antibodies diluted in blocking solution (see table 12) for 60 min. Afterwards, the coverslips were washed with PBS eight times, in ddH_2O once and embedded using Aqua-Poly/Mount. Pictures were taken at a confocal Olympus Fluoview1000ix81 laser scanning microscope.

2.4.2 Immunohistochemical stainings

Immunolabelling of slices was performed in 12-well plates with 40 µm tissue slices floating in the respective solution. First, slices were washed with PBS once, followed by 1 h incubation in blocking solution on a shaker at RT. Next, the slices were incubated in blocking solution

containing the primary antibodies of the respective dilution (table 12) at 4°C overnight in a humidified chamber. The antibodies were washed of three times with washing solution for 10 min and then the slices were incubated in blocking solution containing the secondary antibodies for 90 min at RT. Three washing steps of 10 min with washing solution and one washing step with PBS for 10 min followed. Next, cell nuclei were labelled by incubating the slices for 5 min in 0.4 ng/ml Dapi in PBS. Finally, the slices were washed twice in PBS for 10 min and embedded in Aqua-Poly/Mount.

Table 12: Antibodies
ICC= immunocytochemistry; WB=western blot; IHC= immunohistochemistry; NG2= NG2 proteoglycan; Map2= microtubule associated protein 2; vGlut1= vesicular glutamate transporter 1; vGat = vesicular GABA transporter; STIM 1/2 = stromal interacting molecule 1/2 ; Cy 3/5 = cyanine 3/5; HRP = horseradish peroxidase

Antibody	**Company (clone, reference number)**	**Application and dilution**
mouse anti c-Myc	Santa Cruz (9E10,SC40)	ICC 1:100; WB1:3000
rabbit anti NG2	Millipore (AB5320)	ICC 1: 1000
rabbit anti HA-tag	Abcam (AB9110)	ICC 1:500
mouse anti HA.11 16B12	Covance (MMS-101R)	ICC 1:500
chicken anti Map2	Abcam	ICC 1:2000
mouse anti Map2	Sigma Aldrich	IHC 1:400
rabbit anti Homer1	Synaptic systems	ICC 1:400
rabbit anti Calnexin	Enzo	ICC 1:1000
goat anti Calnexin	SICGen	IHC 1:500 of 0,55 µg/µl
rabbit anti vGlut1	Synaptic systems	ICC 1:2000
guinea pig anti vGat	Synaptic system	ICC 1:400
chicken anti Neurofilament heavy chain	Millipore	ICC 1:10.000
rabbit anti Tau	Sigma	ICC 1:1000
Rabbit anti STIM1	Cell signalling (4916)	ICC 1:200
Rabbit anti STIM2	Cell signalling (4917)	ICC 1:200
Rabbit anti Esterase	Abcam (ABI 1875)	WB 1:5000
Donkey anti guinea pig Cy5	Jackson Immuno research	ICC 1:800

Donkey anti chicken Dylight 649	Jackson Immuno research	ICC 1:800
Goat anti mouse Cy3	Jackson Immuno research	ICC 1:800
Donkey anti rabbit Dylight 488	Jackson Immuno research	ICC 1:800
Goat anti chicken 488	Life technologies	ICC 1:800
Goat anti rabbit HRP	Jackson Immuno research	WB1:10.000
Goat anti mouse HRP	Jackson Immuno research	WB 1:10.000

2.4.3 Image processing

Images were acquired with the Fluoview IX81 microscope equipped with the Olympus FV1000 confocal laser scanning system, FVD10 SPD spectral detector and diode lasers of 405 nm, 473 nm, 559 nm, and 635 nm. The confocal pinhole was set to one Airy disc and 12-bit z-stacks were prepared using the using an Olympus UPLSAPO60x oil or 40x oil objective. Images were processed with the ImageJ software and either confocal single z-planes were used or several z-planes were merged as a maximum intensity projection as stated in the figures. Final figure preparation was performed with Adobe Photoshop CS5 and pictures are shown as RGB images.

2.5 Proteinbiochemistry

2.5.1 Protein isolation

120.000 HeLa cells were seeded in 3.5 cm cell cultures dishes in medium with 10 % FBS and 1 % penicillin/streptomycin and cultured overnight at 37°C and 5% CO_2. Then, cells were transfected using the lipofectamine method described above (2.2.2). Two days after transfection, proteins were isolated. For this, cells were washed with PBS once and then collected in 200 µl protein lysis buffer. To open the cells the lysates were treated with a sonifier (75% 5 s) and subsequently incubated on ice for 15 min. Cell debris were removed by centrifugation at 4°C for 10 min at full speed and the supernatant was used for further analysis. The total protein concentration was determined by using the Pierce BCA Protein Assay Kit. Protein lysates were mixed with 1x protein sample buffer, cooked for 5 min at 95°C and stored at -20°C or -80°C until analysis.

2.5.2 SDS-polyacrylamide gel electrophoresis

8 and 10 % separation SDS-polyacrylamide gels were prepared with a 5% SDS-polyacrylamide stacking gel on top and loaded with 10 µg of the protein lysates and 5 µl of PageRuler prestained protein ladder, a protein size standard. Gels were run at 200 V and 0.2 A with max 30 W for 90 min in electrophoresis buffer.

2.5.3 Western Blot, protein detection, and development

In preparation for protein transfer a PVDF membrane was incubated in methanol for 3-5 min. Afterwards, the methanol was gradually replaced by transfer buffer and the PVDF membrane and the gels were incubated in transfer buffer for 45 min. Proteins were transferred from the gel onto the membrane in a semidry blotting chamber at 640 mA, 50 W and 30 V for 40 min. During the procedure the gel and membrane were kept humid by extra thick filter papers soaked in transfer buffer. Following the transfer, the membranes were incubated in blocking solution for 1h at RT, and in blocking solution containing the primary antibodies at 4°C overnight on a shaker. The membranes were then washed with TBS-T 4-5 time 10 min at RT and then incubated in blocking solution containing the secondary antibodies. Another washing step, 4-5 washes for 10 min each with TBS-T, followed. To visualize the proteins the ECL prime kit was used according to manufacturer`s instructions. The membranes were then wrapped in foil and further processed in a dark room. Luminescence was detected by placing a light sensitive film on the membranes for few seconds and the films were then developed.

3 Results

This study aimed at deciphering calcium homeostasis in primary neurons at rest focusing on the role of the ER calcium store. Therefore, it was necessary to find a tool enabling the direct imaging of ER calcium signals in undisturbed neurons. Targeted-esterase induced dye loading was known to provide such a tool. This method was developed in earlier work in order to investigate ER calcium signalling in cultured cells (Jaepel and Blum, 2011; Rehberg et al., 2008) but some relevant questions remained unsolved. It was examined whether the fusion of the red fluorescent protein TagRFP-T to the carboxylesterase influenced the esterase activity and whether a neuron specific promoter can further enhance TED. Furthermore, the applicability of TED to cultured hippocampal neurons was confirmed in more detail and calcium homeostasis in cultured neurons was investigated. In addition, a transgenic mouse line expressing the TED RedCES2 reporter construct was successfully generated.

3.1 Methodical part

3.1.1 Introduction to original TED vector constructs mCES2 and RedCES2

Synthetic calcium indicators of the acetoxymethyl ester family are per se cell membrane permeable, insensitive to calcium ions, and not fluorescent. To use them as calcium indicators, they have to be converted by cleaving of the AM group by an esterase activity. Within most cells types, esterases are present in the cytosol and in the ER that are capable to convert AM calcium indicators. But the TED method aims at visualizing solely ER calcium ions (see also introduction). Therefore, a reporter protein was designed, that provides a high esterase activity in the ER to convert the AM indicator. The cloning steps described in this chapter 3.1.1 were conducted by others and are summarized here (and in figure 8) in order to provide a complete picture of the process to establish the TED method. Plasmid numbers in bracelets are numbers according to the AG Blum plasmid library.

As described in (Rehberg et al., 2008) the mouse carboxylesterase 2 (mCES2) is able to convert AM dyes. The RNA sequence coding for mCES2 (Acc. No. BC015290) had therefore been isolated from mouse liver and cloned into the vector pcDNA3.1 behind the CMV promoter. The result is plasmid number 433, “**mCES2”**.

In parallel, this sequence had been cloned into the lentiviral FUGW vector (Lois et al., 2002) (result: 434). The FUGW vector is equipped with sequences coding for the promoter of the ubiquitin gene (UBQ) and lentiviral elements needed to generate lentiviral particles.

In an alternative approach the sequence for **"mCES2^{OPT}"** had been generated by first amplifying the mCES2 sequence exclusive of its ER signal peptide and 3`end. Then the amplicon was cloned into the plasmid pCMV-myc-ER in frame in a position 3´ of an optimized ER signal peptide and 5` of the sequence coding for a c-Myc-tag and ER retention motif (HKDEL*) (result: 593) (Jaepel and Blum, 2011).

As mentioned in (Jaepel and Blum, 2011) the sequence coding for the luminal red fluorescent protein TagRFP-T (Shaner et al., 2008) had been added to the mCES2^{OPT} sequence enabling the identification of cells expressing the reporter protein (result: 603).

The resulting "**RedCES2**" sequence had been subcloned into the lentiviral FUGW vector (result: 712).

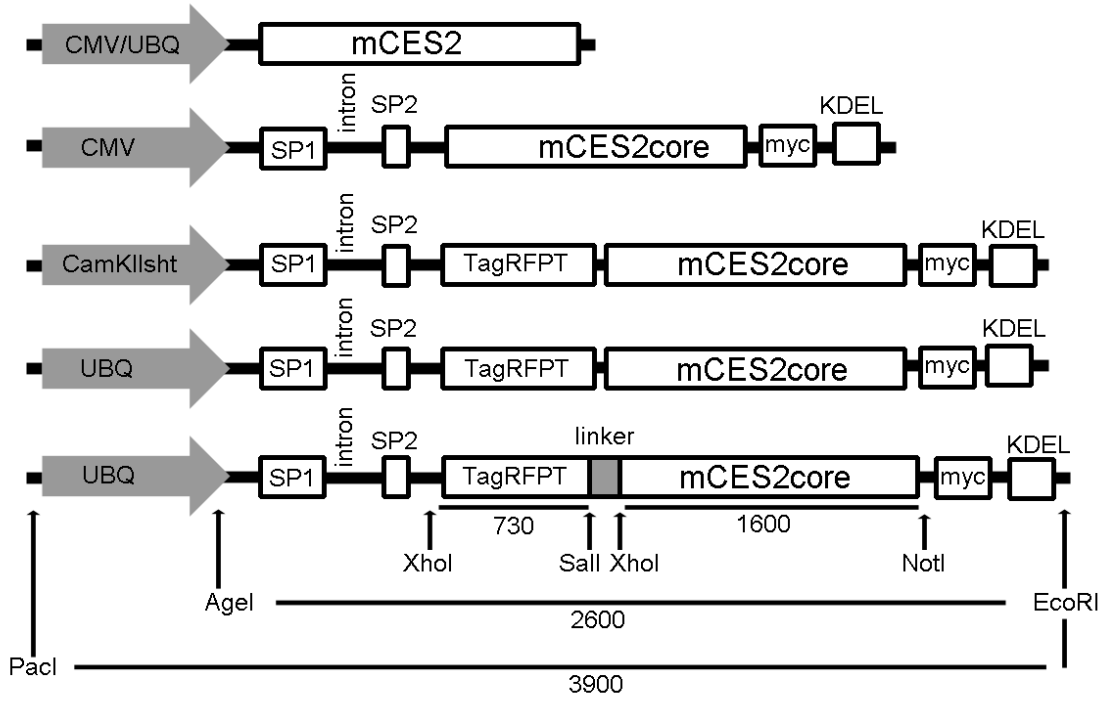

Figure 8: Overview of "old and new" TED vector constructs
For the first TED vector the total mRNA sequence coding for mouse Carboxyleterase2 (mCES2) was cloned (mCES2, upper row). This sequence - except for its signalling peptide and ER retention motif- was cloned into a new backbone, thus adding an improved ER signal peptide, ER retention motif, and a c-Myc-tag (myc) to the carboxylesterase (mCES2^{OPT}, second row). This sequence was then further improved by fusing it to the red fluorescent protein TagRFP-T either directly (RedCES2) or via a Glycine-Serine rich linker. The RedCES2 sequence proved to be most suitable for TED and was therefore cloned behind the UBQ and CamKII short promoter of lentiviral vectors. Numbers are numbers of base pairs and the length of single elements is not to scale. SP1 /SP2 = first and second exon of the signal peptide; KDEL = ER retention motif; arrows indicate positions of restriction sites.

3.1.2 Optimization of RedCES2 by inclusion of a linker region

Although existing TED vector constructs were suitable for ER calcium imaging in neuronal cells, it was not clear whether fusion of the TagRFP-T sequence directly to the mCES2 sequence reduced the esterase activity of the total fusion protein. To avoid such detrimental

effect, we added a flexible linker sequence between the mCES2 sequence and the TagRFP-T sequence. The sequence coding for the amino acid sequence GGSGGSGG flanked 5`by a SalI restriction site and 3´by a XhoI site was inserted yielding the sequence **"Red^{LNK}CES2"** (see also figure 8) (result: 768).

Then, the Red^{LNK}CES2 sequence was subcloned into FUGW (result: vector 804) and used to generate lentiviral particles. As depicted in figure 9 transduced hippocampal neurons could be loaded with Fluo5N, AM and used for live cell calcium imaging. As expected (see below), the fluorescence increased upon stimulation with 100 µM glutamate and decreased during stimulation with 40 mM caffeine.

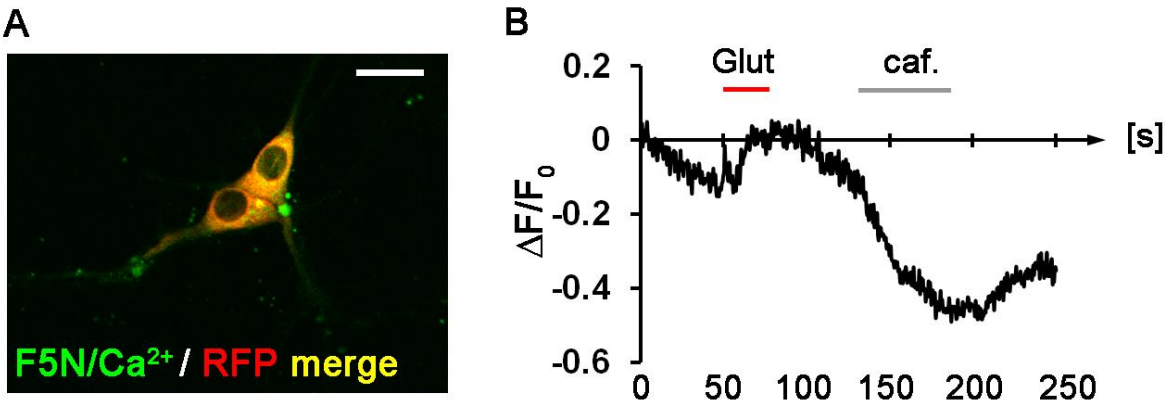

Figure 9: Red^{LNK}CES2 enables TED imaging in hippocampal neurons
Cultured hippocampal neurons were transduced with the Red^{LNK}CES2 construct and loaded with Fluo5M, AM. **A)** Picture of transduced hippocampal neurons under live cell imaging conditions. **B)** Mean fluorescence trace representing ER calcium levels of 4 neurons stimulated with 100 µM glutamate and 40 mM caffeine as indicated confirming the functionality of the reporter construct.

3.1.3 Expression and processing of TED vector constructs in HeLa cells

Because it was not clear how the various TED reporter proteins behaved in cells regarding expression strength, localization and processing, western blot analysis and immunocytochemical stainings were performed.

HeLa cells were transfected with expression constructs coding for mCES2, mCES2^{OPT}, RedCES2, and Red^{LNK}CES2. The cells were then cultured for 2 more days to allow synthesis of the respective reporter proteins and then total protein lysates were isolated. The protein lysates were separated by a SDS-Polyacrylamide gel and blotted on a PVDF membrane for immuno detection using anti esterase and anti c-Myc antibodies.

The western blot, shown in figure 10, revealed that all constructs are expressed in HeLa cells suggesting that the sequences of the vector constructs were correct. Interestingly, RedCES2 fusion proteins were detected with the antibody directed against the c-Myc-tag but not by the anti esterase antibody. Possibly, the anti esterase antibody binding site was hidden by the TagRFP-T protein. This was not altered by addition of the flexible glycine-serine linker

between both protein moieties. The Red^{LNK}CES2 protein was also only detectable by the anti c-Myc antibody whereas the mCES2^{OPT} protein was detected with both antibodies.
Overexpression of mCES2 led to a double band with a weaker upper band, whereas all other proteins caused single bands only. The upper band is probably caused by proteins in which the signalling peptide was not cleaved off and which would therefore not be localized to the ER. Addition of the optimized ER signal peptide and ER retention motive successfully solved this problem.

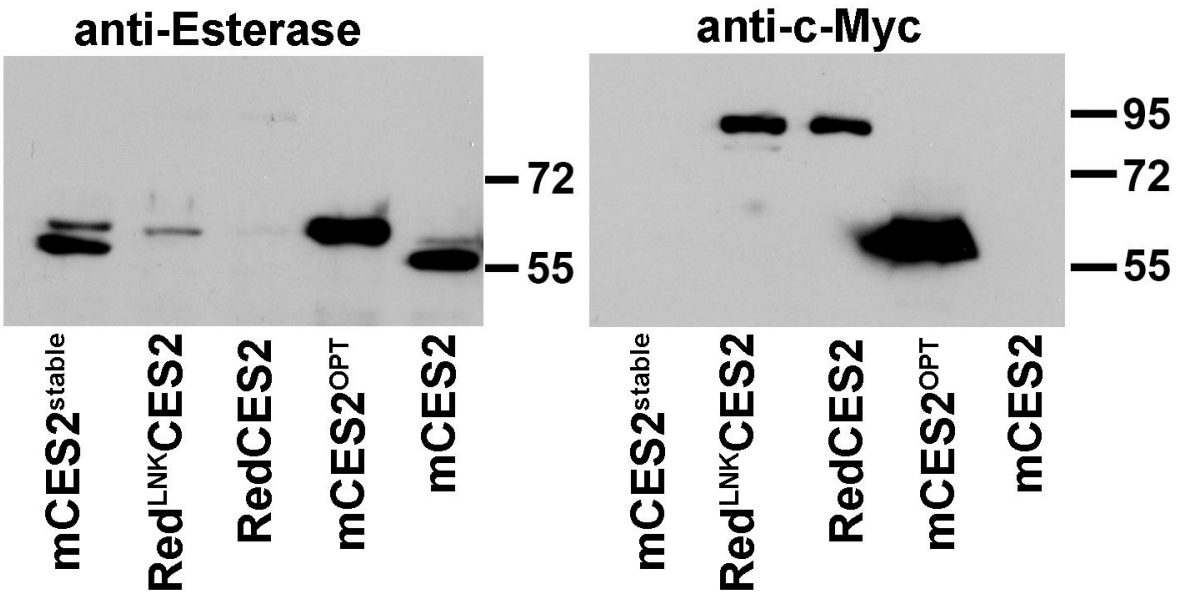

Figure 10: Western Blot analysis of TED reporter constructs
HeLa cells were transfected with TED reporter plasmids. The total protein lysates were isolated and analysed via western blotting. For immuno detection an anti esterase and an anti c-Myc antibody were used. Carboxylesterases bearing the improved ER signal peptide and ER retention motif are correctly processed whereas the native mCES2 protein gives a double band. Carboxylesterases fused to the TagRFP-T can only be detected with an anti c-Myc antibody but not with the anti esterase antibody. mCES2^{stable} = protein lysates from a HeLa cell line stably expressing mCES2.

3.1.4 Performance of different TED vector constructs in HeLa cells using Fluo5N, AM

We screened the performance of different TED constructs to identify the most efficient CES fusion protein in cleaving AM dyes and to examine how the addition of the TagRFP-T and the linker region influenced the carboxylesterase activity. For this experiment, HeLa cells were seeded on 10 mm glass cover slips and transfected with mCES2, RedCES2, Red^{LNK}CES2 and rat CES3. Two days after transfection the cells were incubated in 5 µM F5N, AM solution for 30 min and analysed with a confocal laser scanning microscope. During laser scanning cells were kept under continuous perfusion with HEPES buffer containing 1 mM $CaCl_2$. Inline heater and imaging chamber were set to 37 °C. For each construct 20 cells were analysed in 3 independent experiments by measuring the fluorescence of 10 z-layers

1.5 µm apart. The mean fluorescence of all cells and z-layers caused by the F5N/Ca^{2+} complexes was determined (figure 11). The highest fluorescence values, representing Fluo5N-release and Fluo5N/Ca^{2+} complex formation, were achieved by using the Red^{LNK}CES2 construct with 497 ± 176 (for all arbitrary units (a.u.) ± standard error of the mean (S.E.M.)) directly followed by the CES2 construct which led to a fluorescence value of 462 ± 117. Usage of the RedCES2 construct was in the same range with 362 ± 159, whereas the rat CES3 (66 ± 4) and untransfected cells (78 ± 11) produced hardly any fluorescence at all.

RedCES2 was chosen for consecutive experiments because it allows the identification of cells by their red fluorescence and gave satisfactory levels of calcium fluorescence.

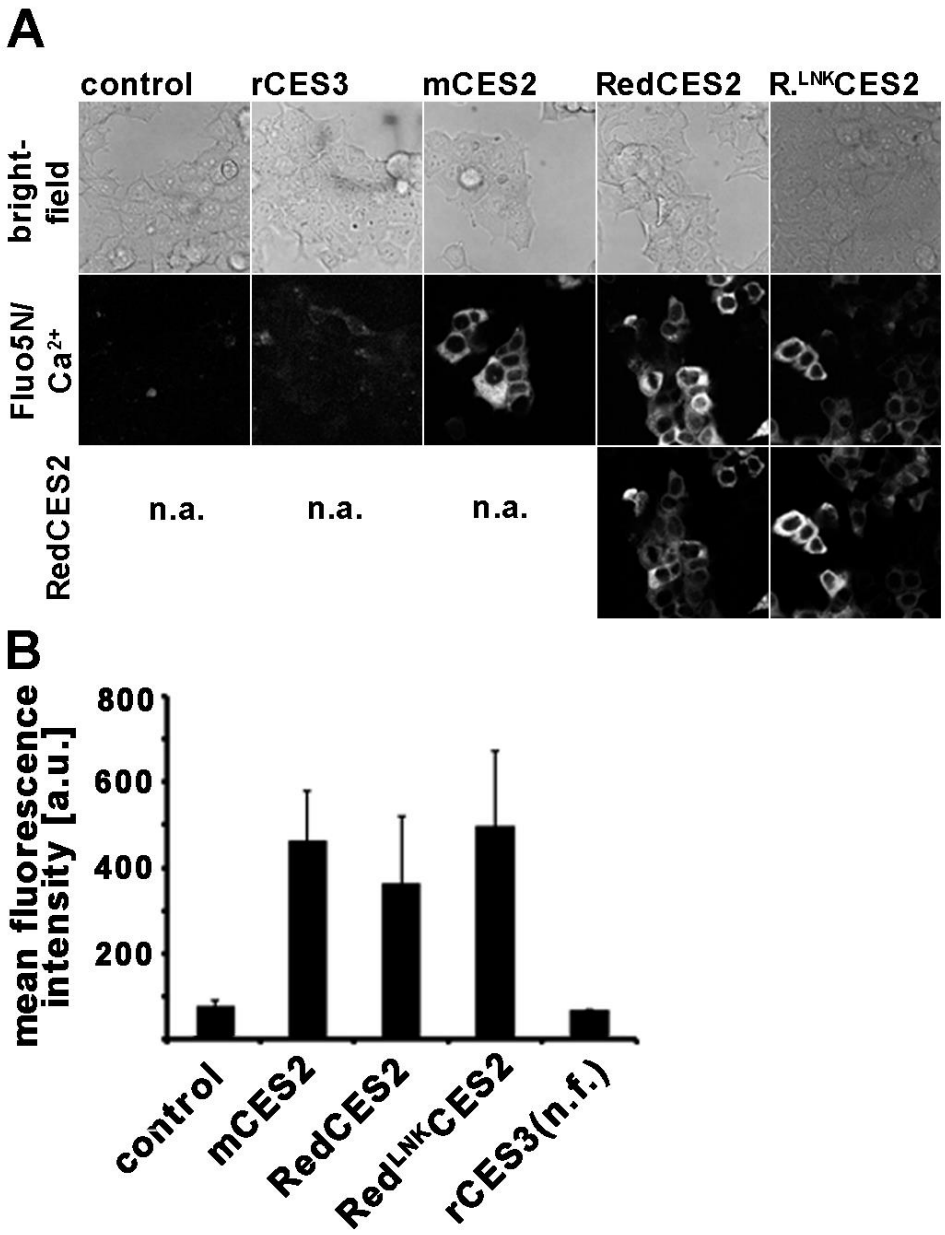

Figure 11: TED reporter performance in Fluo5N, AM conversion
HeLa cells were transfected with TED reporter plasmids and loaded with F5N, AM. For each construct 20 cells were analysed in 3 experiments. Confocal z-stacks of 10 pictures were taken at a Leica SP5

microscope. **A**) Representative pictures taken from different experiments. **B)** Bars represent the mean fluorescence of all cells of 3 independent experiments ± SEM. n.a. = not applicable; n.f. = non functional. The dye loading performance did not differ profoundly between the constructs.

3.1.5 Performance of different TED vector constructs in HeLa cells using Mag-Fluo-4, AM

Various synthetic AM calcium indicator dyes are available but most of them have a high calcium affinity (Paredes et al., 2008). For the analysis of high calcium concentration, low-affinity calcium indicators are essential. The most suitable synthetic calcium indicators for the analysis of high calcium concentrations are F5N with a K_D in the range of 90 µM, and Mag-Fluo-4, AM (MF4) with a rather low calcium affinity of ca. K_D 22 µM (http://probes.invitrogen.com/handbook/tables/0355.html (Paredes et al., 2008))**.** Therefore, MF4 is an alternative to F5N and was also used to investigate the activity of the TED vector constructs. In this experiment an Olympus confocal FX100xi81 microscope was used.

HeLa cells grown on confocal IBIDI cell culture dishes were transiently transfected with mCES2, mCES2^{OPT}, RedCES2 and Red^{LNK}CES2 or no DNA for control. Two days later, cells were loaded with 1 µM MF4, AM for 15 min and analysed. For each vector construct and independent experiment around 100 cells were scored by determining the fluorescence in 6 z-layers 2 µm apart. For mCES2, mCES2^{OPT} and RedCES2 three independent experiments were performed and for Red^{LNK}CES2 and control cells without plasmid DNA two experiments. The mean of all fluorescence values per construct were calculated and are depicted in figure 12A and 12B.

Untransfected cells showed a mean fluorescence of ca. 219 a.u. Cells expressing the mouse carboxylesterase had a higher fluorescence. mCES2 led to a fluorescence of 570 ± 97 a.u. ± S.E.M and mCES2^{OPT} to 356 ±124. RedCES2 resulted in highest fluorescence values of 901 ± 141 a.u. ± S.E.M. That is an enhancement of 4.1 fold compared to control. Contrasting to the F5N experiment, the RedCES2 construct, but not Red^{LNK}CES2 with 709 a.u. increased the fluorescence most.

The used Olympus confocal microscopic setup was also suitable to analyse cells at a resolution that allowed the visualization of subcellular organelles (figure 12C). Here, HeLa cells were transfected with RedCES2 and loaded with MF4, AM. RFP fluorescence was restricted to ER structures, but was excluded from the nucleus and a structure close to the nucleus (arrow), the prospective Golgi apparatus. The Golgi apparatus had a strong MF4 label.

This result met all requirements regarding spatial resolution. Next, experiments were performed to find out how the TED reporter constructs are expressed and localized in cultured hippocampal neurons.

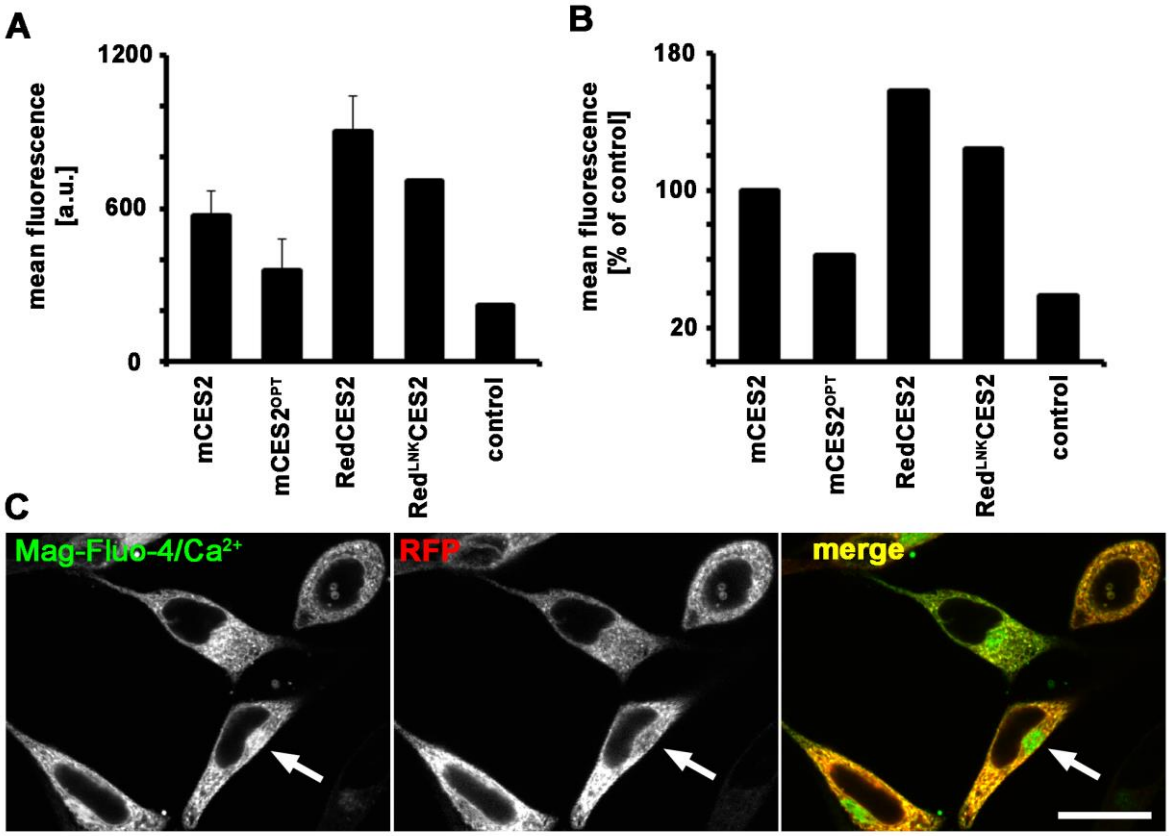

Figure 12: Performance of TED reporter proteins in MF4, AM conversion
HeLa cells were transfected with the indicated TED reporter constructs and loaded with 1 µM Mag-Fluo-4, AM for 15 min. Analysis was then performed at the confocal Olympus Fluoview1000ix81 microscope. Fluorescence of 6 z-layers 2 µm apart of 200-300 cells in total were analysed for each construct. For mCES2, mCES2^{OPT} and RedCES2 three independent experiments were performed and for Red^{LNK}CES2 and control cells (no plasmid DNA) two experiments. **A)** Mean raw fluorescence values of all cells in arbitrary units (a.u.) ± SEM. **B**) Mean fluorescence given as percent of mCES2 fluorescence as a standard. Contrasting to the F5N, AM loading performance, RedCES2 performed best leading to highest fluorescence. **C)** Confocal high resolution image of HeLa cells transfected with RedCES2 and loaded with MF4. Subcellular organelles can be visualized; the arrow points out the prospective Golgi apparatus which is MF4-positive but negative for the ER targeted RFP. Scale bar = 20 µm.

3.1.6 Expression and localization of RedCES2 in hippocampal neurons

There is compelling evidence that the ER is a continuous membranous organelle that functions as a single, calcium store (Choi et al., 2006). On the other hand some parts of the ER are known to serve as regionally restricted calcium stores, for example the spine apparatus in dendritic spines or growth cones (Goldberg et al., 2003; Higley and Sabatini, 2012; Jedlicka et al., 2008).

In order to define the localization of RedCES2 in cultured hippocampal neurons, immunocytochemical analysis was performed. For this, hippocampal neurons were infected with a lentivirus expressing RedCES2. After 15 days in vitro, RedCES2 was co-stained with Calnexin, a calcium binding protein that resides in the ER membrane under resting

conditions. Dendrites were identified by antibodies against the Microtubule associated protein 2 (Map2) and axons were identified by detection of Neurofilament, heavy chain (Nf). The anti Tau antibody used in this experiment detects the microtubule associated protein Tau in axons and dendrites. Furthermore, glutamatergic synapses were identified using antibodies directed against the presynaptic protein vesicular glutamate transporter (vGlut) and GABAergic synapses were identified with antibodies directed against the presynaptic vesicular GABA transporter (vGAT). Postsynaptic structures were identified by antibodies directed against Homer1, a protein of the postsynaptic density core scaffold structure (Andreska et al., 2014; Sugiyama et al., 2005).

As a first result, it became clear that the reporter RedCES2 protein was localized in the ER. Both, Calnexin and c-Myc labelling overlapped with Map2 positive dendrites (figure 13). This suggested a localization of the RedCES2 protein in the somato-dendritic ER lumen. The anti c-Myc antibody was well suited to detect the RedCES2 construct and did not label non-infected control cells (figure 14A1).

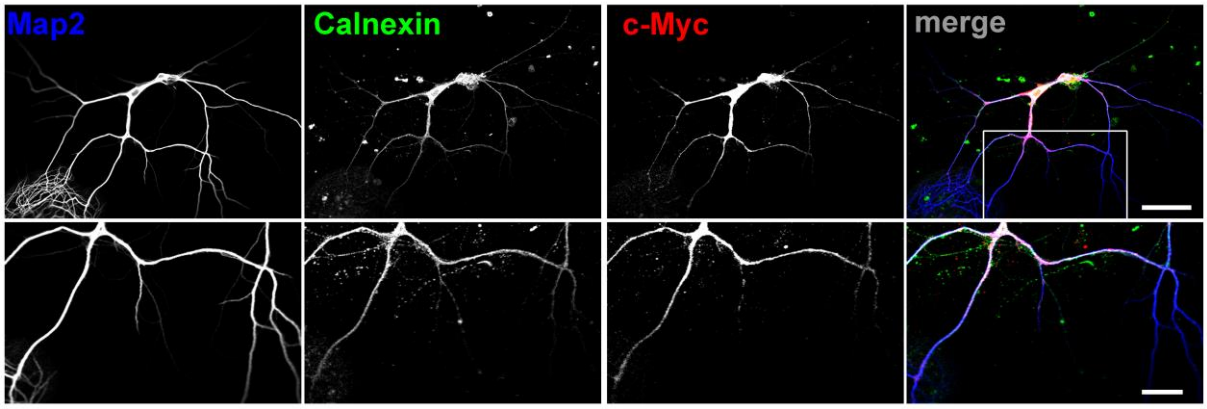

Figure 13: Detection of RedCES2 in the somato-dendritic region of hippocampal neurons
Cultured hippocampal neurons were infected with RedCES2 and used for immunostaining at DIV15. Strong overlap was observed between Map2, the ER marker Calnexin, and RedCES2, here detected wit help of anti c-Myc antibody. Upper scale bar: 50 µm, lower scale bar: 20 µm.

Next, infected neurons were stained with anti Neurofilament antibody and anti c-Myc antibody. A representative result is shown in figure 14. Here, the overlap between Nf-positive axons and the reporter protein was weak. Mostly, but not always, Nf-positive protrusions and c-Myc positive protrusions were juxtaposed to each other, but not overlapping (compare figure 14D1, D2 and D3).

Furthermore, it was investigated whether the localization pattern of RedCES2 in the somato-dendritic ER of hippocampal neurons remains stable over longer expression periods. It was important to find out whether long-term expression of RedCES2 causes RedCES2 accumulations or protein aggregates. As shown in figure 15A, RedCES2 showed no signs of

aggregates at DIV 3, 15 and 37. The red fluorescence remained evenly distributed in the somatodendritic compartments of the neurons in all age groups. However, it was noted that usage of anti Neurofilament, -Map2 and –Tau antibodies did not lead to an unambiguous distinction of axons from dendrites. Rather, axons and dendrites were usually intermingled beyond the resolution of light microscopy.

Taking all these facts into account it was concluded that the RedCES2 reporter protein has a preferential localization to the somato-dendritic part of the cultured neurons. Next, infected neurons were examined using antibodies against synaptic marker proteins. Figure 15B shows that the c-Myc labelling continued into the finest branches of Map2 positive dendrites, but was not found to overlap with postsynaptic bars positive for Homer 1 (Andreska et al., 2014). Presynaptic elements positive for vGlut and vGat were not found to overlap with RedCES2, indicating that the RedCES2 reporter does not reach pre- or postsynaptic structures, at least in cultured neurons. On the other hand, the volume of the ER in synapses is small and might therefore not contain enough protein for proper immuno detection.

Regarding the application of the RedCES2 reporter protein in calcium detection it was concluded that mainly ER calcium of somatic and dendritic regions, but not axonal or synaptic compartments is detected.

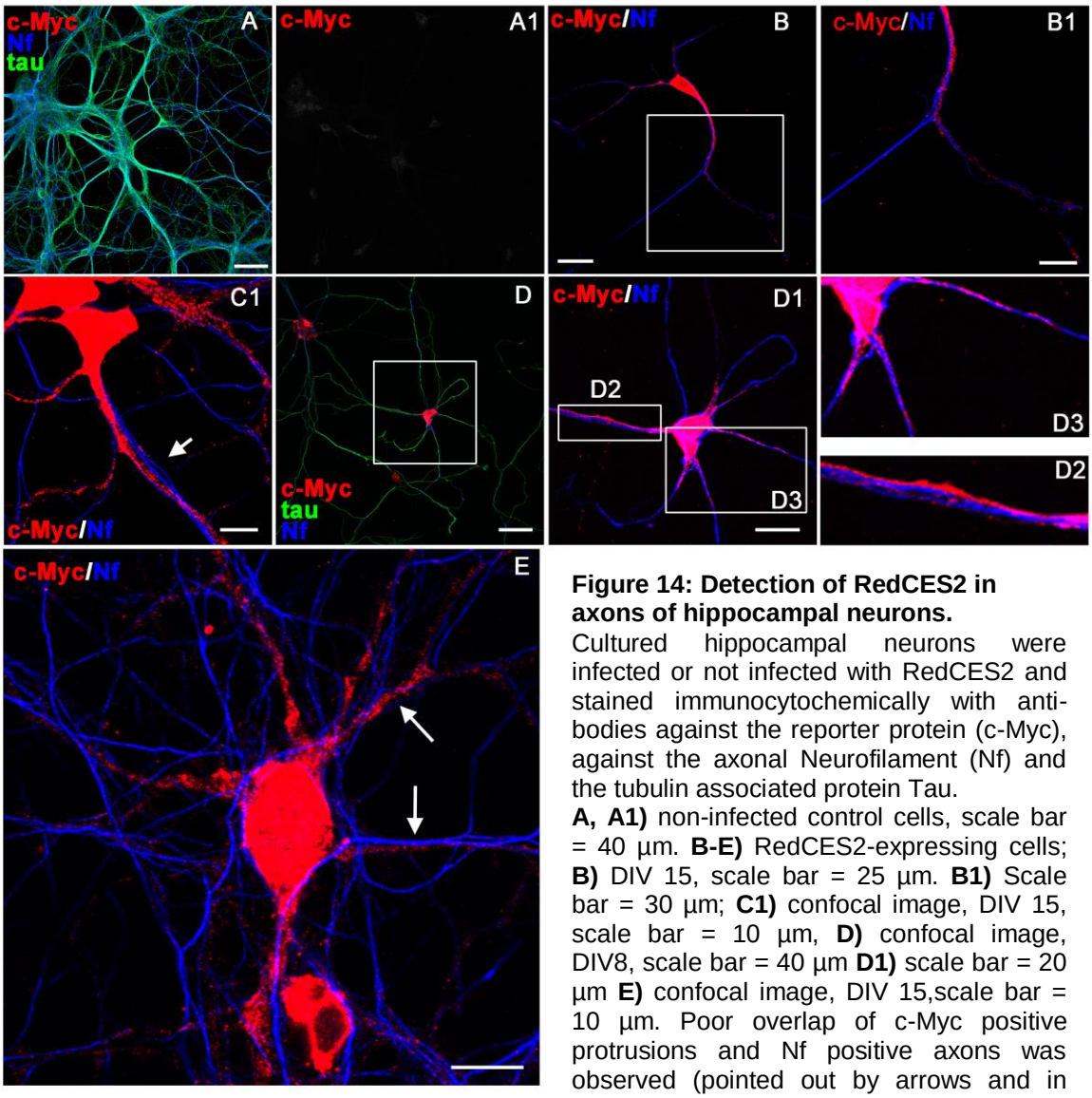

Figure 14: Detection of RedCES2 in axons of hippocampal neurons.
Cultured hippocampal neurons were infected or not infected with RedCES2 and stained immunocytochemically with antibodies against the reporter protein (c-Myc), against the axonal Neurofilament (Nf) and the tubulin associated protein Tau.
A, A1) non-infected control cells, scale bar = 40 µm. **B-E)** RedCES2-expressing cells; **B)** DIV 15, scale bar = 25 µm. **B1)** Scale bar = 30 µm; **C1)** confocal image, DIV 15, scale bar = 10 µm, **D)** confocal image, DIV8, scale bar = 40 µm **D1)** scale bar = 20 µm **E)** confocal image, DIV 15,scale bar = 10 µm. Poor overlap of c-Myc positive protrusions and Nf positive axons was observed (pointed out by arrows and in magnification D2).

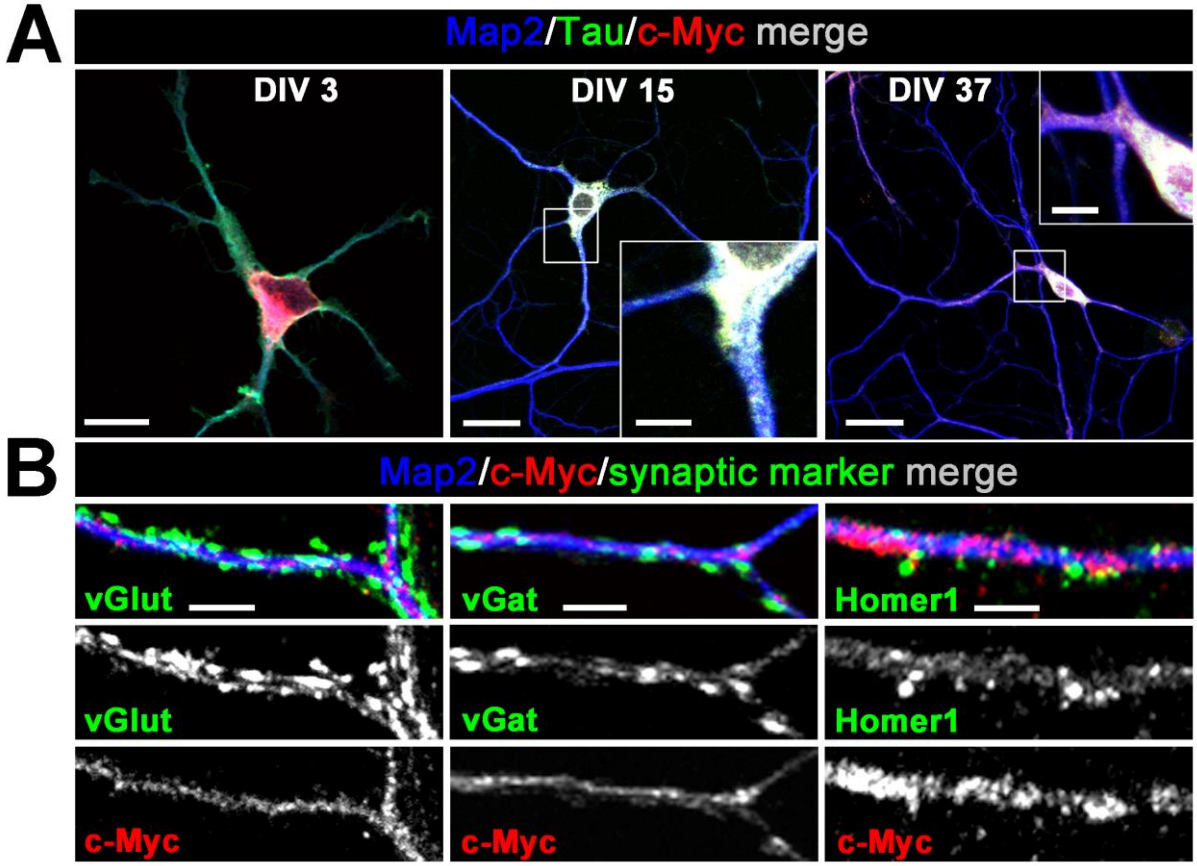

Figure 15: Detection of RedCES2 in synapses and hippocampal neurons of different age
Cultured hippocampal neurons were infected with RedCES2 and stained immunocytochemically. **A**) Neurons were labelled for Tau (axons), for Map2 (dendrites) and with anti c-Myc antibody to detect the reporter protein. The reporter protein gave a strong signal in somatic and dendritic regions of the neurons at all ages. DIV 3 scale bar = 15 µm, DIV 15 and DIV 37 scale bars 20 µm and 5 µm in inserts. Several z-layers were merged to visualize somatic and dendritic regions in one image. **B)** Immunolabelling of synapses of cultured hippocampal neurons revealed only weak signals of the TED reporter protein in synaptic structures. vGat: DIV 15, scale bar = 4 µm; vGlut: DIV 16, scale bar = 5 µm; Homer1: DIV 21, scale bar = 3 µm; confocal images.

3.1.7 Optimization of RedCES2 by usage of the CamKII promoter

In order to restrict TED-based, direct ER calcium imaging to neurons, the RedCES2 sequence was subcloned into the vector FCK, a lentiviral vector (Dittgen et al., 2004) providing the sequence of the CamKII promoter and additional sequences needed for lentiviral production. To achieve this, the RedCES2 sequence was isolated from the existing vector RedCES2 (603) of the plasmid library using the restriction enzymes AgeI and EcoRI. The DNA insert was then ligated into the FCK backbone in a directed manner, again using the restriction site for AgeI and EcoRI. The resulting vector (772) was later used to produce lentiviral particles.

Both CamKII promoter controlled and UBQ promoter controlled RedCES2 reporter proteins were used in this study. In comparative experiments it was found that the UBQ promoter is

useful to gain a high protein expression in neurons at DIV 5-12. CamKII promoter driven reporter was strongest expressed in cultures older than DIV14, although some weak expression was detectable in younger neurons. As expected, the CamKII promoter driven RedCES2 expression was restricted to neurons. Figure 16 depicts this specificity. In immunocytochemical stainings it was observed that RedCES2 expressing cells were also positive for the neuronal markers Map2 and vGlut. Furthermore, when CamKII RedCES2 transduced cells were used for live cell imaging, almost all RFP expressing cells reacted with a calcium peak upon AMPA stimulation (figure 16C).

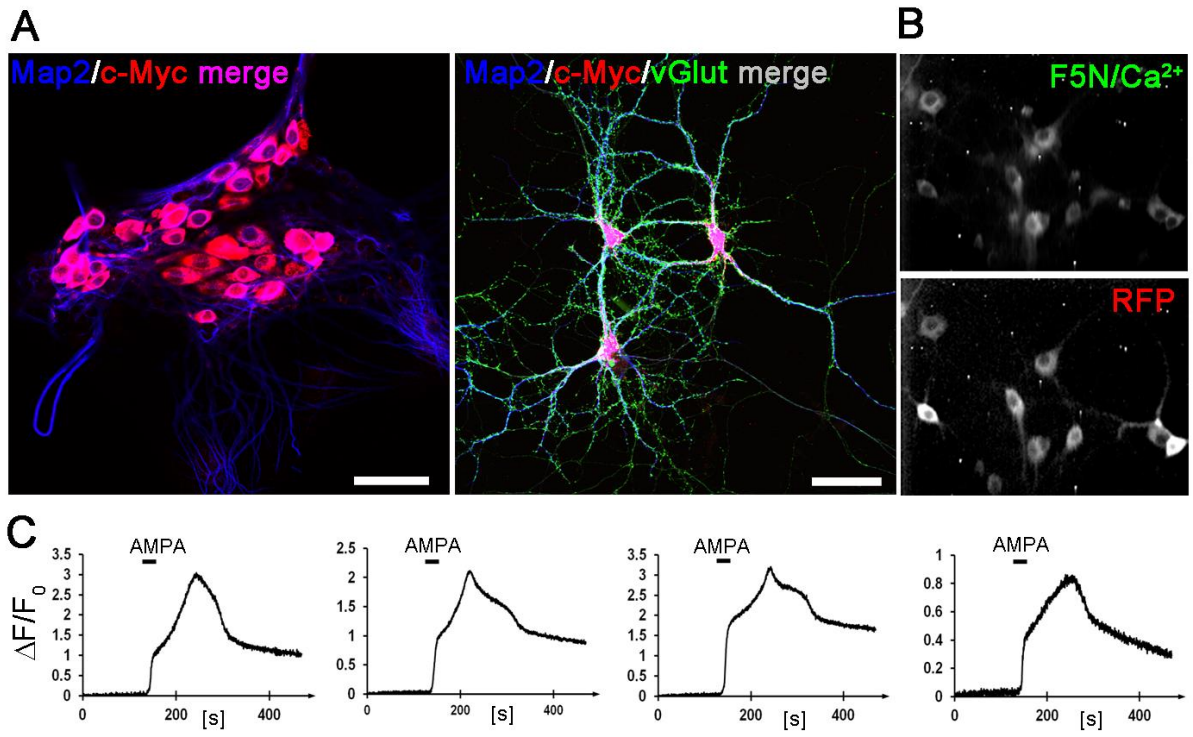

Figure 16: The CamKII RedCES2 reporter construct is specific to neurons
A) Representative immunocytochemical stainings of cultured hippocampal neurons transduced with the CamKII RedCES2 reporter construct. All cells expressing the RFP were positive for the neuronal marker Map2 and were also positive for the presynaptic marker vGlut (right picture). Left picture: scale bar = 40 µm; right picture: scale bar = 50 µm. **B)** Cultured hippocampal neurons transduced with the CamKII RedCES2 reporter construct at DIV 15 under non confocal live cell imaging conditions. The RFP expressing cells were loaded with F5N, AM and stimulated with 30 µM AMPA for 30s. All nine neurons reacted to AMPA. **C)** Single cell fluorescence curves of neurons depicted in B showing the neurons` response to AMPA. Four representative out of all nine curves are shown.

3.1.8 Optimization of RedCES2 by coexpression of the $P2Y_1$ receptor

This part of the study was conducted in collaboration with the student Hannes Hofmann and is also described in his bachelor thesis "*In vitro* investigations on endoplasmic reticulum Ca^{2+} dynamics in the course of recombinant $P2Y_1$ overexpression" (2012).

Here, the GPcR $P2Y_1$ was added to the RedCES2 construct to investigate whether a heterologous expressed receptor can be used to induce ER calcium release in neurons.

The purinergic receptor $P2Y_1$ is a G-protein coupled receptor that is expressed in glial cells and some types of neurons (Köles et al., 2011). It is activated by adenosine diphosphate (ADP) and to a lesser extent by adenosine triphosphate. Upon activation $P2Y_1$ conveys signals via activation of $G_{q/11}$ or $G_{i/0}$ proteins which activate the phosholipase C β (PLC β) in turn, leading to IP_3 production (Erb et al., 2006; Ralevic and Burnstock, 1998). For glial cells it was shown that this culminates in calcium release from the ER (Abbracchio and Ceruti, 2006).

Therefore, $P2Y_1$ was chosen to be overexpressed in the same cells as the TED reporter constructs. Activation of the receptor with ADP was expected to activate the G-protein signalling cascade which would lead to a calcium release from the ER.

In order to generate a vector construct enabling this, an internal ribosomal entry site (IRES) sequence followed by the $P2Y_1$ sequence was cloned 3´ of the RedCES2 sequence. In this way the $P2Y_1$ receptor is co-expressed in RedCES2 expressing cells, but 2 separate molecules are generated. The RedCES2 protein was expected to be localized in the ER due to its ER signalling peptide and ER retention motive and the $P2Y_1$ receptor was expected to be integrated into the membrane of cells since the native sequence was not altered.

An IRES2 sequence was amplified and BamHI restriction sites were added by performing a PCR reaction using the primers forward 5`TCGGATCCTAGAATTC CCGCTACGTAAATTCC 3` (underlined EcoRI site and BamHI site) and reverse 5`ATGGATCCGGTTGTGGCCATATTATCATCG 3` (underlined BamHI site). The PCR product was restricted with BamHI and purified. Next, the resulting insert was ligated into the BamHI site of the vector pcDNA-CMV-His-P2Y1-HA (kind gift from Prof. Dr. Carsten Hoffman, Würzburg; plasmid library 775), which resulted in an intermediate IRES2-His-P2Y1-HA cassette (787 in the plasmid library). The complete insert coding for IRES2-His-tag-P2Y1-HA-tag was isolated from the intermediate product using EcoRI and cloned into the EcoRI site of FUGW-RedCES2 (712 of the plasmid library). Clones bearing the correct insert orientation were selected using restriction digestion and the sequence was partially confirmed via DNA sequencing. An outline of the resulting construct (result: 786) is given in figure 17A.

In order to investigate the proteins expressed by this new plasmid, HEK293T cells were transfected using the lipofectamine method and stained immunocytochemically using antibodies directed against the c-Myc-tag of the RedCES2 protein, and the HA-tag of the $P2Y_1$ receptor. Nuclei were detected using Dapi reagent. Figure 17B shows a representative image.

As expected, the RedCES2 protein showed an ER-like staining pattern, whereas the $P2Y_1$ receptor was localized at the margins of the cells, conceivably the plasma membrane.

Furthermore, cultured primary neural cells were transduced with this expression construct and stained immunocytochemically. Neurons were detected by using a Map2 antibody, the $P2Y_1$ receptor was detected by an anti HA-tag antibody and the RedCES2 protein was detected by its red fluorescence. It was observed that in glial cells, which were negative for Map2, the $P2Y_1$ protein was located to the margins of the cells and the RedCES2 protein was located in the centre, comparable to HEK293T cells. In Map2 positive neurons the $P2Y_1$ immunoreactivity was distributed like the RedCES2. However, contrasting to Hek293T and glial cells neurons are not spread out flat and it is therefore not possible to conclude on the exact localization of the $P2Y_1$ protein in this experiment.

Under live cell imaging conditions (figure 17C) neurons transduced with the new construct could be loaded with F5N, AM, but it remained unclear whether these cells were reactive to ADP. The functional verification of the $P2Y_1$ construct remains open for future studies.

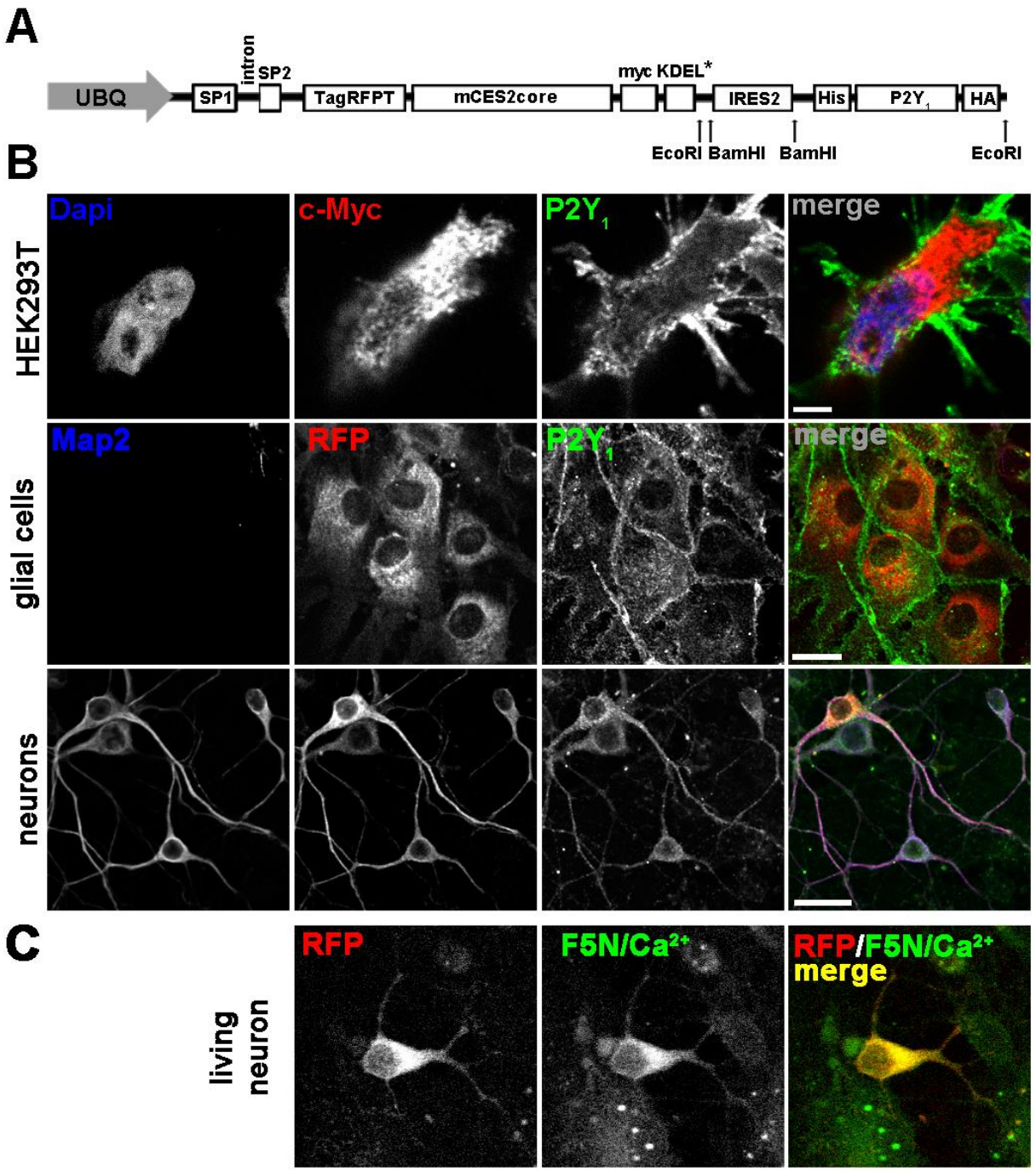

Figure 17: Cloning and application of the RedCES2-IRES2-P2Y$_1$ reporter construct
A) Scheme of the RedCES2-IRES2-P2Y$_1$ reporter sequence. **B)** Transfected HEK293T cells (upper row, picture taken by H. Hofmann), transduced primary glial cells (middle) and transduced primary hippocampal neurons (lower row) expressing the UBQ RedCES2-IRES2-P2Y$_1$ construct were stained immunocytochemically using antibodies against Map2 to identify neurons, antibodies directed against the HA-tag to identify the P2Y$_1$ receptor and antibodies against the c-Myc tag to identify the RedCES2 protein. Cell nuclei were identified with Dapi staining. **C)** Cultured hippocampal neurons, transduced with the RedCES2-IRES2-P2Y$_1$ reporter construct, could be loaded with Fluo5N, AM and were analysed under live cell imaging conditions.

3.1.9 Performance of various synthetic calcium indicators with TED

Previous results showed that the RedCES2 TED vector construct had a carboxylesterase activity sufficient to increase calcium indicator conversion in the ER of cells. In addition, it seemed that by usage of MF4 with HeLa cells it was possible to visualize ER calcium (figure 12C). It was therefore next examined what calcium indicator can best be applied to visualize ER calcium in cultured hippocampal cells.

In order to find the most suitable calcium indicator for TED, three common AM dyes were compared including the low affinity calcium indicators F5N and MF4. For this, cultured hippocampal neurons were incubated for 15 min in ACSF containing 5 µM of the respective AM dye: Fluo5N, AM, Mag-Fluo-4, AM and Mag-Fura-2, AM (MF2). Oregon Green 488 BAPTA-1, AM (OGB1) has a very high affinity to calcium and was therefore not included in this experiment (see figure 22 for Oregon green staining of neurons). For each AM dye, one coverslip bearing RedCES2 infected neurons and one cover slip bearing uninfected control neurons were used.

The cells were examined for brightness and calcium indicator localization at the confocal Olympus Fluoview microscope and representative pictures are shown in figure 18.

MF2 strongly labelled both infected and uninfected neurons. The largest proportion of indicator was present in the cytosol and nucleus. MF2 was therefore excluded as a potential candidate to use for TED.

MF4 (K_D = 22µM) showed a preferential localization to the ER. Remarkably, this was observed in infected and uninfected control cells. MF4 can therefore potentially be used to monitor ER calcium in resting neurons. However, using HeLa cells and higher magnification it was observed that MF4 accumulated in a structure with Golgi-like features (figure12C). Another drawback of MF4 is its higher calcium affinity. It bears the risk to detect cytosolic calcium signals, especially after activation of neurons by e.g. glutamate and AMPA that lead to a rise in cytosolic calcium concentration. In addition, subtle changes in ER calcium might not be detected or the drop in fluorescence could be delayed.

The best result was obtained with Fluo5N, AM. It has a low calcium affinity (K_D = 90 µM) and only labelled infected neurons. Because uninfected neurons were not labelled, the risk of detecting cytosolic calcium is low. In addition, Fluo5N was accumulated in the ER of the neurons which made it ideally suited for TED imaging of ER calcium in neurons, as described earlier (Jaepel and Blum, 2011; Rehberg et al., 2008).

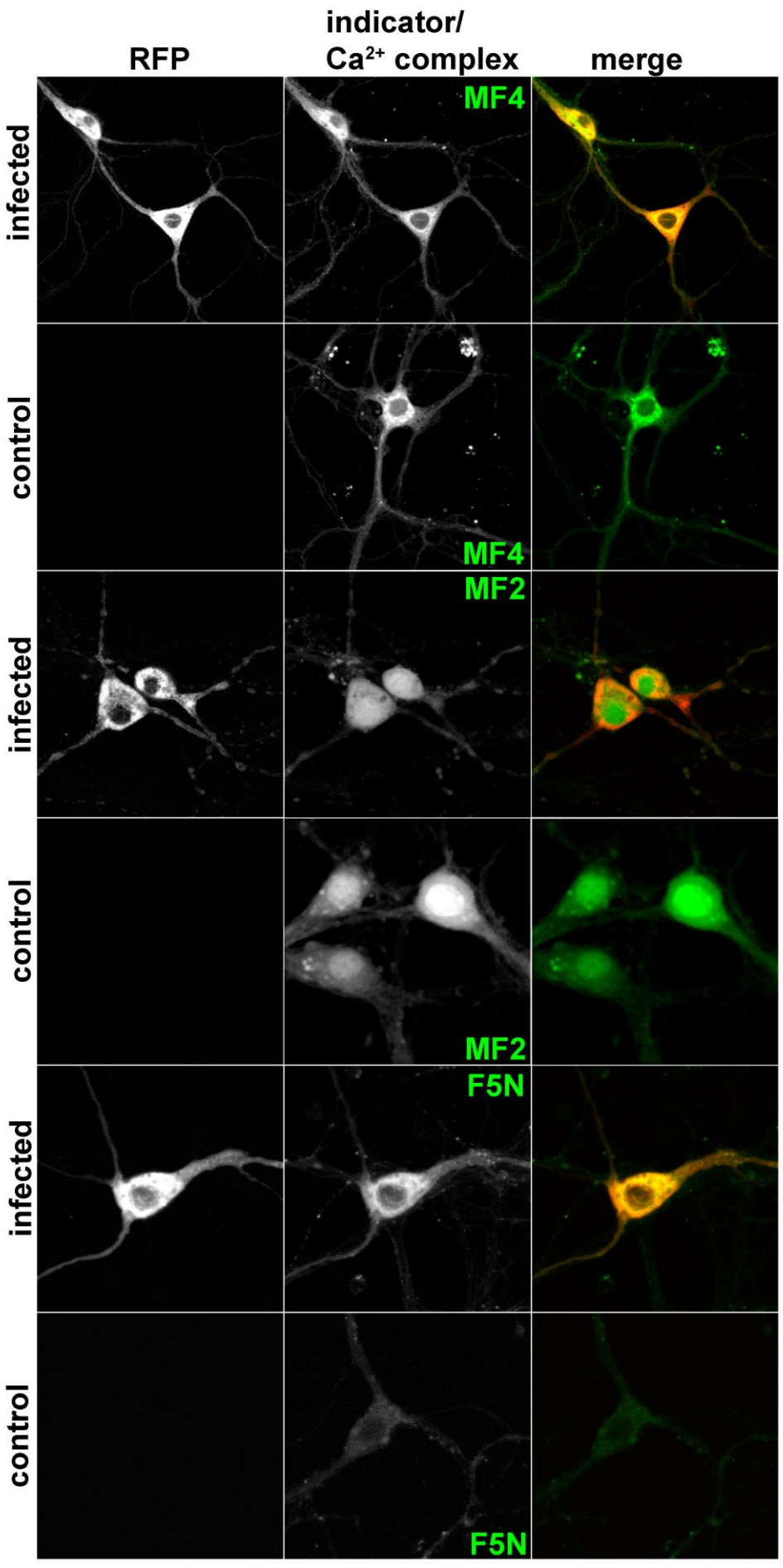
RFP
indicator/
Ca2+ complex
merge
infected
MF4
control
MF4
infected
MF2
control
MF2
infected
F5N
control
F5N

Figure 18: Comparison of synthetic calcium indicators potentially used with TED
Both RedCES2 infected and uninfected control neurons were loaded with either of the calcium indicator dyes Mag-Fluo-4, AM (MF4), Mag-Fura-2, AM (MF2) or Fluo5N, AM (F5N). The cells were then examined using a confocal laser scanning microscope. Fluo5N is the most suitable calcium indicator dye because it provides a bright label of ER calcium under resting conditions, and has the lowest affinity for calcium in comparison to other available low-affinity calcium indicators such as MF4.

3.1.10 Optimization of RedCES2 by using the Thy1.2 promoter and generation of transgenic Thy1.2 RedCES2 mouse lines

It was examined whether RedCES2 expression under control of the mouse Thy1.2 promoter would be beneficial for the generation of a transgenic mouse line. This promoter is known to drive expression of the transgene only in neurons (Feng et al., 2000). Although the exact expression pattern seems to vary among different Thy1.2 mouse lines, it was reported that the Thy1.2 promoter is mainly active in principal neurons of the central nervous system, i.e. pyramidal cells of the hippocampus and projection neurons (Caroni, 1997; Deguchi et al., 2011; Feng et al., 2000; Porrero et al., 2010). In addition, it was reported that in all transgenic mouse lines created with the Thy1.2 promoter, expression of the reporter proteins was strong in hippocampal areas and was found in somatic, axonal and dendritic regions of the expressing neurons (Feng et al., 2000; Guoping Feng et al., 2000; Hirrlinger et al., 2005). Although expression of the respective reporter protein in these studies was mainly found to start at postnatal stages, i.e. P6 - P10 in mice, at least one study found earlier expression in some neuronal tissues (Campsall et al., 2002).

The RedCES2 construct was cloned into the Thy1.2 vector that was originally published by Pico Caroni (Caroni, 1997). The RedCES2 reporter sequence was isolated from plasmid 772 from the AG Blum plasmid library using the restriction enzymes AgeI and EcoRI and blunt-end cloned into the XhoI site of the Thy1.2 vector (vector and map kind gift from P. Caroni lab, Zürich). In the Thy1.2 gene the exons Ia, Ib, parts of II and IV contain regulatory sequences, whereas parts of exon II, exon III and parts of exon IV comprise the protein coding sequence. By using the XhoI restriction site the RedCES2 sequence, from Kozak sequence to stop codon, replaces the entire sequence coding for the Thy1 protein (Caroni, 1997).

Figure 19 shows in A the original construct published in 1997 and in B the vector map in which the RedCES2 construct was cloned into the XhoI site. The insert orientation was determined by restriction digestion and sequencing. To check whether the clone was indeed able to lead to RedCES2 expression in hippocampal neurons, the plasmid was transfected into hippocampal neurons. Figure 19C shows representative pictures of cultured hippocampal neurons at DIV12 that were transfected at DIV2 with the calcium chloride method. The cells were stained with 5 µM Fluo5N, AM for 15 min und observed under a cell culture microscope. Compared to the control cells transfected with the CamKII RedCES2

vector construct, no difference was observed regarding RFP expression or dye loading. In transfected neurons RFP and Fluo5N fluorescence was observed in all regions of the cell but the nucleus .This clone was therefore chosen for pronucleus injection in order to generate a transgenic mouse line.

To this end the plasmid was cut with the restriction enymes PvuI and EcoRI and the insert was isolated and purified (see 2.3.4 in methods part). The DNA was then sent to the transgenic unit of the Institute of Molecular Genetics, academy of sciences of the Czech republic (ASCR) were it was injected into the pronucleus from oocytes of mice from the C57BL/6N strain. The DNA from the founder mice was analysed using a PCR reaction with primers directed against the TagRFP-T sequence. Mice that were positive for the transgene showed a DNA band of 188 bp on an agarose gel (figure 7) and were chosen for further breeding.

A

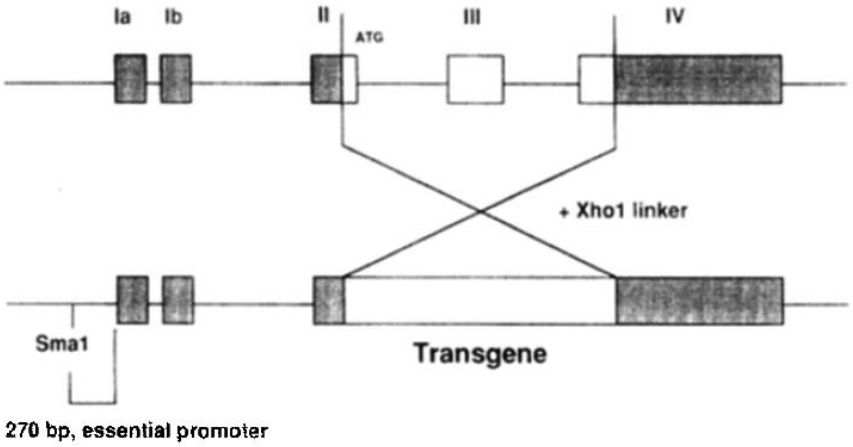
Ia
Ib
II
ATG
III
IV
+ Xho1 linker
Sma1
Transgene
270 bp, essential promoter

B

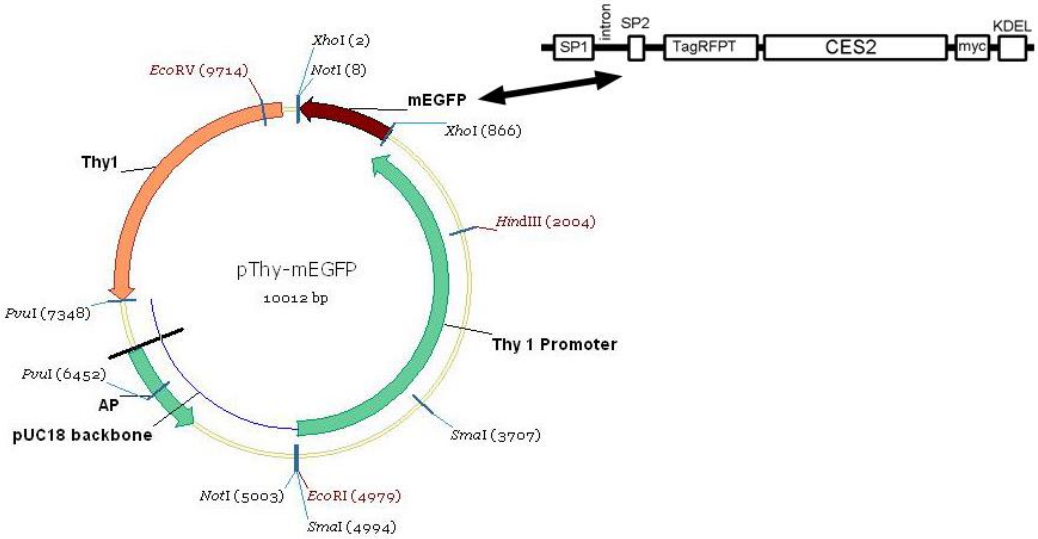
intron
SP2
SP1
TagRFPT
CES2
myc
KDEL
XhoI (2)
EcoRV (9714)
NotI (8)
mEGFP
XhoI (866)
Thy1
HindIII (2004)
pThy-mEGFP
10012 bp
PvuI (7348)
Thy 1 Promoter
PvuI (6452)
AP
pUC18 backbone
SmaI (3707)
NotI (5003)
EcoRI (4979)
SmaI (4994)

C

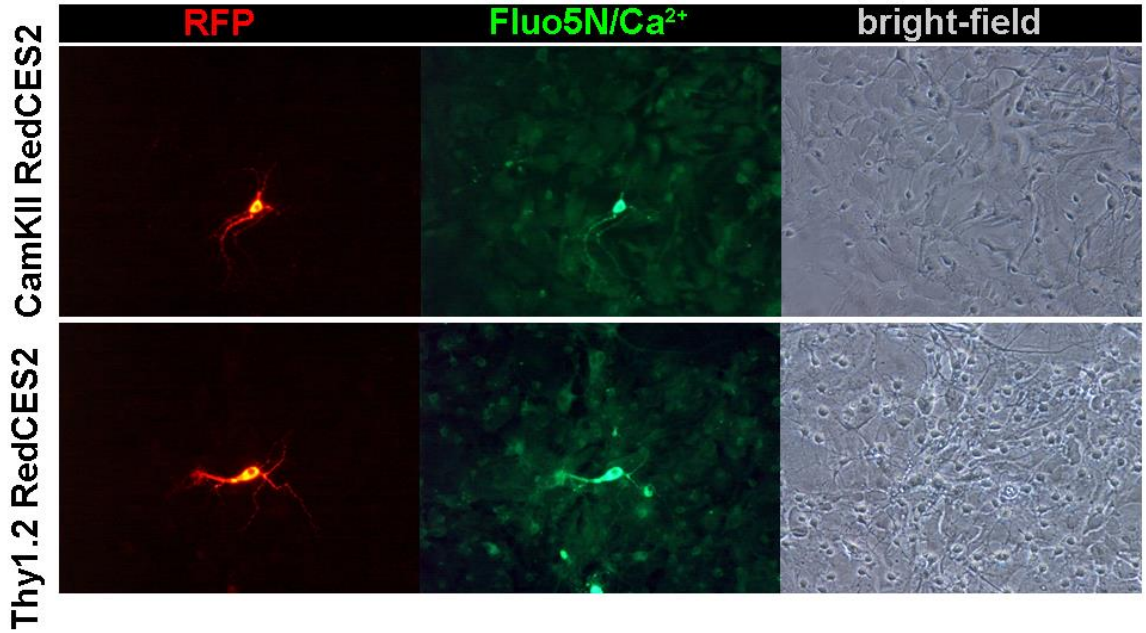
RFP
Fluo5N/Ca2+
bright-field
CamKII RedCES2
Thy1.2 RedCES2

Figure 19: Cloning and analysis of the Thy1.2 RedCES2 construct.
A) Scheme of the Thy1.2 expression construct, from (Caroni, 1997). **B)** Vector map of the Thy1.2 vector used to generate transgenic mouse lines. The RedCES2 construct was cloned into the XhoI site. **C)** Cultured hippocampal neurons were transfected with Thy1 RedCES2 or CamKII RedCES2 as a control. Living cells were then loaded with F5N, AM. Both vectors led to a similar expression of the RedCES2 protein and similar F5N fluorescence 10 days after transfection**.**

3.1.11 Analysis of a Thy1.2 promoter-driven RedCES2 founder mouse

With pronucleus injection techniques, seven Thy1.2 promoter-driven RedCES2 mouse lines (Thy1::RedCES2) were obtained by the TGU Prague and were transferred to the animal house of the Institute for Clinical Neurobiology. Unexpectedly, individual Thy1::RedCES2 lines showed a reduced life span and showed pronounced hindlimb clasping, indicating neurological/motor impairments in individual strains. The reason for this phenotype is not clear, yet. To find out whether the Thy1::RedCES2 mice showed the expression of the corresponding gene fragment individual mice were perfused and fixed with 4% PFA, the brain was dissected, embedded in 6 % agarose and 40 µm brain slices were prepared with a vibratome and kept in cryoprotection solution at 4°C. Later, immunohistochemical stainings were performed. The ER was detected by an anti Calnexin antibody, neurons were labelled by anti Map2 staining, and endogenous red fluorescence of RedCES2 was used to identify neurons expressing the transgene. Nuclei were labelled by Dapi (figure 20). Generally, RedCES2 reporter expression was strong in Map2-positive neurons. Higher magnification revealed that the endogenous RedCES2 fluorescence showed a pronounced overlap with the ER specific Calnexin immunoreactivity. The RedCES2 reporter signal was pronounced in the somatic area of the pyramidal neurons in the Cornu ammonis (CA) 1 region of the hippocampus. In the CA3 region the red fluorescence was also found to be pronounced in the dendrites of the pyramidal neurons that extend into the molecular layer (see inlet in figure 20A CA3).

This analysis only confirms the expression of the RedCES2 in this transgenic strain. To obtain enough transgenic animals for a more detailed analysis, establishment of a Thy1::RedCES2 pedigree was started.

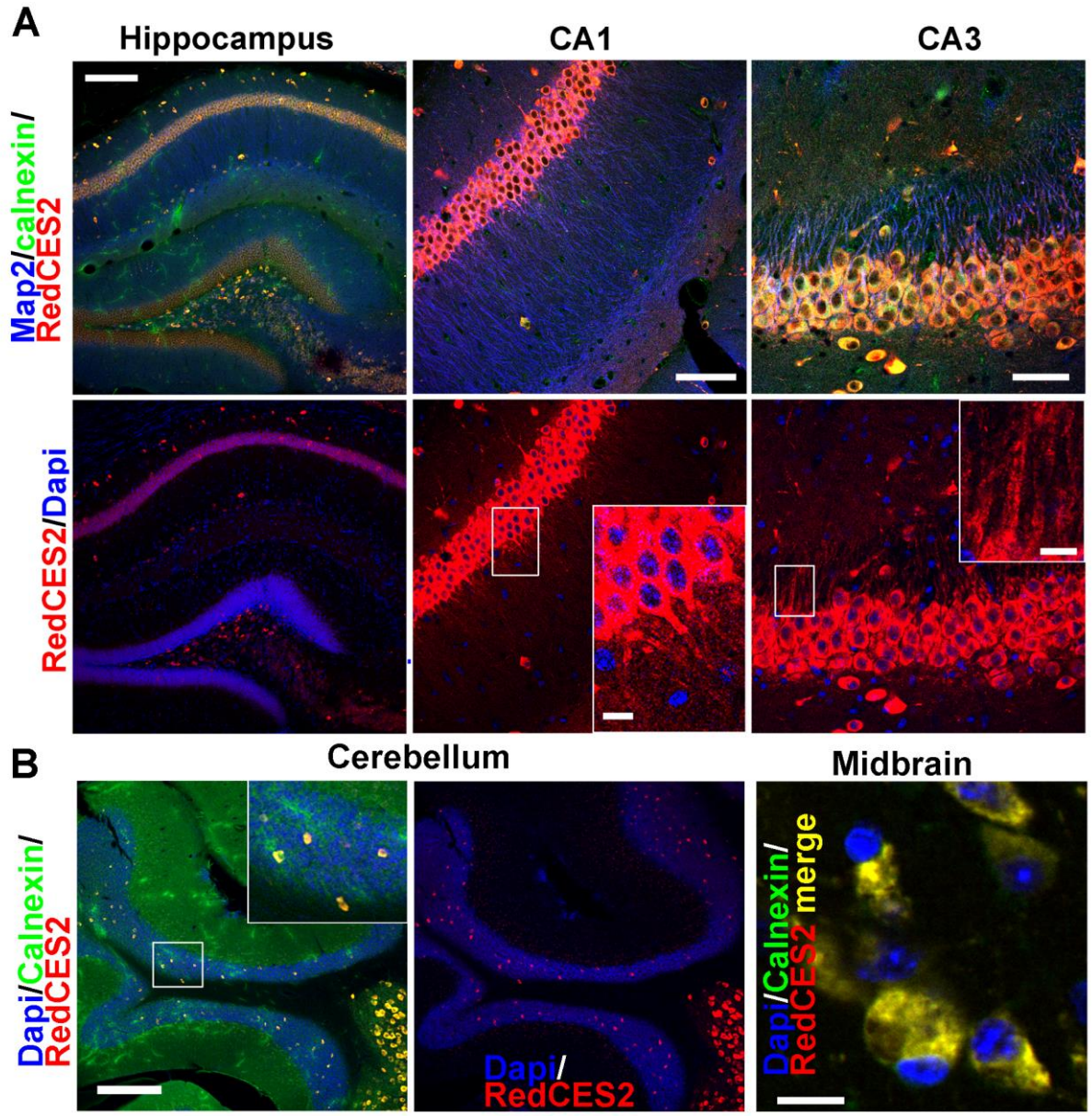

Figure 20: Thy1::RedCES2 transgenic founder mice
A and B) Immunohistochemical staining of brain slices from founder 145IV #23389. The mouse was perfused and fixed with 4% PFA, and brain slices were prepared and stored in cryo-protection solution. Expression of the RedCES2 reporter protein (endogenous fluorescence) was detected in most areas of the brain. **A)** Scale bars represent in the overview picture (left) 200 µm, in the CA1 (middle) 70 µm and in the insert 10 µm, in the CA3 (right) 50 µm and in the insert 10 µm. B) Scale bar represents in the overview pictures 200 µm and in the higher magnification of the cells 10 µm. Overlap between the ER marker Calnexin and the reporter protein RedCES2 was observed.

3.1.12 Optimization of RedCES2 by usage of the GFAP promoter for glial cells

It was shown that TED is well suited to analyse the ER calcium dynamic in astrocytes (see result 3.3.6 (Blum et al., 2010; Jaepel and Blum, 2011). In order to start the generation of a transgenic mouse model expressing RedCES2 under control of a glial cell-specific promoter, RedCES2 was cloned under the control of a human GFAP promoter (Hirrlinger et al., 2005).

The *gfap* gene codes for the glial fribrillary acidic protein (GFAP), an intermediate filament protein and usage of the human GFAP promoter restricts transgene expression to astrocytes (Hirrlinger et al., 2005).

This part of the project was conducted in collaboration with the student Klara Thein and the hGFAP plasmid backbone was a gift from Dr. Anja Scheller, Institute for Physiology, University of Saarland. A scheme of the plasmid map and cloning step are depicted in figure 21A.

The original plasmid (819 in plasmid library) was restricted using the enzymes EcoRI and AgeI to remove the RFP insert and the RedCES2 insert, equally restricted with EcoRI and AgeI, was ligated into it. One clone was selected by further restriction digestion and sequencing (plasmid 839 in AG Blum plasmid library).

In order to examine the performance of the new construct, primary glial cells were transfected with the lipofectamine procedure (see methods) and stained immunocytochemically. The RedCES2 reporter protein was detected using an anti c-Myc antibody, astrocytes were identified using an anti GFAP antibody and cells from the oligodendrocyte lineage were detected using an anti Ng2 antibody. Figure 21B shows two representative pictures from this analysis. Cells expressing the RedCES2 protein were positively labelled for GFAP, but not Ng2, thus identifying these cells as astrocytes, as expected. However, it still needs to be examined whether astrocytes transfected or transduced with this GFAP RedCES2construct can be loaded with F5N, AM and used for live cell imaging.

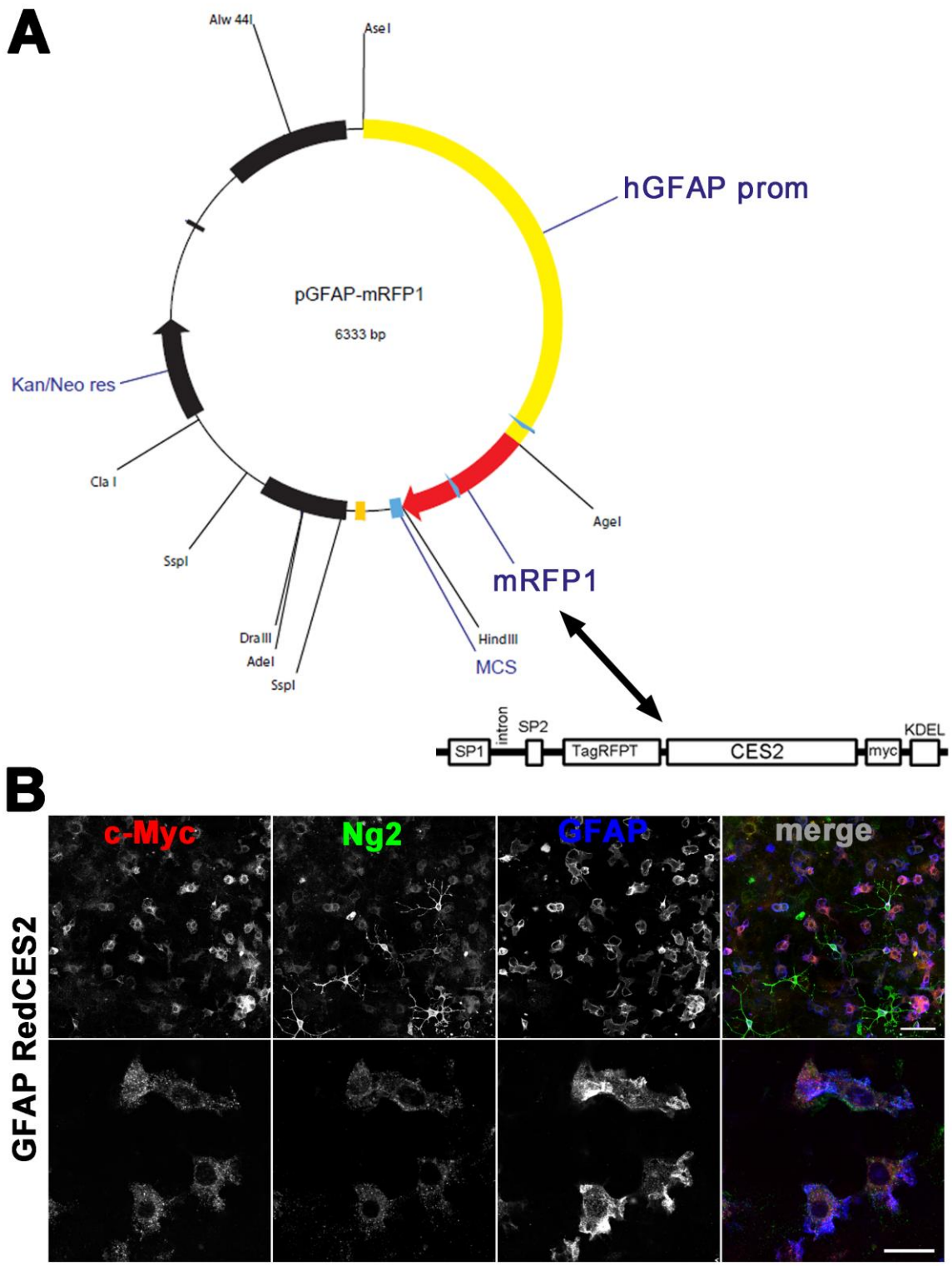

Figure 21: Cloning and expression of the GFAP RedCES2 construct
A) Vector map of the GFAP expression construct from A. Scheller and the RedCES2 insert that was cloned to replace the mRFP1 sequence. **B)** Cultured glial cells transfected with the GFAP RedCES2 construct were immunocytochemically stained with anti Ng2 antibodies to identify cells from the oligodendrocyte lineage and anti GFAP antibodies to identify astrocytes. The RedCES2 protein was detected with anti c-Myc antibodies. The RedCES2 protein was detected in GFAP positive astrocytes. Upper scale bar = 50 µm, lower scale bar = 20 µm.

3.2 Establishing ER live cell calcium imaging in cultured neurons

3.2.1 Visualization of free calcium in the ER and cytosol of neurons

In order to investigate the ER calcium dynamics in neurons, primary hippocampal neurons were transduced with lentiviral vectors encoding RedCES2 and incubated in Fluo5N, AM. In order to visualize the cytosolic calcium content non-infected cultured neurons were incubated in Oregon Green 488 BAPTA-1, AM (OGB1). As depicted in figure 22, OGB1 labelling was stronger than F5N, was localized to all areas of the neurons, and fluorescence signals were strongest in the nuclear region. F5N labelling was localized to all areas of the cell but the nucleus and localized with the fluorescence of the TagRFP-T from the reporter protein.

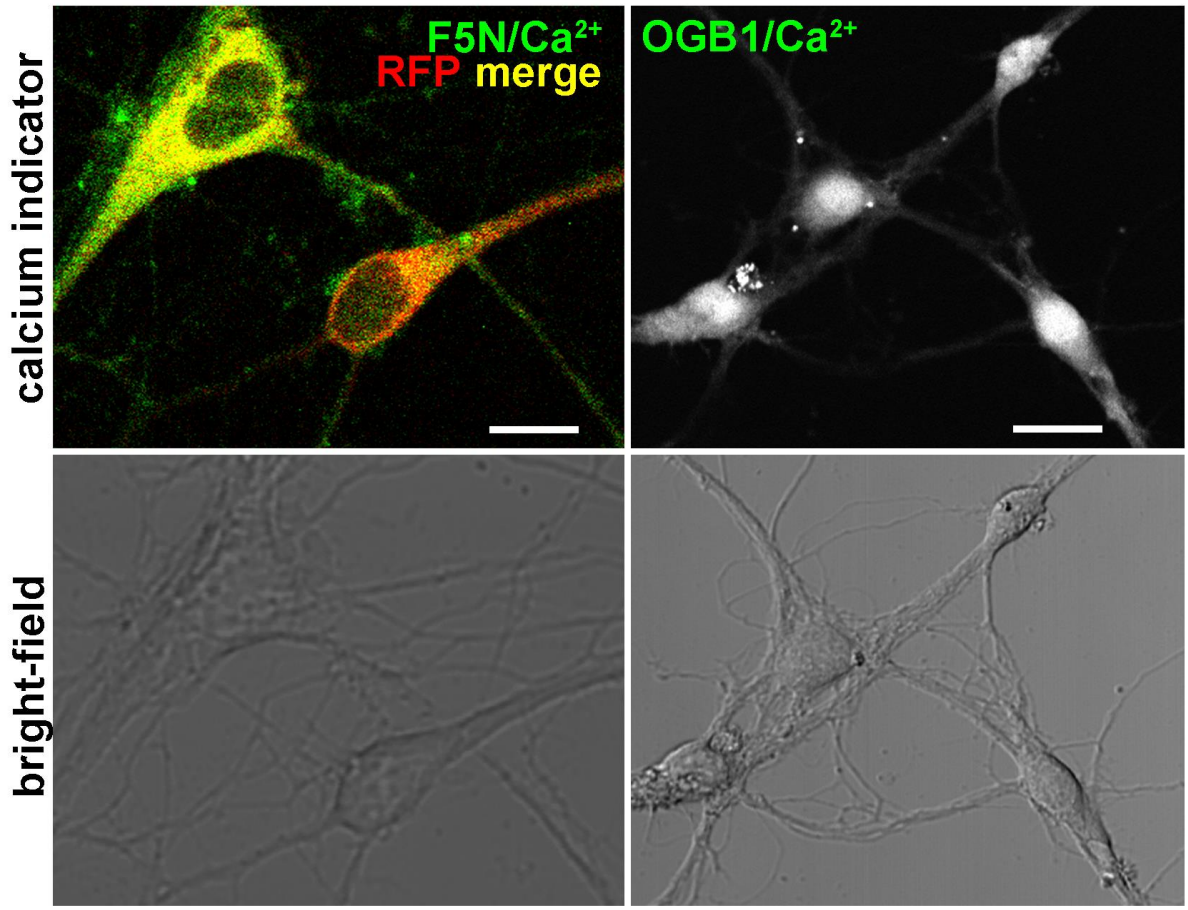

Figure 22: Comparison of cytosolic and ER calcium imaging
Left: Cultured hippocampal neurons were infected with RedCES2 and incubated with Fluo5N, AM to visualize the ER calcium. Confocal image; scale bar = 10 µm. Right: Non-infected control cells were incubated in Oregon Green 488 BAPTA-1, AM to visualize the cytosolic calcium. Non-confocal image; scale bar = 20 µm.

3.2.2 Live cell ER calcium imaging in hippocampal neurons during stimulation

Next, TED imaging was used in order to visualize ER calcium signals that were evoked by stimulation of neurons. For this, the neurons were treated as described before for TED

calcium imaging and mounted in a live cell setup. Different agonists were applied by perfusion with ACSF containing the agonist. Figure 23 depicts results obtained that exemplify some issues that were observed occasionally. In figure 23A neurons showing a perfect ER localization of the F5N dye (in green) were stimulated with 90 mM potassium. This depolarizes neurons and leads to an influx of calcium via Ca_vs. After the stimulation it was observed that the F5N dye also gave a strong signal in the nuclear region suggesting a non ER derived calcium signal. Interestingly, this phenomenon occurred only in those cells that were recorded during the stimulation but not in the surrounding cells, as pointed out by the arrow. It was concluded that the excitation light but not the stimulation itself was the cause of this effect. Therefore, for consecutive experiments the excitation light was drastically reduced which indeed nearly completely abolished this effect.

However, a similar problem was sometimes observed when neurons were strongly stimulated with agonists like glutamate, AMPA, kainate or a high potassium concentration which all lead to a massive influx of calcium into the cytosol. It was observed occasionally (figure 23B example 1 compared to example 2) that strong stimulation led to an increase in fluorescence in both the perinuclear, i.e. ER, and nuclear compartment of the neuron. After 1-2 min, the nuclear level decreased again. It is possible, that cytosolic calcium levels jumped to a concentration high enough to be detected by cytosolic F5N for this short time window. Alternatively, some ER structures of the nuclear region became visible that are usually not detected, possibly because of a very low calcium content. More experiments are needed in order to clarify the nature of this effect.

In order to verify that F5N is mainly converted and hold within the ER, cell membranes were permeabilized with the ionophore ionomycin. After treatment of F5N labelled cells with 10 µM ionomycin for several minutes (figure 23C) the neurons lost their ER label and the cytosol became visible. This demonstrates that some F5N is converted in the cytosol and that a strong calcium influx is necessary for the formation of fluorescent F5N/Ca^{2+} complexes in the cytosol. Under normal resting conditions the cytosolic F5N/Ca^{2+} is not detected.

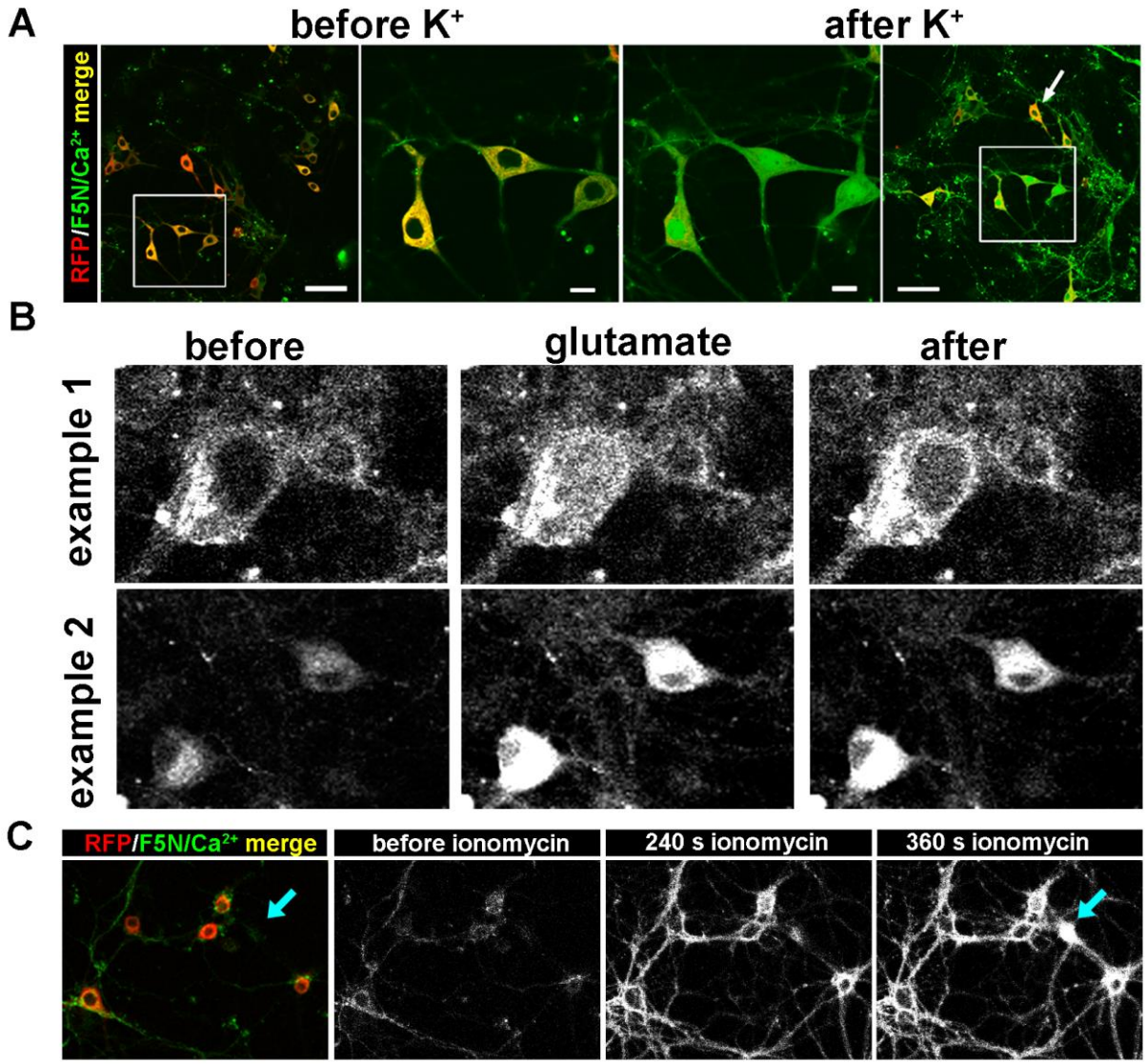

Figure 23: TED using RedCES2 and Fluo5N, AM in hippocampal neurons
Initial experiments in which cultured hippocampal neurons were infected with RedCES2 and loaded with Fluo5N, AM revealed potential advantages and disadvantages with TED. Live cell imaging was performed at a confocal microscope. **A)** In some experiments it was observed that the ER calcium label was lost after strong illumination. Before stimulation with potassium, the calcium labelling was restricted to the ER regions (left) but after stimulation, the nucleus became labelled. In contrast, the effect was not observed in neurons that were not illuminated, but also stimulated (arrow). **B)** Pictures taken from two representative TED movies. In example 1 100 µM glutamate were applied which led to detection of fluorescence signals in the nuclear region in addition to a calcium rise in the ER. In example 2 200 µM glutamate were applied. Here, the nuclear region of the cells remained dark and only ER calcium levels were detected. **C)** Fluo5N loaded cells were treated with 10 µM of the ionophore ionomycin. Only after membrane permeation did the cells show a bright cytosolic fluorescence signal. The non-infected cell (cyan arrow) became only visible at the very end of the experiment.

3.2.3 Activation of ryanodine receptors using caffeine

Neurons possess RyR in the ER membrane which can conduct calcium release signals from the ER. Three types of RyR receptors, RyR1, RyR2 and RyR3 were detected in the hippocampus of mice (Galeotti et al., 2008) and RyR3 was found to be functionally expressed in hippocampal neurons (Lanner et al., 2010). In (Seymour-Laurent and Barish,

1995) the localization of RyR receptors within cultured hippocampal neurons was described. RyRs were found in all regions of the neurons but fine dendrites. However, this study did not distinguish between RyR isoforms.

RyR are known to be activated by caffeine in neurons (Beck et al., 2004; Korkotian and Segal, 1999; McPherson et al., 1991; Seymour-Laurent and Barish, 1995) and therefore caffeine was used to generate calcium release signals from the ER of neurons. TED calcium imaging was applied to neurons at DIV 6-21 and ACSF containing 40 mM caffeine was applied for 1-2 min and ER calcium levels were analysed for the somatic and dendritic regions separately (figure 24A1 and A2). In some experiments it was observed that application of glutamate or potassium to neurons increased the ER calcium levels (figure 24C) suggesting that the ER of neurons might not *per se* be full with calcium. Therefore, a short pulse of 10-20 mM potassium was given to the neurons before caffeine in order to "load" the ER if necessary. Indeed, potassium elicited an increase in calcium in some ROIs but not in others (see results 3.3 1 and figure 25 for potassium "precharging"). As figure 24 depicts, caffeine led to a decrease in ER calcium and no major difference was observed between somatic (figure 24A1) and dendritic (figure 24A2) ROIs. This potassium-caffeine protocol led to results comparable to the ones shown here in 12 experiments with 2-6 neurons each. When the same experimental protocol was applied to neurons loaded with MF4 a peak in fluorescence was observed upon potassium application and a drop in fluorescence during caffeine application (figure 24A4). Altogether a drop in ER fluorescence in presence of calcium was observed in 33 experiments (29 with F5N and 4 with MF4) on 23 independent cover slips. However, the recovery after caffeine application was often very weak. By comparison, in 6 experiments on 5 coverslips the reaction to caffeine was not clear. However, artefacts caused by caffeine application were described before. First, it was demonstrated that the calcium indicators indo-1, Mag-Fura-2, magnesium green, fura-2 and fluo-3 interact with caffeine in millimolar concentrations. This interaction leads to quenching of the fluorescence in a calcium-, caffeine- and dye-concentration dependent manner (McKemy et al., 2000; Muschol et al. 1999). Furthermore, the group of Sandor Györke described that caffeine in combination with Fluo5N causes a fluorescence quenching of roughly 10 % compared to Fluo5N usage with other agonists (Belevych et al., 2007; Kubalova et al., 2004).

To find out whether caffeine caused an artefact in our Fluo5N experiments a test experiment was performed. In conditions comparable to the ones before, caffeine was applied to neurons and the fluorescence changes were recorded simultaneously for the Fluo5N (473 nm) and RFP (559 nm) laserline (figure 24B).The known fluorescence reduction and recovery in the Fluo5N channel was observed, whereas the RFP channel fluorescence remained stable with the exception of continuous bleaching. The bright-field signal, which

was illuminated by the 559 nm laserline, is not confocal and showed only small artefacts. The imaged turned blurry. Prompted by these observations a quenching assay was conducted. The non-confocal BX51WI microscope was used instead of the confocal microscope because i) it was difficult to know the correct confocal focal plane and ii.) it was known that very weak fluorescence signals i.e. of an fluorescent coupled antibody diluted in buffer, are not detected at the confocal setup.

To mimic a live cell imaging situation ACSF containing 40 mM caffeine or no caffeine was supplemented with 10 mM HEPES to stabilize the pH and 1 µl of Alexa 488 antibody was added to 1 ml ACSF solution. The live cell imaging chamber was filled with the solution and the solution was excited with an epifluorescence light at 470 nm. The fluorescence was detected for the complete visual field in 48 frames. Fluorescence was corrected for background fluorescence which was determined with ACSF with HEPES and with or without caffeine but no fluorescent antibody. The mean fluorescence values of 4 trials revealed that the fluorescence in ACSF containing caffeine and fluorescent antibody was reduced by 18 % as compared to ACSF containing the antibody but no caffeine.

This means that in this conditions caffeine ACSF has a quenching effect on fluorescence at 470 nm which is the same wavelength used to excite Fluo5N and Oregon Green. Thus the results obtained before might be falsified at least in part by a quenching artefact caused by the agonist caffeine. On the other hand, it remained elusive whether this effect is applicable to the data obtained at the confocal microscope in which only the fluorescence of the cell layer, but not more, was detected. In addition, the effect caused by caffeine was usually larger than an 18% decrease and sometimes occurred not simultaneously with caffeine application. Figure 24A3 shows the fluorescence curve of a neuron that did not recover after caffeine application which excludes the possibility that the drop before was caused by quenching only.

Disregarding the possibility of artefacts, caffeine caused a release of ER calcium in hippocampal neurons in both “default” neurons (as in figure 24A3) and in neurons that were stimulated with potassium (as in figure 24A1, A2 and A4). It was concluded that the ER of neurons is neither empty nor full of free calcium ions and it can therefore be filled up or emptied out of calcium. In addition, these experiments show that TED is able to visualize CiCR-mechanisms and that MF4 can be functionally applied to TED. In this preliminary form, these aspects will be followed in future studies.

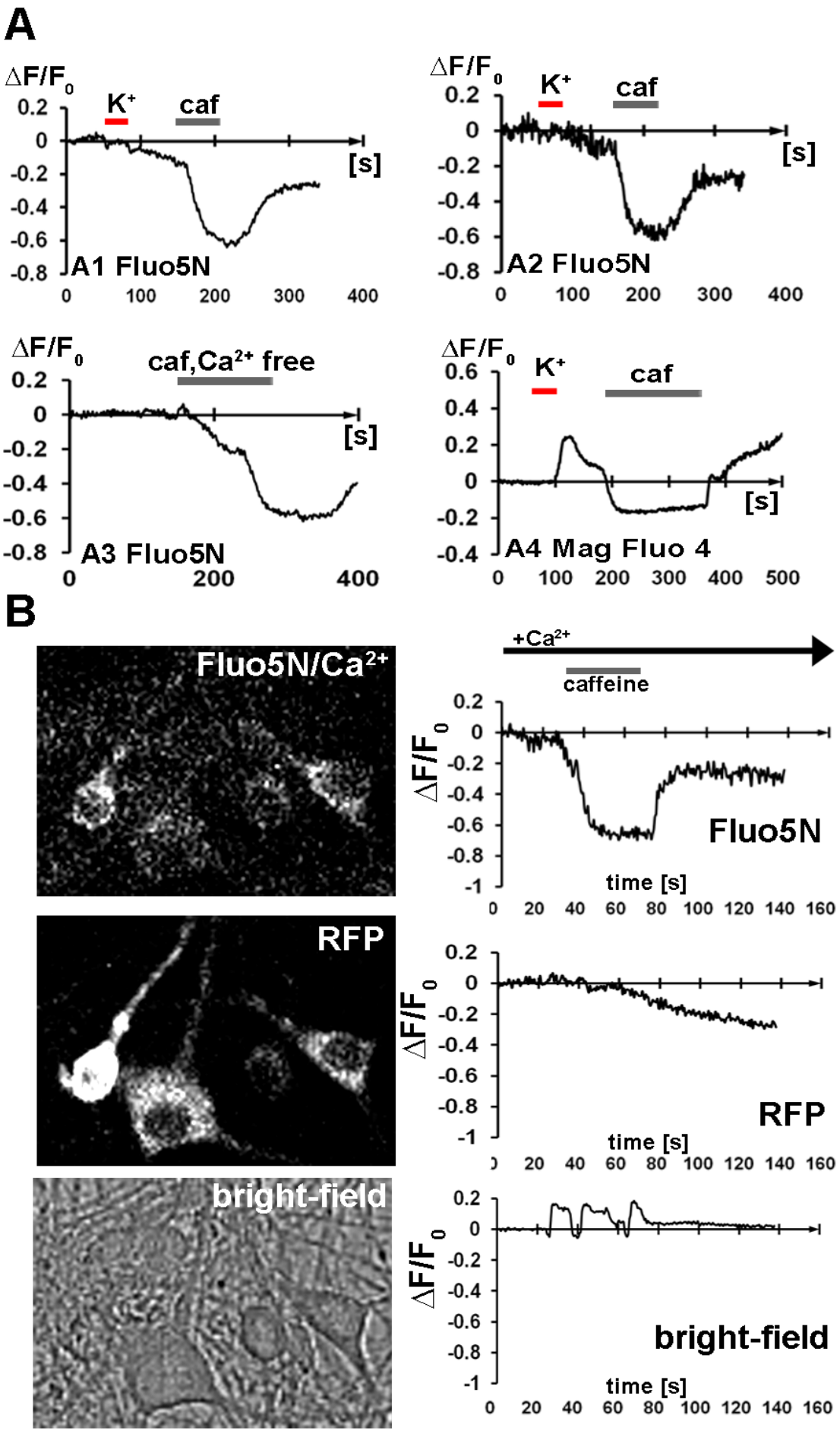
A
ΔF/F0
K+
caf
[s]
A1 Fluo5N
A2 Fluo5N
caf,Ca2+ free
A3 Fluo5N
A4 Mag Fluo 4
B
Fluo5N/Ca2+
RFP
bright-field
+Ca2+
caffeine
Fluo5N
time [s]
RFP
bright-field

Figure 24: caffeine evoked calcium signals and TED
A) Exemplary results obtained by live cell imaging of neurons with TED and F5N or MF4. 11-20 mM Potassium solution and 40 mM caffeine were applied in presence of extracellular calcium as indicated. Potassium evoked a rise in ER calcium in one experiment. Caffeine application led to a decrease in fluorescence of variable magnitude in all experiments shown.
A1 is a curve obtained by analysing only somatic ROIS and **A2** is a curve obtained by analysing only ROIS in processes in the same experiment. **A3** and **A4** are independent experiments.
B) and C) Using the confocal microscope set to "in frame" scan mode, the fluorescence of the Fluo5N/Ca^{2+}, the RFP and non-confocal bright-field fluorescence were recorded.
B) Pictures from the movie before caffeine application. **C)** Mean fluorescence curves of the 4 neurons shown in B for all three channels. Only the Fluo5N/Ca^{2+} fluorescence dropped abruptly during caffeine application.

3.2.4 Ryanodine, cresol, and DHPG failed to evoke calcium signals

RyR can also be activated by their agonist 4-chloro-m-cresol (cresol), a methylphenol. Cresol is mostly applied to muscle cells and led to calcium release from the sarcoplasmic reticulum in concentrations of 200 µM and 1 mM (Westerblad et al., 1998; Zorzato et al., 1993). When applied to cultured astrocytes, 0.5 to 2 mM cresol elicits calcium release (Matyash et al., 2002). At a concentration below 1 mM cresol is specific for RyR and it exerts its effect at 0.5 mM on hippocampal neurons (Wu et al., 2013).

A drawback of cresol is its ability to inhibit SERCA pumps in the sarcoplasmic reticulum of muscle cells (Al-Mousa and Michelangeli, 2009) and both SERCA blockade and RyR activation lead to the decline in ER calcium.

Nevertheless, initial experiments were performed in which 0.5 µM cresol was applied to OGB1 loaded neurons for 20-30 s in 6 experiments on 5 independent cover slips in the presence of extracellular calcium. Recordings were performed at ca. 5 Hz at the non-confocal microscope setup in order to enable the recording of fast release signals, but these signals were never observed.

Another alternative to caffeine is ryanodine itself which can also activate RyRs. Here it needs to be considered that the action of ryanodine is complex and different reports regarding its application exist. Most studies were performed by using cardiac muscle or skeletal muscle cells and electrophysiology. Laporte *et al*. reported that ryanodine at submicromolar concentrations either leads to a full conductance state of the RyR or it leads to stabilization of one of several partially conducting states, which is the more typical effect (Laporte et al., 2004). At micromolar or higher concentrations ryanodine completely closes the RyR channel pores.

(Fill and Copello, 2002) reported that Ryanodine at a 10 nM concentration increases the frequency of single channel opening to normal conductance level, 100 µM ryanodine lock the channel closed and intermediate concentrations were reported to induce very-long-duration open events and a simultaneous reduction in ion conductance through the pore (Rousseau et al., 1987).

In cultured astrocytes application of 10-20 µM ryanodine resulted in intracellular calcium elevation (Matyash et al., 2002) and 5 µM ryanodine locally applied to hippocampal slices activated RyR channels (Liu et al., 2012).

Therefore, cytosolic and ER calcium imaging experiments were conducted in which neurons were perfused with buffer containing 10 nM, 100 nM,1 µM, 2 µM or 20 µM ryanodine for 30 s to two minutes. Neither was a release signal observed in the ER, nor a peak in the cytosol.

This failure to release ER calcium can have two reasons. First, the concentration of ryanodine within the imaging chamber cannot be exactly controlled. Although the concentration of any agonist probably reaches the determined concentration, the concentration is lower while the buffer is flowing in and out. Second, the effect of ryanodine is also dependent on the state the channel is in when ryanodine binds. The channel has to be in an activated state to be blocked open by ryanodine. In dorsal root ganglion neurons the application of 10 µM ryanodine blocked caffeine induced calcium release from the ER only after the neurons were activated by application of caffeine and potassium before (Usachev et al., 1993).

In order to observe ER calcium release caused by activation of metabotropic signalling cascades stimulations with dihydroxyphenylglycine (DHPG) and carbachol were perfomed. DHPG is an agonist specific for metabotropic glutamate receptors type 1 and 5 (mGluR1, mGluR5) and was shown to lead to ER calcium release in cultured neurons (Ng et al., 2011; Rae et al., 2000) and carbachol, an agonist for the muscarinic/metabotropic acetylcholine receptor (mAChR) was reported to induce ER calcium release in cultured hippocampal neurons (Irving and Collingridge, 1998).

Despite these promising facts several attempts to record DHPG or carbachol induced calcium signals in neurons failed, whereas DHPG induced cytosolic calcium signals were repeatedly observed in prospective oligodendrocytes (data not shown).

The cause for the nonreactive neurons remained elusive, but it can be speculated that the application used in our experiments promoted mAChR and mGluR1/5 desensitization, or that the recording conditions were not suitable, or that there is a lack of functional mAChR and mGluR1/5 expression in our mouse hippocampal neurons. In addition, it cannot be excluded, yet, that the esterase activity of RedCES2 interferes with the IICR mechanism in hippocampal neurons.

3.3 Calcium homeostasis in resting hippocampal neurons and glial cells

The results presented above showed that TED in combination with RedCES2 is suitable to investigate ER calcium dynamics in neurons, thus enabling a detailed analysis of ER calcium homeostasis in neurons.

Although reports had been published in which the calcium influx and efflux of neurons was investigated, hardly any information exists regarding calcium homeostasis in neurons at rest. We asked the questions: How do neurons keep the calcium that was taken up by various pathways? How is the resting ER calcium level maintained?

3.3.1 Medial filling state of the ER at rest

One basic question regarding ER calcium homeostasis was whether the ER is full or devoid of free calcium ions at a resting state. To answer this question, neurons at DIV 9-16 were stimulated with 11-20 mM potassium during TED ER calcium imaging in calcium containing ACSF solution and recordings were made at the confocal imaging setup. Out of 86 neurons, 39 neurons showed a reaction. Out of these, 35 neurons showed a fluorescence peak which declined to resting values within almost 70 seconds and only 4 neurons showed a sustained elevation in ER fluorescence (figure 25). This means that at rest the ER is in a “medium-high” filling state. This result is in agreement with the observations made with caffeine application in which it was possible to release ER calcium with and without precharging the ER with potassium (see above 3.2.3).

Furthermore, the background corrected raw fluorescence values of 12-bit images of neurons were determined before and after a CPA stimulus and during an AMPA induced peak (see 3.3.2 and figure 26 for CPA and AMPA fluorescence traces). The initial fluorescence of these 15 neurons in 4 experiments was 767 a.u. ± 52 S.E.M., after ER depletion it was 361 a.u. ± 29 S.E.M. and during the AMPA Peak the mean fluorescence value was at 928 a.u. ± 89 S.E.M. This again proofs that the neuronal ER at rest is initially neither empty nor full. In addition it became apparent that the calcium signals under investigation are within the limits of the F5N detection range.

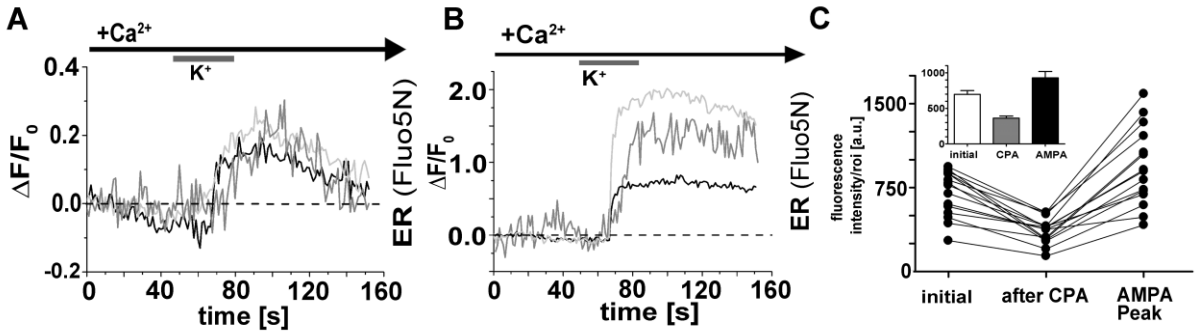

Figure 25: Medial filling state of the neuronal ER
A) and B) Examples of fluorescence traces representing calcium levels in the ER of neurons stimulated with 11-20 mM potassium during live cell calcium imaging in the ER. 35 neurons showed a peak as the three examples in A) and 4 neurons showed a peak as the three examples in B. **C)** Background corrected raw fluorescence values of ER calcium measurements of 15 neurons before and after CPA treatment and during an AMPA stimulus. The ER is initially in a "medial-high" filling state and TED with F5N allows the detection of both, higher and lower ER calcium filling states.

3.3.2 ER calcium leakage in resting neurons

In order to get a first idea about the maintenance of ER calcium levels the SERCA inhibitor cyclopiazonic acid (CPA) was used. Inhibition of SERCA either by thapsigargin or CPA leads to a decline in ER calcium levels due to leakage of calcium from the ER store (Beck et al., 2004; Camello et al., 2002).

TED ER calcium imaging and cytosolic calcium imaging was performed at a confocal imaging setup using an open confocal aperture (800 µm) and a frame rate of 1s. During the experiment the neurons were perfused with ACSF containing 2 mM calcium and 100 nM TTX to prevent action potential firing. After 20 s of recording 30 µM CPA was perfused into the system at a rather slow perfusion speed for 4 min and DMSO was used as a solvent control (figure 26A and C). Then, TTX was washed out of the system for 3-5 min and 20 µM AMPA was given for 30 s to stimulate the neurons (figure 26B and D). It was observed that CPA led to a decline in ER calcium levels in 17 neurons in 4 experiments, whereas DMSO did not alter the ER calcium concentration in 10 neurons in 2 experiments. AMPA application led to a sharp rise in ER calcium concentration. When the same experimental outline was performed and the cytosolic calcium concentration was recorded with OGB1, no change in calcium levels was observed in the DMSO condition in 5 neurons. In CPA treated cells the cytosolic calcium concentration showed only minimal fluctuations in 20 neurons in 3 experiments. Application of AMPA stimulated a sharp increase in cytosolic calcium concentration. The decline in ER calcium by SERCA inhibition is in agreement with other reports and proofs that the ER continuously loses calcium at rest. This also means that continuous SERCA activity is needed to maintain the ER calcium content at rest.

Contrasting to published results, no major changes in cytosolic calcium levels were observed. Therefore, an alternative set of experiments was performed in which the cytosolic

calcium concentration was recorded using the non-confocal imaging setup with a frame rate of 1s and 4 x 4 binning. When 30 µM CPA was applied by a 30 s pulse with a high perfusion speed (figure 26E) a short peak in cytosolic calcium was observed (in 33 of 43 neurons in 7 experiments). When the ER calcium levels were recorded in a similar experiment the ER calcium level dropped and remained low as before and a small recovery of ER calcium was observed after CPA was washed out (36 out of 39 neurons in 7 experiments) (figure 26G). When 30 µM CPA was applied for 4 min with slow perfusion speed, similar calcium curves were recorded. Again, a small and transient cytosolic calcium peak (figure26F) and a sustained reduction in ER calcium (figure26H) were observed (cytosol: 10 of 14 neurons in 3 experiments and ER: 5 of 5 neurons in 1 experiment). After washout of CPA and TTX neurons were stimulated for 30 s with 30 µM AMPA, which resulted in a strong fluorescence peak under all conditions. Figure 26 E-H shows the mean fluorescence curves of all neurons of one representative experiment for each condition.

This set of experiments led to the conclusion that the ER calcium concentration is maintained at rest by active transport of calcium ions by the SERCA pump and therefore ER calcium levels decline when this activity is interrupted, as expected. The interesting observation is that the cytosolic calcium concentration is regulated by the neurons in a way that aims at maintaining the basal calcium concentration. For this reason, only small cytosolic calcium peaks, rather than sustained elevations were observed despite sustained reduction in ER calcium levels.

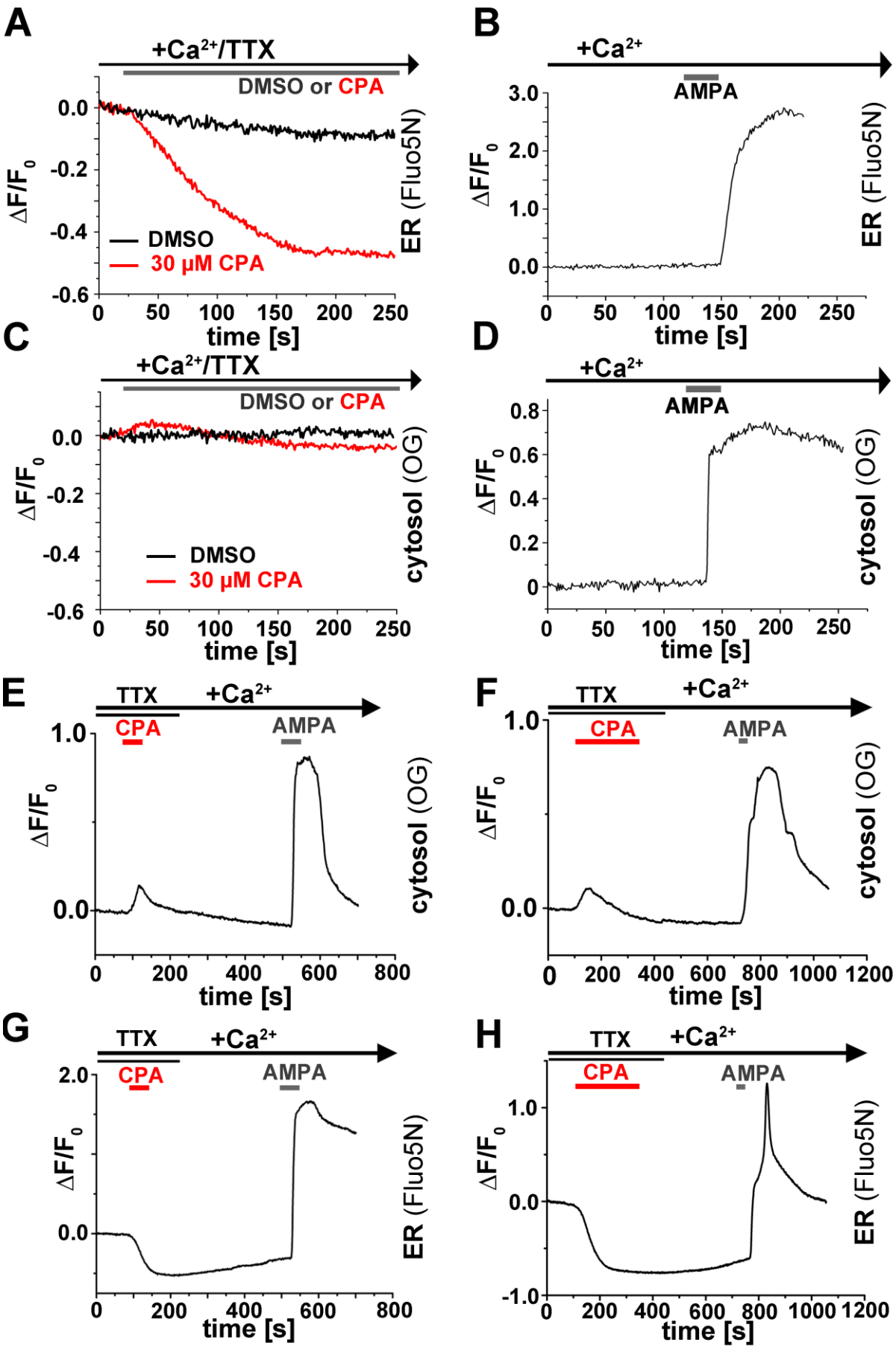
A
+Ca2+/TTX
DMSO or CPA
ΔF/F0
ER (Fluo5N)
DMSO
30 µM CPA
time [s]
B
+Ca2+
AMPA
ΔF/F0
ER (Fluo5N)
time [s]
C
+Ca2+/TTX
DMSO or CPA
ΔF/F0
cytosol (OG)
DMSO
30 µM CPA
time [s]
D
+Ca2+
AMPA
ΔF/F0
cytosol (OG)
time [s]
E
TTX
+Ca2+
CPA
AMPA
ΔF/F0
cytosol (OG)
time [s]
F
TTX
+Ca2+
CPA
AMPA
ΔF/F0
cytosol (OG)
time [s]
G
TTX
+Ca2+
CPA
AMPA
ΔF/F0
ER (Fluo5N)
time [s]
H
TTX
+Ca2+
CPA
AMPA
ΔF/F0
ER (Fluo5N)
time [s]

Figure 26: ER calcium is maintained at rest by SERCA activity
Mean fluorescence traces representing calcium levels obtained under **A)-D)** confocal imaging conditions and **E)-H)** non-confocal imaging conditions. Neurons were perfused with ACSF containing calcium and 100 nM TTX as indicated. **A)** ER calcium levels of neurons treated for 4 min with 30 µM CPA (red curve; 17 neurons in 4 experiments) or DMSO (black curve; 10 neurons in 2 exp.). **B)** ER calcium levels (4 neurons in 1 exp.) after TTX was washed out for 3-5 min and a 30 s pulse of 30 µM AMPA was applied. **C)** Cytosolic calcium levels of neurons treated for 4 min with 30 µM CPA (red curve; 20 neurons in 3 exp.) or DMSO (black curve; 5 neurons in 1 exp.). **D**) Cytosolic calcium levels of neurons (6 neurons in 1 exp.) treated as in B). **E)** Cytosolic calcium levels (6 neurons in 1 exp.) of neurons stimulated with 30 µM CPA for 30 s and 30 µM AMPA for 30 s. **F)** Cytosolic calcium levels (4 neurons in 1 exp.) when CPA is applied for 4 min rather than 30 s. **G)** ER calcium levels (3 neurons in 1 exp.) of neurons treated with 30 µM CPA for 30 s and stimulated with 30 µM AMPA as in E). **H)** ER calcium levels (5 neurons in 1 exp.) of neurons treated with 30 µM CPA for 4 min and 30 µM AMPA as in F). SERCA blockade with CPA led to a sustained decline in ER calcium levels, whereas cytosolic levels showed a transient peak.

3.3.3 Effect of calcium deprivation on resting calcium levels

It was observed before that ER calcium levels are maintained at rest by continuous, SERCA dependent calcium influx. Next, it was addressed whether this influx was dependent on extracellular calcium. Cytosolic and ER calcium levels were recorded in neurons (DIV 9-16) perfused with ACSF containing 100 nM TTX at the confocal live cell imaging setup using a frame rate of 2 or 3 s, an open confocal aperture (800µm) and laserpower of 0.3 to 0.5 %. During the experiments the extracellular calcium was removed for 5-7 min and reapplied. As depicted in figure 27A and B the calcium concentration declined until a minimum was reached and recovered upon calcium re-addition.

In figure 27A pictures from a representative TED imaging movie are shown and in B the mean fluorescence curves of ER and cytosolic calcium levels are shown (black curve = ER calcium level: mean fluorescence of 2 neurons in 1 representative experiment and red = cytosolic curve: mean fluorescence of 2 neurons in one representative experiment).

We determined the time needed from the time point of calcium withdrawal until the ER and the cytosol of somatic regions reached a fluorescence minimum (figure 27C). After 219 ± 18 s (26 cells in 13 experiments; for all mean ± S.E.M.) of calcium withdrawal the ER was empty. The cytosol was depleted of calcium 43 s earlier at 176 ± 30 s (14 cells in 5 experiments).

We did the same measurement for the dendritic regions of the neurons and got a clearer result (figure 27 C). Upon calcium withdrawal it lasted 230 ± 21 s until the ER was depleted of calcium (22 cells in 13 experiments), but the cytosol was significantly faster by 101 s with 131 ± 44 s (8 cells in 5 experiments; $p = 0.0369$).

These results suggest that calcium is first lost from the cytosol and subsequently from the ER. The emptying processes were completed in 3-4 minute. After re-addition of extracellular calcium both cytosolic and ER calcium levels recovered. The onset of this recovery appeared to start at the same point in time for the cytosol and the ER, but the inflowing calcium did not accumulate in the cytosol. Possibly, the calcium was instantly pumped into the ER by the

SERCA pump, which can be achieved since the SERCA pump was found to continuously pump inflowing calcium into the ER (3.3.2 and figure 26). Alternatively, the calcium might enter the ER via microdomains containing the SOCE-molecules and the SERCA pump. Also, both mechanisms could exist in parallel. In this way the calcium could bypass the cytosol but enter the ER via SERCA.

Independent of the influx mechanism, the result demonstrates that in these experiments the ER was not able to store or keep calcium when calcium was lost from the cytosol. Rather, the ER also lost its calcium. It was also concluded that under normal conditions, in presence of extracellular calcium, the following calcium fluxes are active: Calcium enters the neurons from extracellular sites through the cytosol into ER. To achieve a balanced calcium level there must be a continuous calcium efflux from the ER into the cytosol and through the plasma membrane out of the neuron, hence showing that ER calcium leak needs to be replaced from extracellular sites.

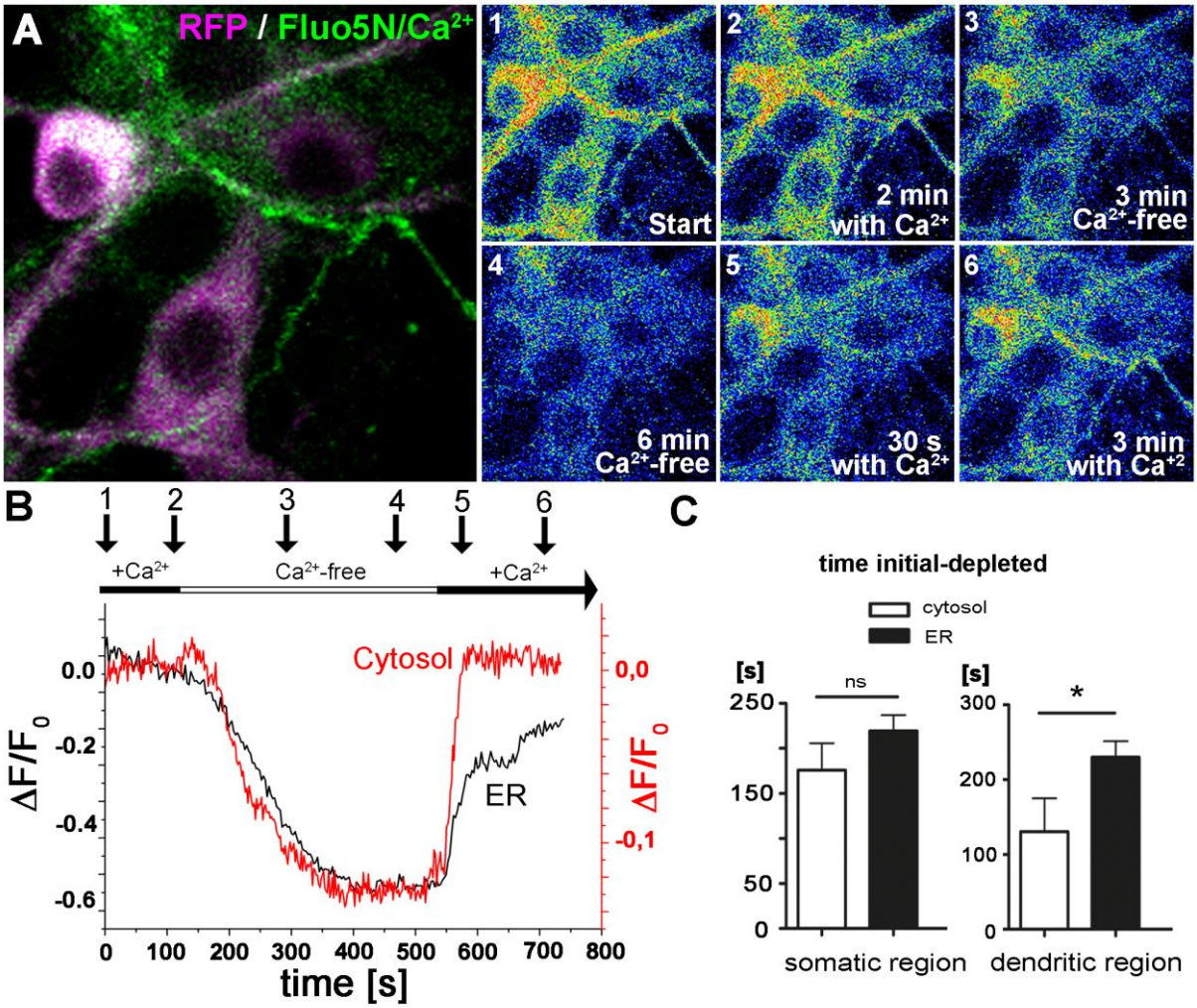

Figure 27: Loss of neuronal calcium by calcium withdrawal
During cytosolic and ER calcium imaging at a confocal imaging setup, neurons were perfused first with ACSF containing 2 mM calcium, then with ACSF without calcium for 7 min and finally calcium was

given back. **A)** Left picture: merge of the RFP and F5N/Ca^{2+} channels of F5N loaded cells. Right: Pictures from a time lapse movie of a representative experiment. **B)** Mean fluorescence of neurons during a representative calcium withdrawal experiment. The red curve represents the cytosolic calcium level (2 neurons in 1 experiment) and the black curve the ER calcium level (2 neurons in 1 experiment). Images from the time points indicated by arrows are shown in A). **C)** Quantification of experiments conducted as in B). The time until the cytosol (white bars) and the ER (black bars) were depleted was determined. Bars represent mean fluorescence ± SEM of the somatic and dendritic region.

3.3.4 Effect of SOCE blockade on resting calcium levels

In neurons, two main routes of calcium entry exist: Influx via Ca_v channels or via ionotropic calcium permeable receptors after activation, and SOCE after ER calcium release (see introduction). Because our neurons were kept in a resting state and treated with a blocker of voltage-gated sodium channels, it was hypothesized that SOCE is responsible for the continuous resting calcium influx that was observed.

To investigate this hypothesis, SKF-96365, a SOCE inhibitor was used to find out whether SOCE is involved in maintenance of ER calcium levels in neurons. SKF-96365 is a prominent inhibitor of SOCE (Lalonde et al., 2014; Varnai et al., 2009). The disadvantage of the blocker is that it interacts with TrpC channels (Boulay et al., 1997) and T-Type Ca_v (Singh et al., 2010) and possibly even Orai channels (Wolkowicz et al., 2011). Nevertheless, SKF-96365 is a commonly used and accepted inhibitor of the SOCE mechanism (Lalonde et al., 2014; Liou et al., 2005; Merritt et al., 1990).

Cytosolic and ER live cell calcium imaging was performed at the non-confocal imaging setup and cultured hippocampal neurons (DIV 9-16) were perfused in HEPES ACSF with calcium containing 100 nM TTX and 25 µM SKF-96365 for 8 min. The camera was set to a frame rate of 0.5 s and 4 x 4 binning. Figure 28 shows in C pictures of a representative ER calcium imaging experiment. The initial ER calcium concentration drops after SKF-96365 reaches the neuron. During stimulation with AMPA the fluorescence abruptly recovered. Three experiments with 16 neurons were conducted with SKF-96365 and 10 neurons in three experiments were treated with the solvent control PBS. We determined the fluorescence levels of SKF and PBS treated cells after 8 min perfusion with ACSF containing calcium and SKF or PBS (the time point indicated in figure 28A by an arrow). The result was a significant additional reduction in ER fluorescence of 17 % in SKF treated neurons as compared to the reduction of PBS controls. (SKF: -0.32 ± 0.03 $\Delta F/F_0$ ± S.E.M., and PBS: -0.15 ± 0.03 $\Delta F/F_0$ ± S.E.M.; p = 0.0029; figure 28E). Figure 28A represents mean ER fluorescence curves of 8 neurons in 2 experiments with SKF-96365 and mean fluorescence of 10 neurons in 3 experiments with PBS and figure 28B shows the mean cytosolic fluorescence of 18 neurons in 4 experiments with PBS control and 54 neurons in 8 experiments with SKF-96365. The ER fluorescence curve in A, as well as the single cell traces in C further show that SKF-96365

caused a decline in ER fluorescence that can clearly be distinguished from the linear rundown in the PBS controls.

Intriguingly, SKF-96365 only caused a loss of calcium in the ER whereas the cytosolic calcium level remained constant. It was concluded that a SOCE-like mechanism is required to maintain ER calcium levels in resting hippocampal neurons.

The results raised the question whether this effect was dependent on the SERCA pump, or if calcium entering the neurons can circumvent the cytosol and SERCA and can enter the ER directly. This issue was addressed in experiments (figure 28F) in which SOCE was induced by calcium withdrawal for 8 min and SERCA blockade with 30 µM CPA for 4 min in the experimental conditions (37 cells in 6 experiments), whereas CPA was replaced by DMSO in control conditions (39 cells in 6 experiments). Experiments were performed at the non-confocal live cell imaging setup (frame rate 0.5 s and 4 x 4 binning) and ER calcium levels were recorded in HEPES ACSF. The mean fluorescence curves are depicted in figure 28F.

In DMSO control conditions ER calcium was refilled upon calcium re-addition to the neurons, whereas CPA blocked the refill process, except for small rise of ca. 3%. This proofs that SERCA was indeed required to maintain the ER calcium level at rest. No considerable alternative route was detected. In summary, this shows that resting ER calcium levels are maintained by a SOCE-like calcium influx and a processing of this calcium influx by the SERCA pump.

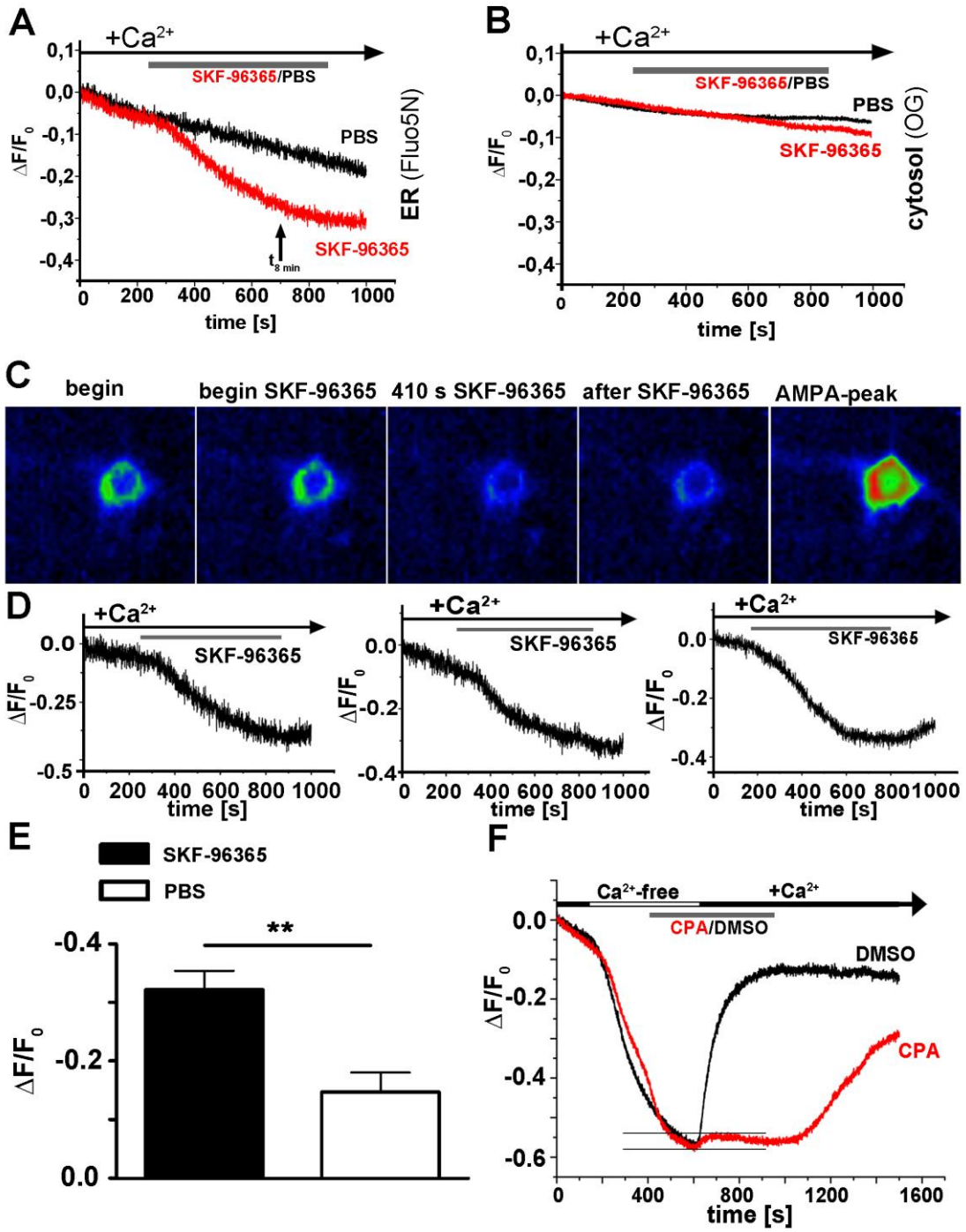

Figure 28: SOCE maintains ER calcium at rest

A) - E) Acute treatment of neurons perfused with HEPES ACSF containing TTX with 25 µM SKF-96365 to inhibit SOCE caused a decline in ER calcium levels. **A)** Mean fluorescence curve representing ER calcium levels during acute SKF-96365 (8 neurons in 2 experiments) or PBS control treatment (10 neurons in 3 experiments). **B)** Mean fluorescence curve representing cytosolic calcium levels during SKF-96365 (54 neurons in 8 experiments) or PBS control treatment (18 neurons in 4 experiments) **C)** Images from a representative neuron during acute SKF treatment and subsequent AMPA stimulation. **D)** Single cell fluorescence traces representing ER calcium levels. **E)** Mean ER fluorescence levels +/- S.E.M. of neurons after 8 min of acute SKF or PBS treatment (PBS:10 neurons in 3 experiments and SKF-96365: 16 neurons in 3 experiments). **F)** Neurons were deprived of extracellular calcium to induce SOCE. Additional treatment with SERCA inhibitor CPA prevented the

recovery of ER calcium after re-addition of extracellular calcium. (Mean ER fluorescence traces of 37 neurons in 6 experiments for CPA and 39 neurons in 6 experiments for DMSO control).

3.3.5 Immunocytochemical detection of STIM1/2 in hippocampal neurons

Inhibition of SOCE by SKF-96365 had a profound effect on ER calcium levels. SKF-96365 is an unspecific SOCE inhibitor that inhibits the STIM-Orai mediated calcium influx (Varnai et al., 2009). The expression of STIM1 and STIM2 was therefore investigated by immunocytochemical detection.

Both STIM1 and STIM2 proteins were detected in cultured hippocampal neurons expressing RedCES2 after lentiviral transduction (figure 29). The STIM1/2 immunoreactivity was detected in the same areas as c-Myc reactivity demonstrating the expected ER localization.

This result is in agreement with other studies. STIM2 was detected in cultures hippocampal neurons in (Berna-Erro et al., 2009) and Korkotian *et al*. reported the detection of STIM1 and Orai 1 (Korkotian et al., 2014).

It was therefore concluded that the proteins affected by SKF-96365 are present in cultured hippocampal neurons.

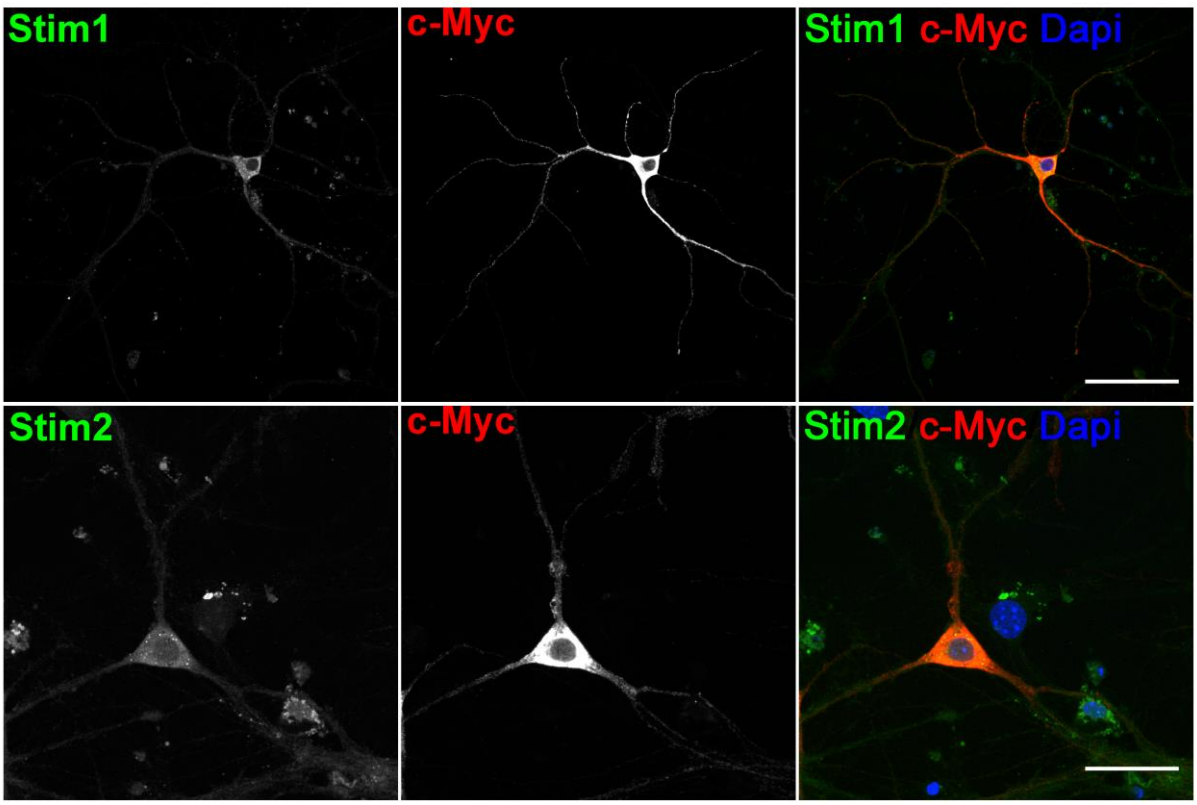

Figure 29: Localization of STIM1 and STIM2 in hippocampal neurons
Cultured hippocampal neurons were transduced to express RedCES2 and immunocytochemical staining was performed. Both, STIM 1 and STIM2 protein were detected in the ER of the neurons. Upper: confocal image, scale bar represent 50 µm; lower: merge of several z-layers to visualize somatic and dendritic areas, scale bar represents 30 µm.

3.3.6 Calcium imaging in the ER of primary glial cells using the RedCES2 construct

TED has been shown to work quite efficiently in glial cells (Blum et al., 2010; Jaepel and Blum, 2011). Therefore, the performance of the lentiviral Red-fluorescent TED construct UBQ RedCES2 was tested in primary glial cells.

Primary glial cells were infected with the UBQ RedCES2 construct and incubated in 5 µM F5N, AM for 15 min to visualize the ER calcium. Figure 30A and figure 31D show exemplary confocal pictures of such RedCES2 expressing, living astrocytes in which the ER calcium is visualized with F5N. The fluorescence signals are evenly distributed throughout the outspread somas of the cells and the nuclei remain dark.

In a first experiment depicted in figure 30 cells were perfused with calcium containing HEPES buffer and 200 µM ATP was applied for 15 s. ATP can be used to release calcium from the ER of astrocytes by stimulation of metabotropic ATP receptors and activation of IP_3 induced calcium release (Salter and Hicks, 1995). Figure 30A shows pictures extracted from a confocal time laps movie and figure 30B gives the corresponding fluorescence values.

After ATP application the fluorescence values of the F5N/Ca^{2+} dropped abruptly and partially recovered ca. 60 s later due to calcium release and re-uptake. The RFP fluorescence was recorded simultaneously and declined slowly but continuously due to bleaching. The result shows that TED in combination with Fluo5N, AM can be used to visualize calcium signals in the ER of intact glial cells in presence of extracellular calcium, while the TagRFP-T signal can serve as a confocal plane control during confocal “in-line” scans of both fluorescent labels.

Next, this imaging strategy was used to examine whether the continuous calcium flux observed in neurons is also present in glial cells.

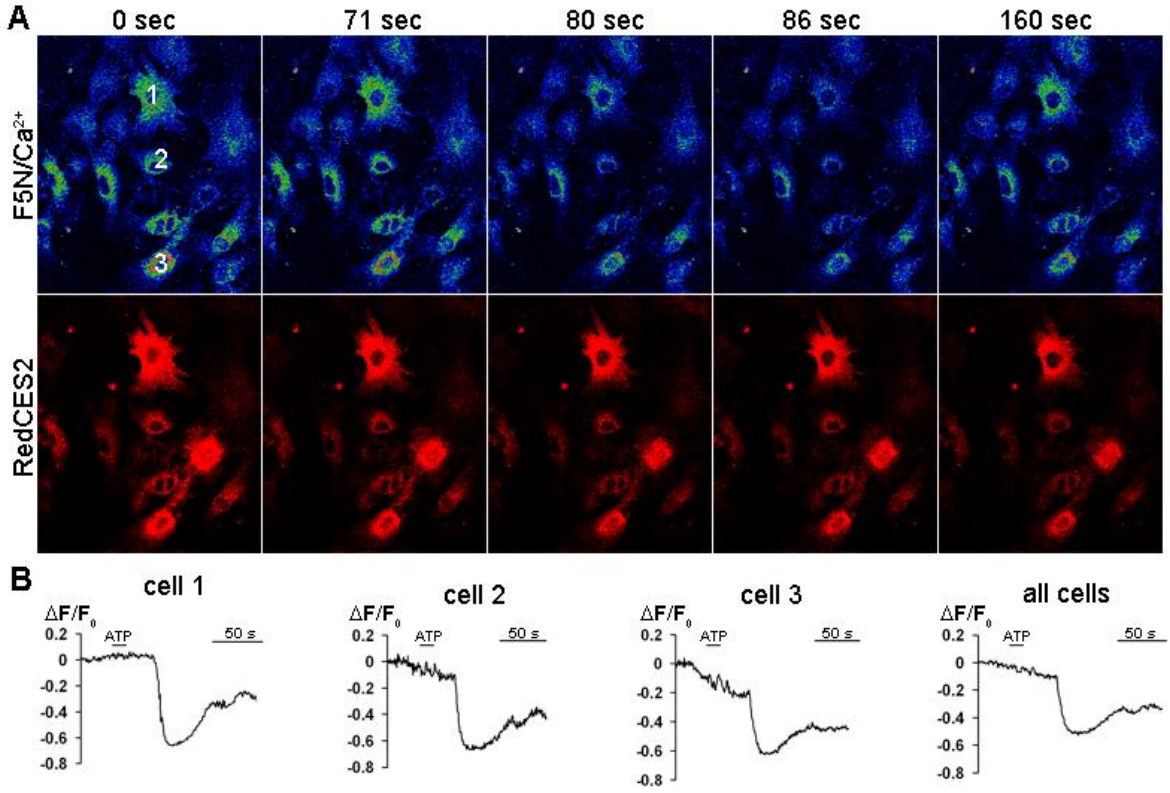

Figure 30: ATP induced calcium signals in primary glial cells
Primary glial cells were grown on cover slips and live cell calcium imaging was performed at a confocal microscope in calcium containing HEPES buffer. The ER calcium levels dropped and recovered after 10 s application of 200 µM ATP. **A**: Pictures from the cells analysed. Cells expressing the RedCES2 can be identified by their red fluorescence and have a strong F5N signal. The ROIS in which the fluorescence was determined are depicted. **B**: Pictures from the live cell calcium imaging movie extracted at the indicated time points. In the upper panel the calcium signal is depicted in false colour. Black-blue = low calcium, green-yellow = medium calcium red= high calcium. The lower panel shows the fluorescence of the RedCES2 fusion protein at the same time points. The fluorescence is constant over time, with the exception of some bleaching. **C**: Fluorescence traces representing ER calcium levels obtained in the experiment in the ROIs depicted in A. Figure from Samtleben *et al*., 2013.

For this, UBQ RedCES2 infected glial cells and uninfected control cells loaded with OGB1, AM were used in imaging experiments at a confocal microscope. The resulting calcium signals are depicted in figure 31 A-C. Cells were perfused with HEPES buffer either with calcium or without calcium and stimulated with 200-500 µM glutamate as indicated in figure 31A-C to activate metabotropic glutamate receptors (mGluR) (Chen et al., 1997; D'Antoni et al., 2008). The ER calcium levels declined upon glutamate stimulation in calcium free buffer and the ER calcium levels were only restored after calcium re-addition (figure 31A) indicating mGluR-induced ER calcium release via the PLC-IP_3 pathway. In figure 31B the same stimulation protocol was used on astrocytes in which the cytosolic calcium was recorded. Here, glutamate stimulation led to an increase of calcium in a calcium free environment demonstrating that this calcium peak is due to an ER calcium release (same result in 2 independent experiments). Cytosolic calcium levels rose after calcium re-addition to the

extracellular buffer. In the control in figure 31 C no such calcium peak was observed when PBS was applied instead of glutamate. Here, calcium deprivation led to a decrease in cytosolic calcium level that recovered after calcium re-addition.

In experiments by MSc Caroline Fecher, Institute of Clinical Neurobiology (Fecher 2012 „Influence of store-operated calcium release and mitochondrial function in neural cells“) it was observed that application of 3 µM thapsigargin to astrocytes led to a rapid decline in ER calcium levels in presence of extracellular calcium.

These results strongly suggest that in cultured astrocytes the ER calcium concentration also depends on calcium influx from the extracellular space and that a continuous, SERCA-dependent calcium flux is necessary to maintain the ER calcium level. Albeit more investigations are necessary in order to provide an understanding of calcium homeostasis at rest in glial cells, these experiments already indicate that a SOCE-like calcium influx at rest is a widespread cellular phenomenon.

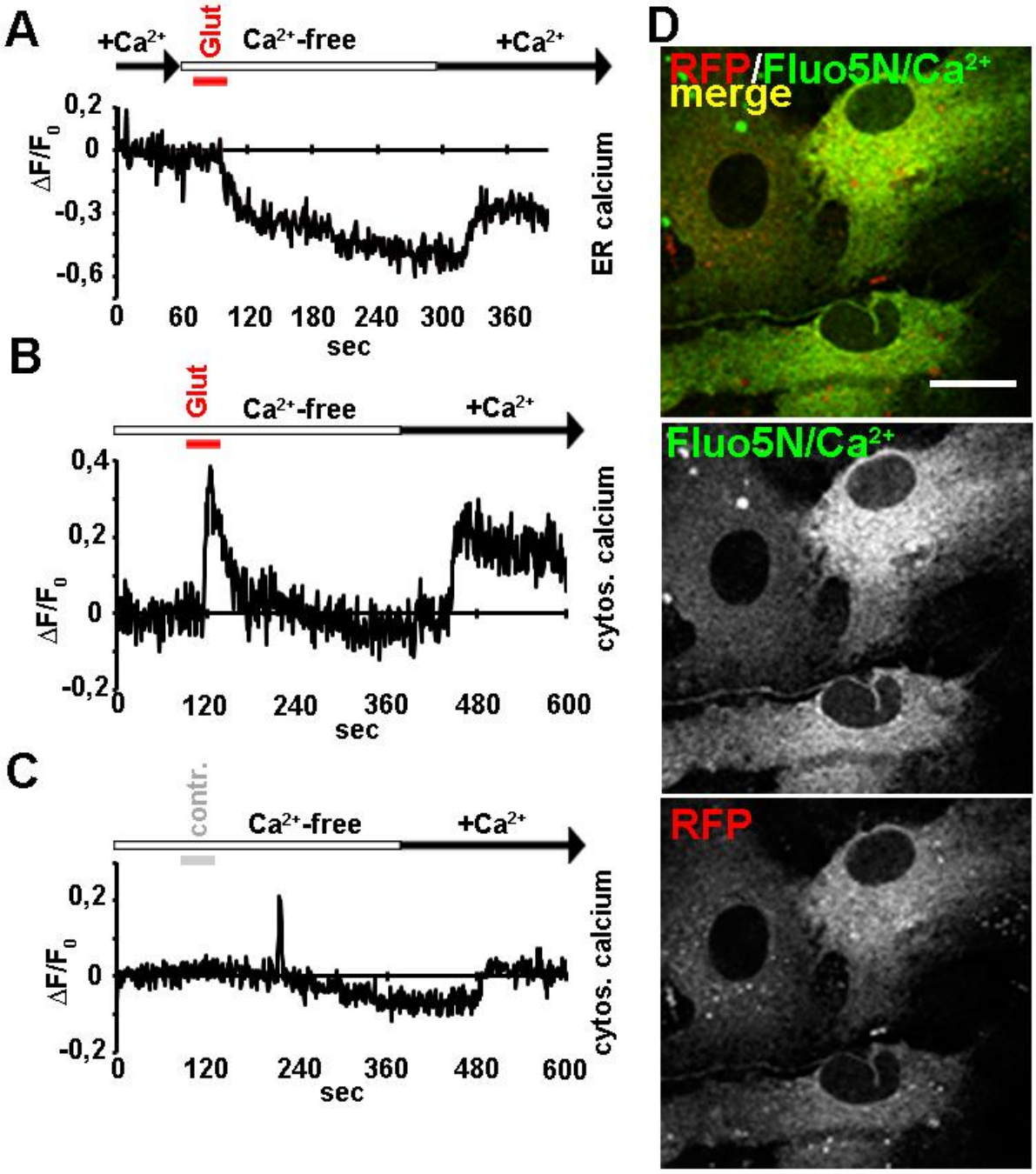

Figure 31: Glutamate induced calcium signals in primary glial cells
Primary glial cells were grown on cover slips and live cell calcium imaging was performed at a confocal microscope. Cells were stimulated with glutamate via perfusion. **A)** Fluorescence curve representing the ER calcium response of RedCES2 expressing cells. Glutamate led to a drop in ER calcium that recovered only after calcium re-addition. Mean fluorescence values of 8 cells. **B)** Cytosolic calcium response visualized with OGB1 of cells treated as in A). The calcium released from the ER elicited a cytosolic calcium peak. Mean fluorescence curve of 10 cells **C)** Cytosolic response of cells treated with a control solution (PBS) rather than glutamate. Except for a small and short spontaneous peak no peaks are observed. Mean fluorescence values of 10 cells **D)** Pictures of primary glia cells infected with UBQ RedCES2 and loaded with F5N, AM. Scale bar = 15 µm.

4 Discussion

4.1 Limitations and Potency of TED

One aim of this study was to visualize calcium signals involving the ER calcium store in neurons. To achieve this, the targeted-esterase induced dye loading technique was used and applied to primary hippocampal neurons. TED is based on the overexpression of the ER-targeted mouse Carboxylesterase 2, which then converts the synthetic AM dye Fluo5N, AM in the ER.

The success of live cell calcium imaging using synthetic calcium indicators is dependent on two main factors. First, when AM dyes are cleaved by esterases, formaldehyde is released as a toxic by-product. Therefore, it is necessary to find a balance between toxicity and a sufficient amount of released dye. Second, any fluorescent light that illuminates the cells causes phototoxicity and can harm, even kill, the cells under investigation. On the other hand, the light must be bright enough to detect the calcium signal. Using F5N and hippocampal neurons the best ER calcium imaging results were achieved by incubating the cells in 5 µM F5N, AM solution for 15 min at 37°C. The ER labelling was clearly visible, obviously distinguished from a cytosolic labelling (figure 22) and no obvious toxic effects were observed.

As described in 3.2.2 and figure 23, one drawback of F5N is its relatively low stability against illumination and rapid bleaching is often observed. Currently, this issue is addressed by shortening illumination- time and -power. Practically, the time lapse movies can be restricted to a short duration or intervals of illumination are interrupted by intervals without illumination.

As demonstrated by the experiments in this thesis, TED currently offers the possibility to monitor ER calcium ions directly and constantly over time periods up to 15 min and experiments of up to 30 min were also successfully conducted (data not shown).

With TED, it was observed that the F5N sometimes emerged in the cell nucleus but does not remain in the ER. This phenomenon was caused by strong stimulation or strong illumination (figure 23 A and B) and its origin is unknown.

Consequently, one needs to carefully examine the movies obtained by TED imaging and, if necessary, choose a weaker stimulation protocol to avoid these calcium signals.

Therefore, it could be worthwhile to combine TED with a different AM dye in the future. Principally, all AM compounds can be converted by the carboxylesterase meaning that TED can be used to convert and trap other fluorescent indicators in the ER. A more bleach

resistant indicator would clearly enhance the TED method and a ratiometric indicator might add even more benefits.

Ratiometric calcium indicators depend on the excitation with two different wavelengths. One wavelength excites the calcium-bound form and the other the calcium-free form. By using the ratio of the two signals disturbing signals like bleaching or focus shifts can be reduced. Ratiometric dyes are commonly used to measure absolute calcium concentrations as well (Paredes et al., 2008). On the other hand, image acquisition speed is reduced. Nonetheless, TED might benefit from a low affinity, ratiometric, AM, more bleach resistant calcium indicator.

In this study it became obvious that TED allows the imaging of ER calcium with a synthetic calcium indicator without disrupting the cellular integrity. For several years synthetic calcium indicators were considered superior compared to GECIS regarding signal-to-noise ratio, dynamic range, which describes the fluorescence change between the calcium bound and calcium free form, and velocity of response kinetics (Palmer et al., 2006).

However, during the last years, GECIs were developed that tackle these and other difficulties. First, a FRET based GECI was developed named ER-D1. It consists of the calcium sensing proteins Calmodulin and a Calmodulin binding peptide derived from skeletal muscle Myosin light chain kinase (skMLCK) cloned between the fluorescent proteins cyan fluorescent protein (CFP) and citrine. Compared to earlier versions of this GECI, the Calmodulin sequence was mutated to prevent interaction of the sensor with endogenous calmodulin. ER-D1 was described to have a low calcium affinity, K_D =69 µM, be ratiometric, have fast on but slow off kinetics and to permit imaging at single cell resolution.(Palmer et al., 2004; Palmer and Tsien, 2006). The GFP-apo-aequorin (GAP) calcium indicators (Rodriguez-Garcia et al., 2014) were developed very recently and its family member “erGAP1” allows ratiometric calcium imaging in the ER. This GECI is based on the jellyfish GFP fused via a linker region to jellyfish apoaequorin. Here, no interaction with endogenous proteins was detected. The dynamic range, is three- to fourfold, and the dissociation constant of calcium was determined to be K_D =12 µM. The authors also generated a transgenic mouse line expressing this calcium sensor. The reporter protein expression was stable during mouse development and it was possible to detect ER calcium release evoked by caffeine in hippocampal slices of 1 month old mice (Rodriguez-Garcia et al., 2014).

In parallel, a group of calcium indicators named CEPIAs (calcium measuring organelle entrapped protein indicators) was developed (Suzuki et al., 2014).

Here, the calcium sensor is based on mutated Calmodulin as a calcium sensor, which was fused to different fluorescent proteins and signalling sequences in order to allow simultaneous imaging of more than one subcellular organelle. For the ER a green fluorescent version (G-CEPIA1er), a red fluorescent version (R-CEPIA1er), and a ratiometric blue green

version (GEM-CEPIA1er) were developed. Their affinity for calcium is very low ranging from K_D = 558 to 672 µM and they have a dynamic range of 21.7 to 4.7.

However, the dynamic range of TED with F5N or another synthetic indicator has never been evaluated but TED in combination with F5N has some advantages over GECIs. First, it enables the detection of ER calcium signals in the range of milliseconds. Calcium release was detected after application of DHPG for 100 ms with a sampling speed of 15 Hz. (Rehberg et al., 2008). Whether this temporal resolution can be achieved with the aforementioned GECIS was not shown. Second, TED imaging depends on the targeted release of the, Fluo5N, AM dye in the ER. Once the dye is cleaved and sensitive to calcium, it is freely diffusible within the ER.

Whether this calcium sensor interacts with endogenous proteins, like it sometimes occurs with GECIs, was not investigated, yet. Furthermore, the small synthetic calcium sensor can be transported with small vesicle-like elements enabling it to reach finest ER structures (Rehberg et al., 2008). In our study small microdomains were not investigated, but calcium microdomains are one focus of attention within the calcium signalling field (Berridge, 2006; Lopreiato et al., 2014; Weinberg and Smith, 2014). In this area of interest, TED could become a very useful method.

To date, TED was only used with transient transfection of cells or lentiviral infection to overexpress the carboxylesterase. Therefore, TED was limited to cultured cells and the risk of detrimental effects due to transfection/transduction remained. It should be possible to transduce either cultured brain slices with TED reporter viruses to enable the examination of calcium signals in neuronal networks. Another possibility is to inject the virus into the ventricle of living mice and to subsequently use acute brain slices. To this end, a mouse line stably expressing the RedCES2 reporter protein in neurons was generated in order to be able to use TED in brain slices as well as cultured cells and to circumvent usage of lentiviral particles. As depicted in figure 20 the Thy 1::RedCES2 mice show a strong expression of the reporter protein indicating a strong esterase activity. Despite these promising observations, more experiments are needed to ascertain whether this mouse line will improve TED.

Altogether, by combining the flexible targeting of proteins with the variability of synthetic AM dyes TED is a very flexible method. TED enables the direct visualization of ER calcium in non-disrupted cells in presence of extracellular calcium.

4.2 Evoked calcium signals in primary neural cells

It was shown before that TED enables the visualization of ER calcium signals in Hek293 cells, BHK21 cells, (Rehberg et al., 2008) HeLa cells (Samtleben et al., 2013; Schäuble et al., 2012) as well as primary cultured astrocytes and cortical neurons (Blum et al., 2010;

Jaepel and Blum, 2011). In the second part of this project TED was applied to cultured primary hippocampal neurons and cultured primary glial cells.

TED gave clear results with prospective astrocytes. The RedCES2 reporter protein was strongly expressed in these cells and led to a bright F5N label after loading. This was achieved by controlling the RedCES2 expression with the UBQ promoter (figure 31). It was shown that ER calcium release signals can be monitored by application of ATP or glutamate activating a metabotropic signalling cascade.

TED proved to be more difficult in combination with cultured neurons. Although RedCES2 expression and F5N, AM loading was fully functional, IP_3 mediated calcium signals could not be observed, which might be due to several reasons.

First, Astrocytes express high affinity metabotropic glutamate receptors (Nash et al., 2002) and $P2Y_1$ receptors (Waldo and Harden, 2004) and the GPcR-IP_3- ER release pathway is very common in this cell type (Volterra et al., 2014). Therefore, it should be easier to induce a metabotropic signal in astrocytes than in neurons. Second, metabotropic calcium release via the IP_3 pathway possibly takes place in specialized microdomains of cultured neurons (Jacob et al., 2005) which we might have overlooked. Third, it is possible that our neurons did not express the appropriate receptors or necessary signalling molecules. Fourth, the mode of drug application influences the experiments. Contrasting to the application via perfusion in this and other studies (Irving and Collingridge, 1998; Young et al., 2005), local application of agonists is also very common. (Hartmann et al., 2014; Holbro et al., 2009; Korkotian and Segal, 1999; Rehberg et al., 2008; Seymour-Laurent and Barish, 1995; Sugawara et al., 2013; Usachev et al., 1993). When using perfusion application it is difficult to achieve a brief stimulation and a sustained exposure of receptors with their ligands can cause the receptors to enter a non-active state.

Apart from metabotropic signals, TED enabled the visualization of calcium release signals by application of CPA, caffeine, and calcium withdrawal.

In summary, it was confirmed that TED can be applied to cultured primary glial cells as well as primary hippocampal neurons.

4.3 Calcium homeostasis in resting neurons

Summary and interpretation of results:

Here, TED was used to investigate ER calcium homeostasis in neurons. It was observed that neurons at rest continuously loose ER calcium through the plasma membrane. To compensate this loss, neurons exhibit a resting calcium influx mechanism which maintains ER calcium levels. The obtained results disagree with a model of ER calcium homeostasis, in which ER calcium loss at rest is rescued by SERCA activity from the cytosol (figure 32 model

1). In addition, SOCE was thought to be a consequence of induced ER calcium release, either by SERCA blockade or by activation of ER release signalling events (Berna-Erro et al., 2012; Hoth and Penner, 1992; Putney, 1986; Targos et al., 2005). The data reported here support a new model (figure 32 model 2) of ER calcium homeostasis, in which the ER calcium leak is compensated with calcium from the extracellular site, thereby keeping cytosolic and ER calcium concentrations constant. The resting calcium fluxes described here are outlined in figure 32.

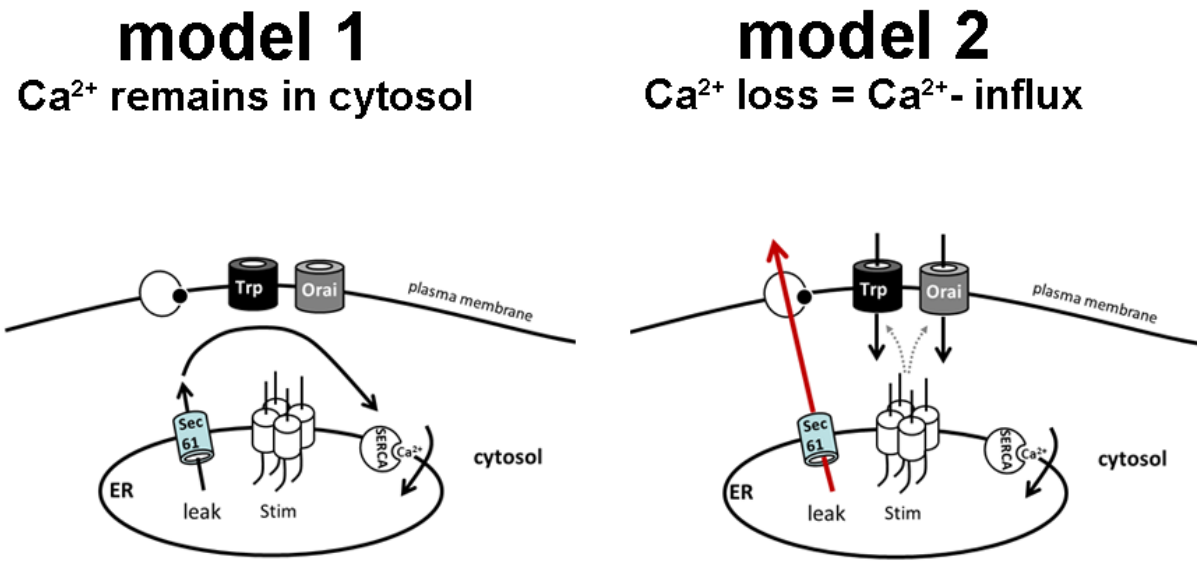

Figure 32: Summary of possible calcium homeostasis models
The Schemes represent possible calcium homeostasis models. In **model 1** calcium ions that leak out of the ER first remain in the cytosol, and are then pumped back into the ER via the Sarco-/endoplasmic reticulum calcium ATPase (SERCA).The new **model 2** is based on our results. Calcium ions leaking from the ER also leave the cytosol and are lost from the cell. This calcium loss is counteracted by a calcium influx mediated by a SOCE-like mechanism and the SERCA pump

First, it was established that the neuronal ER calcium concentration at rest is “medial high”, which enables a high dynamic range for ER calcium release or uptake.

Surprisingly, it was found that a continuous loss of Ca^{2+} into the extracellular space is a prevalent phenomenon in neurons that occurs not only after blockade of the SERCA pump, but also by removal of extracellular calcium. ER calcium, which leaked out of the ER, was not held back in the cytosol but left the neurons through the plasma membrane.

Therefore, it was obvious that a compensatory calcium influx mechanism is needed to maintain resting calcium levels. The finding that acute treatment of neurons with an inhibitor for SOCE caused acute ER calcium loss confirmed for the first time that a SOCE-like calcium influx mechanism is needed to maintain resting ER calcium levels in neurons.

Acute SOCE blockade led to a reduction of ER calcium levels, but did not change cytosolic calcium levels profoundly (figure 28A and B). Rather, transient and sustained SERCA

blockade reduced ER calcium levels, but only transiently changed cytosolic calcium levels. These observations suggest that the calcium fluxes are regulated to achieve a constant cytosolic calcium level.

Although meaningful data were obtained it becomes apparent that measurements of the calcium concentrations would be beneficial for the interpretation, for example to clarify how much calcium remains in the ER and cytosol.

This study is the first thorough study on neuronal ER calcium homeostasis which is based on direct monitoring of ER calcium fluxes at rest.

Before, only indirect evidence for such calcium fluxes were published. Garaschuk *et al.* found that “caffeine depleted calcium stores did not refill in calcium-free saline suggesting that the refilling of the stores depends upon calcium influx through a “capacitative-like” transmembrane influx pathway operating at resting membrane potential” (Garaschuk et al., 1997). Next, STIM2 molecules were identified as regulators of cytosolic and ER calcium levels in a siRNA based screening assay with HeLa cells. STIM2 knockdown lowered the basal cytosolic and ER calcium levels in this cell line, and overexpression increased calcium levels. It was concluded that STIM2 stabilizes basal calcium levels in that cell line (Brandman et al., 2007). However, only cell lines and rough changes by genetic manipulations were used, which can lead to site-effects. Furthermore, results obtained in a cell line can only be indicative for neurons because HeLa cells and neurons differ regarding expression and function of ion channels.

It was also reported that in cultured neurons derived from STIM2$^{-/-}$ mice the amplitude of calcium influx after store depletion by CPA and calcium withdrawal is decreased compared to wildtype controls, and basal cytosolic calcium levels are reduced demonstrating that STIM2 is involved in the regulation of calcium levels in these cells (Berna-Erro et al., 2009). Then, the molecular mechanism was studied in cortical neurons. Using overexpressed, engineered YFP-STIM1 and YFP-STIM2 it was discovered that STIM1 and Orai1 conduct thapsigargin induced SOCE whereas mainly STIM2 regulates resting calcium levels (Gruszczynska-Biegala et al., 2011). This finding was later confirmed with endogenous proteins in cortical neurons using a proximal ligation assay. Here, STIM2-Orai1 complexes were detected after reduction of extracellular calcium, but not after thapsigargin treatment, whereas the number of STIM1-Orai1 complexes increased after thapsigargin treatment (Gruszczynska-Biegala and Kuznicki, 2013).

Recently, it was observed in resting cerebellar granule neurons that SOCE was responsible for the refill of cytosolic calcium after 60 min ca-withdrawal. When calcium was given back to these resting cells, cytosolic calcium levels recovered when all other expressed calcium channels were blocked, but did not rise when SOCE was blocked by SKF-96365 in addition to other calcium permeable channels (Lalonde et al., 2014). Contrasting to our experiments,

in which blockade of SOCE directly influenced the ER calcium levels, SOCE was induced by calcium withdrawal in the Lalonde study.

The Hartmann group reported that STIM1 is essential for the maintenance of basic calcium levels in cerebellar Purkinje neurons. In their study, it was observed that metabotropic or caffeine evoked calcium release signals were absent in Purkinje neurons of conditional Stim1 knockout mice held at resting potential. However, directly after depolarization of these neurons, an ER release signal could be observed, suggesting that only resting ER calcium levels were low (Hartmann et al., 2014). Although this is strong evidence, it can be argued that the complete absence of a main regulator of calcium homeostasis can have more than one specific effect on the cells. By contrast, our neurons were untampered until beginning of the experiments.

All of the above described studies used cytosolic calcium imaging, but neither of the studies directly examined the effect on ER calcium levels. The direct observation that resting ER calcium levels depend on a SOCE-like calcium influx from the extracellular side was not detected before.

It can be concluded from the above studies and our own results that SOCE or at least the SOCE molecular machinery is not only activated after store depletion, but is constantly active in order to maintain resting calcium levels. The molecular machinery responsible for the resting calcium homeostasis is not clear, yet. As summarized above, it appears that different cell types use either STIM1 or STIM2 to regulate basic calcium levels: Cortical and hippocampal neurons use STIM2 and Orai1, but Purkinje neurons use STIM1 (Berna-Erro et al., 2009; Gruszczynska-Biegala and Kuznicki, 2013; Hartmann et al., 2014). Although it was never directly investigated, it can be speculated that the hippocampal neurons used in this project most likely use STIM2 and Orai1 as it was described for hippocampal and cortical neurons. The expression of Orai1 in hippocampal neurons was recently confirmed (Korkotian et al., 2014). Alternatively, low voltage gated calcium channels of the T-type or R-type could mediate the calcium influx. To exclude this possibility the calcium homeostasis experiments would need to be repeated in the presence of nickel ions, which inhibit low voltage activated channels, TTX to block voltage activated sodium channels, CNQX to block AMPA- and kainate receptors and AP-5 to block NMDA-receptors. However, no literature reports point towards the involvement of low voltage activated channels.

At least to our opinion it is unlikely that TrpC channels are responsible for resting calcium fluxes. Best arguments against an involvement of TrpC channels in this process were found when metabotropic signalling cascades were investigated in parallel fibre to Purkinje cell synapses (Hartmann et al., 2008). These studies showed that e.g. TrpC3 loss has no influence on resting ER calcium levels and TrpC3 activity was embedded into the metabotropic glutamate signalling process.

Possible molecular mechanism:

The herein proposed model of resting calcium fluxes presupposes the involvement of a multitude of calcium sensing, regulating, and conducting proteins. Apart from STIM1 or STIM2 and their partner Orai, the molecules mediating these calcium fluxes are unknown but possible candidates exist within the neuronal “calcium toolkit” (Berridge et al., 2000).

Two main mechanisms exist to clear calcium from cells: Plasma membrane calcium ATPases (PMCA) and sodium calcium exchangers (NCX) (Brini and Carafoli, 2011). Isoforms of both molecules are expressed in neurons (Canitano et al., 2002; Kip et al., 2006; Minelli et al., 2007; Strehler and Zacharias, 2001) and were shown to be involved in regulating cytosolic calcium concentration.

All, out of 3, NCX isoforms have a high capacity of pumping calcium but only a low calcium affinity suggesting that they respond to subtle changes in calcium concentration (Brini and Carafoli, 2011).

Some studies reported a functional connection between NCX molecules and the ER calcium store. Wu *et al*. demonstrated in 2008 that NCX operating in reverse mode releases calcium from the ER in cultured neurons (Wu et al., 2008). Additionally, it was reported in 2009 that NCX1 upregulation induced by anoxia in cortical neurons plays a role in refilling the ER calcium store (Sirabella et al., 2009) and Sisalli *et al*. recently reported that upregulation of NXC1 during ischemic preconditioning might control ER calcium levels (Sisalli et al., 2014).

The importance of this molecule in calcium homeostasis was already suggested years ago (Molinaro et al., 2008) and further confirmed in recent reports in which disturbed calcium homeostasis was investigated. In Alzheimer`s disease, Calpain was shown to cleave and inactivate NCX3 and this was suggested to contribute to calcium dysregulation and neuronal dysfunction (Atherton et al., 2014). Furthermore, NCX3, regulated by Collapsin response mediator protein 2, was shown to protect against glutamate induced calcium dysregulation in primary hippocampal neurons (Brustovetsky et al., 2014).

On the other hand, some properties would limit NCX `s potentially constant activity. First, NCX exchanges three Na^+ ions for one Ca^{2+} ion and constant operation of this pump would shift the membrane potential towards depolarization. Furthermore, subtle changes in membrane potential or ion concentration can induce NCX to operate in a reverse mode, pumping Ca^{2+} into the cells (Lytton, 2007).

The second calcium extrusion mechanism of eukaryotic cells involves PMCA pumps. PMCAs were suggested to be the major calcium transport system and responsible for the long term regulation of resting free calcium (Zaidi, 2010). But more recently PMCAs were in focus for being responsible for locally and spatially restricted calcium dynamics because their activity is highly regulated by e.g. Calmodulin/calcium and phosphorylation by protein

kinases (Brini and Carafoli, 2011; Di Leva et al., 2008; Lopreiato et al., 2014). PMCA2 was found to influence locally restricted calcium signals in Purkinje neurons (Roome et al., 2013). Considering all information about the NCX calcium extrusion mechanism and the PMCA pump it appears most likely that a combination of several of those molecules is responsible for the calcium extrusion. This would also allow neurons to adapt their calcium dynamics to environmental changes because the activity, localization, and expression of each single molecule could be regulated according to specific demands (Brini and Carafoli, 2011).

Additionally, molecules providing the sensing and regulatory function exist. In the ER, CBPs can be activated by calcium (see introduction 1.1) and STIM1/2 senses the calcium concentration. In the cytosol the calcium concentration can be sensed by CBPs and by RyRs as well. Several other neuronal calcium sensors exist, that could be involved in the regulation of calcium homeostasis, for example NCS-1, VILIP 1, and hippocalcin (Braunewell and Gundelfinger, 1999; Burgoyne, 2007). Finally, the extracellular calcium concentration is monitored by the calcium sensing receptor CaSR which was already shown to be relevant for local ionic homeostasis, membrane excitability and synaptic transmission (Bandyopadhyay et al., 2010; Ruat and Traiffort, 2013).

All these proteins could conduct the suggested calcium model, but detailed investigations about their functions and possible interrelation is still missing.

Specialized microdomains in the ER:

Considering the different ER functions, from protein-synthesis to calcium homeostasis, and the energy expenses caused by the calcium leakage, it might be beneficial for a neuron to divide the ER into subcompartments specialised for the one or other function. It is known that the ER is a continuous membranous organelle (see introduction), but it was also reported that local molecular arrangements indeed exist in the ER. Orci *et al*. analysed HeLa cells after SOCE induction and reported that the molecules involved in SOCE accumulate in “thin cortical ER” which is enriched with STIM1 but devoid of BIP and ribosomes (Orci et al., 2009).

Such an arrangement would result in ER domains of calcium leakage and protein synthesis and other domains with calcium influx. However, such localized calcium fluxes were not investigated in this study.

Calcium homeostasis of various cell types:

Current literature and own observations suggest that the continuous calcium fluxes are a widely-spread mechanism. Detailed observation were made in cerebellar Purkinje neurons (Hartmann et al., 2014), cerebellar granule neurons (Lalonde et al., 2014) and hippocampal and cortical neurons (Berna-Erro et al., 2009). Another study used cell lines (Brandman et al., 2007). As depicted in figure 31 (see 3.3.6) calcium withdrawal led to a reversible decline in calcium levels in astrocytes as well. SOCE may therefore play a role in calcium

homeostasis in different cell types and, as mentioned before, the detailed nature of the involved mechanism might vary in different cell types and types of neurons.

Physiological function of the calcium flux:

The function or molecular nature of the ER calcium leak is still mostly elusive. It was shown that calcium is lost from the ER via SEC61 complexes during protein transcription at the ribosome covered rough ER (Lang et al., 2011a; Lang et al., 2011b; Schäuble et al., 2012) and ER calcium loss therefore appears to be unavoidable. It is possible that the observed calcium influx is simply a mechanism to counteract this ER calcium loss. Nevertheless, the herein suggested model of calcium fluxes implicates consequences for neurons.

Although discovered in embryonic stem cells, it appears accepted that STIM1 and STIM2 molecules can inhibit Ca_v (Harraz and Altier, 2014; Hooper et al., 2014; Soboloff et al., 2012). As a consequence, STIM activation by SOCE can influence the excitability of neurons directly. Additionally, (Lalonde et al., 2014) discovered that under resting conditions SOCE activated phosphorylation of the transcription factor CREB and led to degradation of the transcription factor Sp4 (Lalonde et al., 2014). Because CREB is known to regulate synaptic plasticity, SOCE may play a role in neuronal excitability.

In addition, the hypothesized model implicates that the neurons invest a lot of energy to operate the involved ion pumps in order to maintain a basal calcium level (Hooper et al., 2014). A challenging question is whether there is a physiological role of the resting calcium fluxes. Neurons are at a higher risk to suffer from a massive and sudden calcium influx e.g. caused by strong neuronal stimulation than from calcium deprivation. The constitutive calcium efflux could prevent the neurons from a permanent calcium overflow. It appears easier, or at least faster, to control a store with a permanent influx and efflux than a less dynamic store. Expressed in an allegory: It is more difficult to overflow a reservoir than a lake. Additionally, this seemingly complicated system could provide a more efficient tool to regulate and integrate all calcium fluxes within a neuron.

References

Abbracchio, M.P., and S. Ceruti. 2006. Roles of P2 receptors in glial cells: focus on astrocytes. *Purinergic signalling*. 2:595-604.

Al-Mousa, F., and F. Michelangeli. 2009. Commonly used ryanodine receptor activator, 4-chloro-m-cresol (4CmC), is also an inhibitor of SERCA Ca2+ pumps. *Pharmacological reports : PR*. 61:838-842.

Andreska, T., S. Aufmkolk, M. Sauer, and R. Blum. 2014. High abundance of BDNF within glutamatergic presynapses of cultured hippocampal neurons. *Frontiers in cellular neuroscience*. 8:107.

Atherton, J., K. Kurbatskaya, M. Bondulich, C.L. Croft, C.J. Garwood, R. Chhabra, S. Wray, A. Jeromin, D.P. Hanger, and W. Noble. 2014. Calpain cleavage and inactivation of the sodium calcium exchanger-3 occur downstream of Abeta in Alzheimer's disease. *Aging cell*. 13:49-59.

Bading, H. 2013. Nuclear calcium signalling in the regulation of brain function. *Nature reviews. Neuroscience*. 14:593-608.

Bandyopadhyay, S., J. Tfelt-Hansen, and N. Chattopadhyay. 2010. Diverse roles of extracellular calcium-sensing receptor in the central nervous system. *Journal of neuroscience research*. 88:2073-2082.

Beck, A., R.Z. Nieden, H.P. Schneider, and J.W. Deitmer. 2004. Calcium release from intracellular stores in rodent astrocytes and neurons in situ. *Cell Calcium*. 35:47-58.

Belevych, A., Z. Kubalova, D. Terentyev, R.L. Hamlin, C.A. Carnes, and S. Gyorke. 2007. Enhanced ryanodine receptor-mediated calcium leak determines reduced sarcoplasmic reticulum calcium content in chronic canine heart failure. *Biophysical journal*. 93:4083-4092.

Berna-Erro, A., A. Braun, R. Kraft, C. Kleinschnitz, M.K. Schuhmann, D. Stegner, T. Wultsch, J. Eilers, S.G. Meuth, G. Stoll, and B. Nieswandt. 2009. STIM2 regulates capacitive Ca2+ entry in neurons and plays a key role in hypoxic neuronal cell death. *Science signaling*. 2:ra67.

Berna-Erro, A., G.E. Woodard, and J.A. Rosado. 2012. Orais and STIMs: physiological mechanisms and disease. *Journal of cellular and molecular medicine*. 16:407-424.

Berridge, M.J. 1998. Neuronal calcium signaling. *Neuron*. 21:13-26.

Berridge, M.J. 2002. The endoplasmic reticulum: a multifunctional signaling organelle. *Cell Calcium*. 32:235-249.

Berridge, M.J. 2006. Calcium microdomains: organization and function. *Cell Calcium*. 40:405-412.

Berridge, M.J., M.D. Bootman, and H.L. Roderick. 2003. Calcium signalling: dynamics, homeostasis and remodelling. *Nature reviews. Molecular cell biology*. 4:517-529.

Berridge, M.J., P. Lipp, and M.D. Bootman. 2000. The versatility and universality of calcium signalling. *Nat Rev Mol Cell Bio*. 1:11-21.

Bezprozvanny, I.B. 2010. Calcium signaling and neurodegeneration. *Acta naturae*. 2:72-82.

Blum, R., O. Petersen, and A. Verkhratsky. 2010. Ca2+ Imaging of Intracellular Organelles: Endoplasmic Reticulum. *Neuromethods*. 43:147-167.

Boulay, G., X. Zhu, M. Peyton, M. Jiang, R. Hurst, E. Stefani, and L. Birnbaumer. 1997. Cloning and expression of a novel mammalian homolog of Drosophila transient

receptor potential (Trp) involved in calcium entry secondary to activation of receptors coupled by the Gq class of G protein. *The Journal of biological chemistry*. 272:29672-29680.

Brandman, O., J. Liou, W.S. Park, and T. Meyer. 2007. STIM2 is a feedback regulator that stabilizes basal cytosolic and endoplasmic reticulum Ca2+ levels. *Cell*. 131:1327-1339.

Braunewell, K.H., and E.D. Gundelfinger. 1999. Intracellular neuronal calcium sensor proteins: a family of EF-hand calcium-binding proteins in search of a function. *Cell and tissue research*. 295:1-12.

Brini, M., and E. Carafoli. 2011. The plasma membrane Ca(2)+ ATPase and the plasma membrane sodium calcium exchanger cooperate in the regulation of cell calcium. *Cold Spring Harbor perspectives in biology*. 3.

Brustovetsky, T., J.J. Pellman, X.F. Yang, R. Khanna, and N. Brustovetsky. 2014. Collapsin response mediator protein 2 (CRMP2) interacts with N-methyl-D-aspartate (NMDA) receptor and Na+/Ca2+ exchanger and regulates their functional activity. *The Journal of biological chemistry*. 289:7470-7482.

Burdakov, D., O.H. Petersen, and A. Verkhratsky. 2005. Intraluminal calcium as a primary regulator of endoplasmic reticulum function. *Cell Calcium*. 38:303-310.

Burgoyne, R.D. 2007. Neuronal calcium sensor proteins: generating diversity in neuronal Ca2+ signalling. *Nature reviews. Neuroscience*. 8:182-193.

Cahalan, M.D. 2009. STIMulating store-operated Ca(2+) entry. *Nature cell biology*. 11:669-677.

Cali, T., D. Ottolini, and M. Brini. 2014. Calcium signaling in Parkinson's disease. *Cell and tissue research*.

Camello, C., R. Lomax, O.H. Petersen, and A.V. Tepikin. 2002. Calcium leak from intracellular stores--the enigma of calcium signalling. *Cell Calcium*. 32:355-361.

Campsall, K.D., C.J. Mazerolle, Y. De Repentingy, R. Kothary, and V.A. Wallace. 2002. Characterization of transgene expression and Cre recombinase activity in a panel of Thy-1 promoter-Cre transgenic mice. *Developmental dynamics : an official publication of the American Association of Anatomists*. 224:135-143.

Canitano, A., M. Papa, F. Boscia, P. Castaldo, S. Sellitti, M. Taglialatela, and L. Annunziato. 2002. Brain distribution of the Na+/Ca2+ exchanger-encoding genes NCX1, NCX2, and NCX3 and their related proteins in the central nervous system. *Annals of the New York Academy of Sciences*. 976:394-404.

Carafoli, E., L. Santella, D. Branca, and M. Brini. 2001. Generation, control, and processing of cellular calcium signals. *Critical reviews in biochemistry and molecular biology*. 36:107-260.

Caroni, P. 1997. Overexpression of growth-associated proteins in the neurons of adult transgenic mice. *Journal of neuroscience methods*. 71:3-9.

Chen, J., K.H. Backus, and J.W. Deitmer. 1997. Intracellular calcium transients and potassium current oscillations evoked by glutamate in cultured rat astrocytes. *The Journal of neuroscience : the official journal of the Society for Neuroscience*. 17:7278-7287.

Choi, Y.M., S.H. Kim, S. Chung, D.Y. Uhm, and M.K. Park. 2006. Regional interaction of endoplasmic reticulum Ca2+ signals between soma and dendrites through rapid luminal Ca2+ diffusion. *The Journal of neuroscience : the official journal of the Society for Neuroscience*. 26:12127-12136.

Cooney, J.R., J.L. Hurlburt, D.K. Selig, K.M. Harris, and J.C. Fiala. 2002. Endosomal compartments serve multiple hippocampal dendritic spines from a widespread rather than a local store of recycling membrane. *The Journal of neuroscience : the official journal of the Society for Neuroscience*. 22:2215-2224.

D'Antoni, S., A. Berretta, C.M. Bonaccorso, V. Bruno, E. Aronica, F. Nicoletti, and M.V. Catania. 2008. Metabotropic glutamate receptors in glial cells. *Neurochemical research*. 33:2436-2443.

Deguchi, Y., F. Donato, I. Galimberti, E. Cabuy, and P. Caroni. 2011. Temporally matched subpopulations of selectively interconnected principal neurons in the hippocampus. *Nature neuroscience*. 14:495-504.

Di Leva, F., T. Domi, L. Fedrizzi, D. Lim, and E. Carafoli. 2008. The plasma membrane Ca2+ ATPase of animal cells: structure, function and regulation. *Archives of biochemistry and biophysics*. 476:65-74.

Dittgen, T., A. Nimmerjahn, S. Komai, P. Licznerski, J. Waters, T.W. Margrie, F. Helmchen, W. Denk, M. Brecht, and P. Osten. 2004. Lentivirus-based genetic manipulations of cortical neurons and their optical and electrophysiological monitoring in vivo. *Proceedings of the National Academy of Sciences of the United States of America*. 101:18206-18211.

Erb, L., Z. Liao, C.I. Seye, and G.A. Weisman. 2006. P2 receptors: intracellular signaling. *Pflugers Archiv : European journal of physiology*. 452:552-562.

Feng, G., R.H. Mellor, M. Bernstein, C. Keller-Peck, Q.T. Nguyen, M. Wallace, J.M. Nerbonne, J.W. Lichtman, and J.R. Sanes. 2000. Imaging neuronal subsets in transgenic mice expressing multiple spectral variants of GFP. *Neuron*. 28:41-51.

Feske, S., Y. Gwack, M. Prakriya, S. Srikanth, S.H. Puppel, B. Tanasa, P.G. Hogan, R.S. Lewis, M. Daly, and A. Rao. 2006. A mutation in Orai1 causes immune deficiency by abrogating CRAC channel function. *Nature*. 441:179-185.

Filippin, L., M.C. Abad, S. Gastaldello, P.J. Magalhaes, D. Sandona, and T. Pozzan. 2005. Improved strategies for the delivery of GFP-based Ca2+ sensors into the mitochondrial matrix. *Cell Calcium*. 37:129-136.

Fill, M., and J.A. Copello. 2002. Ryanodine receptor calcium release channels. *Physiological reviews*. 82:893-922.

Galeotti, N., A. Quattrone, E. Vivoli, M. Norcini, A. Bartolini, and C. Ghelardini. 2008. Different involvement of type 1, 2, and 3 ryanodine receptors in memory processes. *Learning & memory*. 15:315-323.

Gall, D., C. Roussel, I. Susa, E. D'Angelo, P. Rossi, B. Bearzatto, M.C. Galas, D. Blum, S. Schurmans, and S.N. Schiffmann. 2003. Altered neuronal excitability in cerebellar granule cells of mice lacking calretinin. *The Journal of neuroscience : the official journal of the Society for Neuroscience*. 23:9320-9327.

Garaschuk, O., Y. Yaari, and A. Konnerth. 1997. Release and sequestration of calcium by ryanodine-sensitive stores in rat hippocampal neurones. *The Journal of physiology*. 502 (Pt 1):13-30.

Goldberg, J.H., G. Tamas, D. Aronov, and R. Yuste. 2003. Calcium microdomains in aspiny dendrites. *Neuron*. 40:807-821.

Gomez, T.M., and J.Q. Zheng. 2006. The molecular basis for calcium-dependent axon pathfinding. *Nature reviews. Neuroscience*. 7:115-125.

Grienberger, C., and A. Konnerth. 2012. Imaging calcium in neurons. *Neuron*. 73:862-885.

Griesbeck, O., G.S. Baird, R.E. Campbell, D.A. Zacharias, and R.Y. Tsien. 2001. Reducing the environmental sensitivity of yellow fluorescent protein. Mechanism and applications. *The Journal of biological chemistry*. 276:29188-29194.

Gruszczynska-Biegala, J., and J. Kuznicki. 2013. Native STIM2 and ORAI1 proteins form a calcium-sensitive and thapsigargin-insensitive complex in cortical neurons. *Journal of neurochemistry*.

Gruszczynska-Biegala, J., P. Pomorski, M.B. Wisniewska, and J. Kuznicki. 2011. Differential roles for STIM1 and STIM2 in store-operated calcium entry in rat neurons. *PloS one*. 6:e19285.

Guerrero-Hernandez, A., A. Dagnino-Acosta, and A. Verkhratsky. 2010. An intelligent sarco-endoplasmic reticulum Ca2+ store: Release and leak channels have differential access to a concealed Ca2+ pool. *Cell Calcium*. 48:143-149.

Guoping Feng, R.H.M., †, C.K.-P. Michael Bernstein, *, M.W. Quyen T. Nguyen, *, J.W.L. Jeanne M. Nerbonne, *, and a.J.R. Sanes*‡. 2000. Imaging Neuronal Subsets in Transgenic Mice Expressing Multiple Spectral Variants of GFP. *Neuron*. 28: 41–51.

Harraz, O.F., and C. Altier. 2014. STIM1-mediated bidirectional regulation of Ca(2+) entry through voltage-gated calcium channels (VGCC) and calcium-release activated channels (CRAC). *Frontiers in cellular neuroscience*. 8:43.

Hartmann, J., E. Dragicevic, H. Adelsberger, H.A. Henning, M. Sumser, J. Abramowitz, R. Blum, A. Dietrich, M. Freichel, V. Flockerzi, L. Birnbaumer, and A. Konnerth. 2008. TRPC3 channels are required for synaptic transmission and motor coordination. *Neuron*. 59:392-398.

Hartmann, J., R.M. Karl, R.P. Alexander, H. Adelsberger, M.S. Brill, C. Ruhlmann, A. Ansel, K. Sakimura, Y. Baba, T. Kurosaki, T. Misgeld, and A. Konnerth. 2014. STIM1 Controls Neuronal Ca(2+) Signaling, mGluR1-Dependent Synaptic Transmission, and Cerebellar Motor Behavior. *Neuron*. 82:635-644.

Higley, M.J., and B.L. Sabatini. 2012. Calcium signaling in dendritic spines. *Cold Spring Harbor perspectives in biology*. 4:a005686.

Hirrlinger, P.G., A. Scheller, C. Braun, M. Quintela-Schneider, B. Fuss, J. Hirrlinger, and F. Kirchhoff. 2005. Expression of reef coral fluorescent proteins in the central nervous system of transgenic mice. *Molecular and cellular neurosciences*. 30:291-303.

Hofer, A.M., and T.E. Machen. 1993. Technique for in situ measurement of calcium in intracellular inositol 1,4,5-trisphosphate-sensitive stores using the fluorescent indicator mag-fura-2. *Proceedings of the National Academy of Sciences of the United States of America*. 90:2598-2602.

Holbro, N., A. Grunditz, and T.G. Oertner. 2009. Differential distribution of endoplasmic reticulum controls metabotropic signaling and plasticity at hippocampal synapses. *Proceedings of the National Academy of Sciences of the United States of America*. 106:15055-15060.

Hooper, R., B.S. Rothberg, and J. Soboloff. 2014. Neuronal STIMulation at Rest. *Science signaling*. 7:pe18.

Hoth, M., and R. Penner. 1992. Depletion of intracellular calcium stores activates a calcium current in mast cells. *Nature*. 355:353-356.

Huang, G.N., W. Zeng, J.Y. Kim, J.P. Yuan, L. Han, S. Muallem, and P.F. Worley. 2006. STIM1 carboxyl-terminus activates native SOC, I(crac) and TRPC1 channels. *Nature cell biology*. 8:1003-1010.

Irving, A.J., and G.L. Collingridge. 1998. A characterization of muscarinic receptor-mediated intracellular Ca2+ mobilization in cultured rat hippocampal neurones. *The Journal of physiology*. 511 (Pt 3):747-759.

Jacob, S.N., C.U. Choe, P. Uhlen, B. DeGray, M.F. Yeckel, and B.E. Ehrlich. 2005. Signaling microdomains regulate inositol 1,4,5-trisphosphate-mediated intracellular calcium transients in cultured neurons. *The Journal of neuroscience : the official journal of the Society for Neuroscience*. 25:2853-2864.

Jaepel, J., and R. Blum. 2011. Capturing ER calcium dynamics. *European journal of cell biology*. 90:613-619.

Jardin, I., J.J. Lopez, G.M. Salido, and J.A. Rosado. 2008. Orai1 mediates the interaction between STIM1 and hTRPC1 and regulates the mode of activation of hTRPC1-forming Ca2+ channels. *The Journal of biological chemistry*. 283:25296-25304.

Jedlicka, P., A. Vlachos, S.W. Schwarzacher, and T. Deller. 2008. A role for the spine apparatus in LTP and spatial learning. *Behav Brain Res*. 192:12-19.

Kip, S.N., N.W. Gray, A. Burette, A. Canbay, R.J. Weinberg, and E.E. Strehler. 2006. Changes in the expression of plasma membrane calcium extrusion systems during the maturation of hippocampal neurons. *Hippocampus*. 16:20-34.

Koles, L., A. Leichsenring, P. Rubini, and P. Illes. 2011. P2 receptor signaling in neurons and glial cells of the central nervous system. *Advances in pharmacology*. 61:441-493

Korkotian, E., M. Frotscher, and M. Segal. 2014. Synaptopodin regulates spine plasticity: mediation by calcium stores. *The Journal of neuroscience : the official journal of the Society for Neuroscience*. 34:11641-11651.

Korkotian, E., and M. Segal. 1999. Release of calcium from stores alters the morphology of dendritic spines in cultured hippocampal neurons. *Proceedings of the National Academy of Sciences of the United States of America*. 96:12068-12072.

Krause, K.H., and M. Michalak. 1997. Calreticulin. *Cell*. 88:439-443.

Kubalova, Z., I. Gyorke, R. Terentyeva, S. Viatchenko-Karpinski, D. Terentyev, S.C. Williams, and S. Gyorke. 2004. Modulation of cytosolic and intra-sarcoplasmic reticulum calcium waves by calsequestrin in rat cardiac myocytes. *The Journal of physiology*. 561:515-524.

Lalonde, J., G. Saia, and G. Gill. 2014. Store-operated calcium entry promotes the degradation of the transcription factor Sp4 in resting neurons. *Science signaling*. 7:ra51.

Lang, S., F. Erdmann, M. Jung, R. Wagner, A. Cavalie, and R. Zimmermann. 2011a. Sec61 complexes form ubiquitous ER Ca2+ leak channels. *Channels (Austin)*. 5:228-235.

Lang, S., N. Schauble, A. Cavalie, and R. Zimmermann. 2011b. Live cell calcium imaging combined with siRNA mediated gene silencing identifies Ca(2)(+) leak channels in the ER membrane and their regulatory mechanisms. *Journal of visualized experiments : JoVE*:e2730.

Lanner, J.T., D.K. Georgiou, A.D. Joshi, and S.L. Hamilton. 2010. Ryanodine receptors: structure, expression, molecular details, and function in calcium release. *Cold Spring Harbor perspectives in biology*. 2:a003996.

Laporte, R., A. Hui, and I. Laher. 2004. Pharmacological modulation of sarcoplasmic reticulum function in smooth muscle. *Pharmacological reviews*. 56:439-513.

Lewis, R.S. 2011. Store-operated calcium channels: new perspectives on mechanism and function. *Cold Spring Harbor perspectives in biology*. 3.

Liao, Y., N.W. Plummer, M.D. George, J. Abramowitz, M.X. Zhu, and L. Birnbaumer. 2009. A role for Orai in TRPC-mediated Ca2+ entry suggests that a TRPC:Orai complex may mediate store and receptor operated Ca2+ entry. *Proceedings of the National Academy of Sciences of the United States of America*. 106:3202-3206.

Liou, J., M.L. Kim, W.D. Heo, J.T. Jones, J.W. Myers, J.E. Ferrell, Jr., and T. Meyer. 2005. STIM is a Ca2+ sensor essential for Ca2+-store-depletion-triggered Ca2+ influx. *Current biology : CB*. 15:1235-1241.

Liu, X., M.J. Betzenhauser, S. Reiken, A.C. Meli, W. Xie, B.X. Chen, O. Arancio, and A.R. Marks. 2012. Role of leaky neuronal ryanodine receptors in stress-induced cognitive dysfunction. *Cell*. 150:1055-1067.

Lois, C., E.J. Hong, S. Pease, E.J. Brown, and D. Baltimore. 2002. Germline transmission and tissue-specific expression of transgenes delivered by lentiviral vectors. *Science*. 295:868-872.

Lopreiato, R., M. Giacomello, and E. Carafoli. 2014. The plasma membrane calcium pump: new ways to look at an old enzyme. *The Journal of biological chemistry*. 289:10261-10268.

Luik, R.M., M.M. Wu, J. Buchanan, and R.S. Lewis. 2006. The elementary unit of store-operated Ca2+ entry: local activation of CRAC channels by STIM1 at ER-plasma membrane junctions. *The Journal of cell biology*. 174:815-825.

Marambaud, P., U. Dreses-Werringloer, and V. Vingtdeux. 2009. Calcium signaling in neurodegeneration. *Molecular neurodegeneration*. 4:20.

Matyash, M., V. Matyash, C. Nolte, V. Sorrentino, and H. Kettenmann. 2002. Requirement of functional ryanodine receptor type 3 for astrocyte migration. *FASEB journal : official publication of the Federation of American Societies for Experimental Biology*. 16:84-86.

McKemy, D.D., W. Welch, J.A. Airey, and J.L. Sutko. 2000. Concentrations of caffeine greater than 20 mM increase the indo-1 fluorescence ratio in a Ca(2+)-independent manner. *Cell Calcium*. 27:117-124.

McPherson, P.S., Y.K. Kim, H. Valdivia, C.M. Knudson, H. Takekura, C. Franzini-Armstrong, R. Coronado, and K.P. Campbell. 1991. The brain ryanodine receptor: a caffeine-sensitive calcium release channel. *Neuron*. 7:17-25.

Medda, S., and R.L. Proia. 1992. The carboxylesterase family exhibits C-terminal sequence diversity reflecting the presence or absence of endoplasmic-reticulum-retention sequences. *European journal of biochemistry / FEBS*. 206:801-806.

Mellstrom, B., M. Savignac, R. Gomez-Villafuertes, and J.R. Naranjo. 2008. Ca2+-operated transcriptional networks: molecular mechanisms and in vivo models. *Physiological reviews*. 88:421-449.

Merritt, J.E., W.P. Armstrong, C.D. Benham, T.J. Hallam, R. Jacob, A. Jaxa-Chamiec, B.K. Leigh, S.A. McCarthy, K.E. Moores, and T.J. Rink. 1990. SK&F 96365, a novel inhibitor of receptor-mediated calcium entry. *The Biochemical journal*. 271:515-522.

Miller, R.J. 1991. The control of neuronal Ca2+ homeostasis. *Progress in neurobiology*. 37:255-285.

Minelli, A., P. Castaldo, P. Gobbi, S. Salucci, S. Magi, and S. Amoroso. 2007. Cellular and subcellular localization of Na+-Ca2+ exchanger protein isoforms, NCX1, NCX2, and NCX3 in cerebral cortex and hippocampus of adult rat. *Cell Calcium*. 41:221-234.

Mitchell, C.B., R.J. Gasperini, D.H. Small, and L. Foa. 2012. STIM1 is necessary for store-operated calcium entry in turning growth cones. *Journal of neurochemistry*. 122:1155-1166.

Miyawaki, A., J. Llopis, R. Heim, J.M. McCaffery, J.A. Adams, M. Ikura, and R.Y. Tsien. 1997. Fluorescent indicators for Ca2+ based on green fluorescent proteins and calmodulin. *Nature*. 388:882-887.

Molinaro, P., O. Cuomo, G. Pignataro, F. Boscia, R. Sirabella, A. Pannaccione, A. Secondo, A. Scorziello, A. Adornetto, R. Gala, D. Viggiano, S. Sokolow, A. Herchuelz, S. Schurmans, G. Di Renzo, and L. Annunziato. 2008. Targeted disruption of Na+/Ca2+ exchanger 3 (NCX3) gene leads to a worsening of ischemic brain damage. *The Journal of neuroscience : the official journal of the Society for Neuroscience*. 28:1179-1184.

Nagai, T., A. Sawano, E.S. Park, and A. Miyawaki. 2001. Circularly permuted green fluorescent proteins engineered to sense Ca2+. *Proceedings of the National Academy of Sciences of the United States of America*. 98:3197-3202.

Nakai, J., M. Ohkura, and K. Imoto. 2001. A high signal-to-noise Ca(2+) probe composed of a single green fluorescent protein. *Nature biotechnology*. 19:137-141.

Nash, M.S., M.J. Schell, P.J. Atkinson, N.R. Johnston, S.R. Nahorski, and R.A. Challiss. 2002. Determinants of metabotropic glutamate receptor-5-mediated Ca2+ and inositol 1,4,5-trisphosphate oscillation frequency. Receptor density versus agonist concentration. *The Journal of biological chemistry*. 277:35947-35960.

Ng, A.N., M. Krogh, and H. Toresson. 2011. Dendritic EGFP-STIM1 activation after type I metabotropic glutamate and muscarinic acetylcholine receptor stimulation in hippocampal neuron. *Journal of neuroscience research*. 89:1235-1244.

Orci, L., M. Ravazzola, M. Le Coadic, W.W. Shen, N. Demaurex, and P. Cosson. 2009. From the Cover: STIM1-induced precortical and cortical subdomains of the endoplasmic reticulum. *Proceedings of the National Academy of Sciences of the United States of America*. 106:19358-19362.

Palmer, A.E., M. Giacomello, T. Kortemme, S.A. Hires, V. Lev-Ram, D. Baker, and R.Y. Tsien. 2006. Ca2+ indicators based on computationally redesigned calmodulin-peptide pairs. *Chemistry & biology*. 13:521-530.

Palmer, A.E., C. Jin, J.C. Reed, and R.Y. Tsien. 2004. Bcl-2-mediated alterations in endoplasmic reticulum Ca2+ analyzed with an improved genetically encoded fluorescent sensor. *Proceedings of the National Academy of Sciences of the United States of America*. 101:17404-17409.

Palmer, A.E., and R.Y. Tsien. 2006. Measuring calcium signaling using genetically targetable fluorescent indicators. *Nature protocols*. 1:1057-1065.

Paredes, R.M., J.C. Etzler, L.T. Watts, W. Zheng, and J.D. Lechleiter. 2008. Chemical calcium indicators. *Methods*. 46:143-151.

Park, M.K., Y.M. Choi, Y.K. Kang, and O.H. Petersen. 2008. The endoplasmic reticulum as an integrator of multiple dendritic events. *The Neuroscientist : a review journal bringing neurobiology, neurology and psychiatry*. 14:68-77.

Porrero, C., P. Rubio-Garrido, C. Avendano, and F. Clasca. 2010. Mapping of fluorescent protein-expressing neurons and axon pathways in adult and developing Thy1-eYFP-H transgenic mice. *Brain research*. 1345:59-72.

Putney, J.W., Jr. 1986. A model for receptor-regulated calcium entry. *Cell Calcium*. 7:1-12.

Putney, J.W., Jr. 2007. New molecular players in capacitative Ca2+ entry. *Journal of cell science*. 120:1959-1965.

Rae, M.G., D.J. Martin, G.L. Collingridge, and A.J. Irving. 2000. Role of Ca2+ stores in metabotropic L-glutamate receptor-mediated supralinear Ca2+ signaling in rat hippocampal neurons. *The Journal of neuroscience : the official journal of the Society for Neuroscience*. 20:8628-8636.

Ralevic, V., and G. Burnstock. 1998. Receptors for purines and pyrimidines. *Pharmacological reviews*. 50:413-492.

Ramirez, O.A., and A. Couve. 2011. The endoplasmic reticulum and protein trafficking in dendrites and axons. *Trends in cell biology*. 21:219-227.

Rehberg, M., A. Lepier, B. Solchenberger, P. Osten, and R. Blum. 2008. A new non-disruptive strategy to target calcium indicator dyes to the endoplasmic reticulum. *Cell Calcium*. 44:386-399.

Rizzuto, R., A.W. Simpson, M. Brini, and T. Pozzan. 1992. Rapid changes of mitochondrial Ca2+ revealed by specifically targeted recombinant aequorin. *Nature*. 358:325-327.

Rodriguez-Garcia, A., J. Rojo-Ruiz, P. Navas-Navarro, F.J. Aulestia, S. Gallego-Sandin, J. Garcia-Sancho, and M.T. Alonso. 2014. GAP, an aequorin-based fluorescent indicator for imaging Ca2+ in organelles. *Proceedings of the National Academy of Sciences of the United States of America*. 111:2584-2589.

Roome, C.J., T. Knopfel, and R.M. Empson. 2013. Functional contributions of the plasma membrane calcium ATPase and the sodium-calcium exchanger at mouse parallel fibre to Purkinje neuron synapses. *Pflugers Archiv : European journal of physiology*. 465:319-331.

Roos, J., P.J. DiGregorio, A.V. Yeromin, K. Ohlsen, M. Lioudyno, S. Zhang, O. Safrina, J.A. Kozak, S.L. Wagner, M.D. Cahalan, G. Velicelebi, and K.A. Stauderman. 2005. STIM1, an essential and conserved component of store-operated Ca2+ channel function. *The Journal of cell biology*. 169:435-445.

Rose, C.R., and A. Konnerth. 2001. Stores not just for storage. intracellular calcium release and synaptic plasticity. *Neuron*. 31:519-522.

Rousseau, E., J.S. Smith, and G. Meissner. 1987. Ryanodine modifies conductance and gating behavior of single Ca2+ release channel. *The American journal of physiology*. 253:C364-368.

Roussel, C., T. Erneux, S.N. Schiffmann, and D. Gall. 2006. Modulation of neuronal excitability by intracellular calcium buffering: from spiking to bursting. *Cell Calcium*. 39:455-466.

Ruat, M., and E. Traiffort. 2013. Roles of the calcium sensing receptor in the central nervous system. *Best practice & research. Clinical endocrinology & metabolism*. 27:429-442.

Salter, M.W., and J.L. Hicks. 1995. ATP causes release of intracellular Ca2+ via the phospholipase C beta/IP3 pathway in astrocytes from the dorsal spinal cord. *The Journal of neuroscience : the official journal of the Society for Neuroscience*. 15:2961-2971.

Samtleben, S., J. Jaepel, C. Fecher, T. Andreska, M. Rehberg, and R. Blum. 2013. Direct imaging of ER calcium with targeted-esterase induced dye loading (TED). *Journal of visualized experiments : JoVE*:e50317.

Satoh, T., and M. Hosokawa. 2006. Structure, function and regulation of carboxylesterases. *Chemico-biological interactions*. 162:195-211.

Schäuble, N., S. Lang, M. Jung, S. Cappel, S. Schorr, O. Ulucan, J. Linxweiler, J. Dudek, R. Blum, V. Helms, A.W. Paton, J.C. Paton, A. Cavalie, and R. Zimmermann. 2012. BiP-mediated closing of the Sec61 channel limits Ca2+ leakage from the ER. *The EMBO journal*. 31:3282-3296.

Schmidt, H., and J. Eilers. 2009. Spine neck geometry determines spino-dendritic cross-talk in the presence of mobile endogenous calcium binding proteins. *J Comput Neurosci*. 27:229-243.

Seymour-Laurent, K.J., and M.E. Barish. 1995. Inositol 1,4,5-trisphosphate and ryanodine receptor distributions and patterns of acetylcholine- and caffeine-induced calcium release in cultured mouse hippocampal neurons. *The Journal of neuroscience : the official journal of the Society for Neuroscience*. 15:2592-2608.

Shaner, N.C., M.Z. Lin, M.R. McKeown, P.A. Steinbach, K.L. Hazelwood, M.W. Davidson, and R.Y. Tsien. 2008. Improving the photostability of bright monomeric orange and red fluorescent proteins. *Nature methods*. 5:545-551.

Shen, W.W., M. Frieden, and N. Demaurex. 2011. Remodelling of the endoplasmic reticulum during store-operated calcium entry. *Biology of the cell / under the auspices of the European Cell Biology Organization*. 103:365-380.

Singh, A., M.E. Hildebrand, E. Garcia, and T.P. Snutch. 2010. The transient receptor potential channel antagonist SKF96365 is a potent blocker of low-voltage-activated T-type calcium channels. *British journal of pharmacology*. 160:1464-1475.

Sirabella, R., A. Secondo, A. Pannaccione, A. Scorziello, V. Valsecchi, A. Adornetto, L. Bilo, G. Di Renzo, and L. Annunziato. 2009. Anoxia-induced NF-kappaB-dependent upregulation of NCX1 contributes to Ca2+ refilling into endoplasmic reticulum in cortical neurons. *Stroke; a journal of cerebral circulation*. 40:922-929.

Sisalli, M.J., A. Secondo, A. Esposito, V. Valsecchi, C. Savoia, G.F. Di Renzo, L. Annunziato, and A. Scorziello. 2014. Endoplasmic reticulum refilling and mitochondrial calcium extrusion promoted in neurons by NCX1 and NCX3 in ischemic preconditioning are determinant for neuroprotection. *Cell death and differentiation*.

Soboloff, J., B.S. Rothberg, M. Madesh, and D.L. Gill. 2012. STIM proteins: dynamic calcium signal transducers. *Nature reviews. Molecular cell biology*. 13:549-565.

Solovyova, N., and A. Verkhratsky. 2002. Monitoring of free calcium in the neuronal endoplasmic reticulum: an overview of modern approaches. *Journal of neuroscience methods*. 122:1-12.

Solovyova, N., and A. Verkhratsky. 2003. Neuronal endoplasmic reticulum acts as a single functional Ca2+ store shared by ryanodine and inositol-1,4,5-trisphosphate receptors as revealed by intra-ER [Ca2+] recordings in single rat sensory neurones. *Pflugers Archiv : European journal of physiology*. 446:447-454.

Solovyova, N., N. Veselovsky, E.C. Toescu, and A. Verkhratsky. 2002. Ca(2+) dynamics in the lumen of the endoplasmic reticulum in sensory neurons: direct visualization of Ca(2+)-induced Ca(2+) release triggered by physiological Ca(2+) entry. *The EMBO journal*. 21:622-630.

Spacek, J., and K.M. Harris. 1997. Three-dimensional organization of smooth endoplasmic reticulum in hippocampal CA1 dendrites and dendritic spines of the immature and mature rat. *The Journal of neuroscience : the official journal of the Society for Neuroscience*. 17:190-203.

Stathopulos, P.B., R. Schindl, M. Fahrner, L. Zheng, G.M. Gasmi-Seabrook, M. Muik, C. Romanin, and M. Ikura. 2013. STIM1/Orai1 coiled-coil interplay in the regulation of store-operated calcium entry. *Nature communications*. 4:2963.

Streb, H., R.F. Irvine, M.J. Berridge, and I. Schulz. 1983. Release of Ca2+ from a nonmitochondrial intracellular store in pancreatic acinar cells by inositol-1,4,5-trisphosphate. *Nature*. 306:67-69.

Strehler, E.E., and D.A. Zacharias. 2001. Role of alternative splicing in generating isoform diversity among plasma membrane calcium pumps. *Physiological reviews*. 81:21-50.

Sugawara, Y., R. Echigo, K. Kashima, H. Minami, M. Watanabe, Y. Nishikawa, M. Muranishi, M. Yoneda, and T. Ohno-Shosaku. 2013. Intracellular calcium level is an important factor influencing ion channel modulations by PLC-coupled metabotropic receptors in hippocampal neurons. *Brain research*. 1512:9-21.

Sugiyama, Y., I. Kawabata, K. Sobue, and S. Okabe. 2005. Determination of absolute protein numbers in single synapses by a GFP-based calibration technique. *Nature methods*. 2:677-684.

Supnet, C., and I. Bezprozvanny. 2011. Presenilins function in ER calcium leak and Alzheimer's disease pathogenesis. *Cell Calcium*. 50:303-309.

Suzuki, J., K. Kanemaru, K. Ishii, M. Ohkura, Y. Okubo, and M. Iino. 2014. Imaging intraorganellar Ca2+ at subcellular resolution using CEPIA. *Nature communications*. 5:4153.

Targos, B., J. Baranska, and P. Pomorski. 2005. Store-operated calcium entry in physiology and pathology of mammalian cells. *Acta biochimica Polonica*. 52:397-409.

Thomas, D., S.C. Tovey, T.J. Collins, M.D. Bootman, M.J. Berridge, and P. Lipp. 2000. A comparison of fluorescent Ca2+ indicator properties and their use in measuring elementary and global Ca2+ signals. *Cell Calcium*. 28:213-223.

Tsien, R.Y. 1981. A non-disruptive technique for loading calcium buffers and indicators into cells. *Nature*. 290:527-528.

Tu, H., O. Nelson, A. Bezprozvanny, Z. Wang, S.F. Lee, Y.H. Hao, L. Serneels, B. De Strooper, G. Yu, and I. Bezprozvanny. 2006. Presenilins form ER Ca2+ leak channels, a function disrupted by familial Alzheimer's disease-linked mutations. *Cell*. 126:981-993.

Usachev, Y., A. Shmigol, N. Pronchuk, P. Kostyuk, and A. Verkhratsky. 1993. Caffeine-induced calcium release from internal stores in cultured rat sensory neurons. *Neuroscience*. 57:845-859.

Varnai, P., L. Hunyady, and T. Balla. 2009. STIM and Orai: the long-awaited constituents of store-operated calcium entry. *Trends in pharmacological sciences*. 30:118-128.

Verkhratsky, A. 2005. Physiology and pathophysiology of the calcium store in the endoplasmic reticulum of neurons. *Physiological reviews*. 85:201-279.

Vig, M., C. Peinelt, A. Beck, D.L. Koomoa, D. Rabah, M. Koblan-Huberson, S. Kraft, H. Turner, A. Fleig, R. Penner, and J.P. Kinet. 2006. CRACM1 is a plasma membrane protein essential for store-operated Ca2+ entry. *Science*. 312:1220-1223.

Villegas, R., N.W. Martinez, J. Lillo, P. Pihan, D. Hernandez, J.L. Twiss, and F.A. Court. 2014. Calcium release from intra-axonal endoplasmic reticulum leads to axon degeneration through mitochondrial dysfunction. *The Journal of neuroscience : the official journal of the Society for Neuroscience*. 34:7179-7189.

Volterra, A., N. Liaudet, and I. Savtchouk. 2014. Astrocyte Ca(2)(+) signalling: an unexpected complexity. *Nature reviews. Neuroscience*. 15:327-335.

Waldo, G.L., and T.K. Harden. 2004. Agonist binding and Gq-stimulating activities of the purified human P2Y1 receptor. *Molecular pharmacology*. 65:426-436.

Wang, Y., X. Deng, and D.L. Gill. 2010a. Calcium signaling by STIM and Orai: intimate coupling details revealed. *Science signaling*. 3:pe42.

Wang, Y., X. Deng, S. Mancarella, E. Hendron, S. Eguchi, J. Soboloff, X.D. Tang, and D.L. Gill. 2010b. The calcium store sensor, STIM1, reciprocally controls Orai and CaV1.2 channels. *Science*. 330:105-109.

Weinberg, S.H., and G.D. Smith. 2014. The influence of Ca(2)(+) buffers on free [Ca(2)(+)] fluctuations and the effective volume of Ca(2)(+) microdomains. *Biophysical journal*. 106:2693-2709.

Westerblad, H., F.H. Andrade, and M.S. Islam. 1998. Effects of ryanodine receptor agonist 4-chloro-m-cresol on myoplasmic free Ca2+ concentration and force of contraction in mouse skeletal muscle. *Cell Calcium*. 24:105-115.

Wolkowicz, P.E., J. Huang, P.K. Umeda, O.F. Sharifov, E. Tabengwa, B.A. Halloran, F. Urthaler, and H.E. Grenett. 2011. Pharmacological evidence for Orai channel

activation as a source of cardiac abnormal automaticity. *European journal of pharmacology*. 668:208-216.

Wu, B., H. Yamaguchi, F.A. Lai, and J. Shen. 2013. Presenilins regulate calcium homeostasis and presynaptic function via ryanodine receptors in hippocampal neurons. *Proceedings of the National Academy of Sciences of the United States of America*. 110:15091-15096.

Wu, M.M., J. Buchanan, R.M. Luik, and R.S. Lewis. 2006. Ca2+ store depletion causes STIM1 to accumulate in ER regions closely associated with the plasma membrane. *The Journal of cell biology*. 174:803-813.

Wu, M.P., L.S. Kao, H.T. Liao, and C.Y. Pan. 2008. Reverse mode Na+/Ca2+ exchangers trigger the release of Ca2+ from intracellular Ca2+ stores in cultured rat embryonic cortical neurons. *Brain research*. 1201:41-51.

Young, K.W., D. Billups, C.P. Nelson, N. Johnston, J.M. Willets, M.J. Schell, R.A. Challiss, and S.R. Nahorski. 2005. Muscarinic acetylcholine receptor activation enhances hippocampal neuron excitability and potentiates synaptically evoked Ca(2+) signals via phosphatidylinositol 4,5-bisphosphate depletion. *Molecular and cellular neurosciences*. 30:48-57.

Zaidi, A. 2010. Plasma membrane Ca-ATPases: Targets of oxidative stress in brain aging and neurodegeneration. *World journal of biological chemistry*. 1:271-280.

Zhang, S.L., A.V. Yeromin, X.H. Zhang, Y. Yu, O. Safrina, A. Penna, J. Roos, K.A. Stauderman, and M.D. Cahalan. 2006. Genome-wide RNAi screen of Ca(2+) influx identifies genes that regulate Ca(2+) release-activated Ca(2+) channel activity. *Proceedings of the National Academy of Sciences of the United States of America*. 103:9357-9362.

Zhang, S.L., Y. Yu, J. Roos, J.A. Kozak, T.J. Deerinck, M.H. Ellisman, K.A. Stauderman, and M.D. Cahalan. 2005. STIM1 is a Ca2+ sensor that activates CRAC channels and migrates from the Ca2+ store to the plasma membrane. *Nature*. 437:902-905.

Zorzato, F., E. Scutari, V. Tegazzin, E. Clementi, and S. Treves. 1993. Chlorocresol: an activator of ryanodine receptor-mediated Ca2+ release. *Molecular pharmacology*. 44:1192-1201.

Zufferey, R., T. Dull, R.J. Mandel, A. Bukovsky, D. Quiroz, L. Naldini, and D. Trono. 1998. Self-inactivating lentivirus vector for safe and efficient in vivo gene delivery. *Journal of virology*. 72:9873-9880.

Affidavit

I hereby confirm that my thesis entitled “Investigation of homeostatic calcium fluxes in hippocampal neurons by means of targeted-esterase induced dye loading (TED)” is the result of my own work. I did not receive any help or support from commercial consultants. All sources and / or materials applied are listed and specified in the thesis.

Furthermore, I confirm that this thesis has not yet been submitted as part of another examination process neither in identical nor in similar form.

Place, Date

Signature

Eidesstattliche Erklärung

Hiermit erkläre ich an Eides statt, die Dissertation mit dem Titel „Untersuchung von homöostatischen Kalziumströmen in hippokampalen Neuronen mittels “targeted-esterase induced dye loading (TED)”” eigenständig, d.h. insbesondere selbständig und ohne Hilfe eines kommerziellen Promotionsberaters, angefertigt und keine anderen als die von mir angegebenen Quellen und Hilfsmittel verwendet zu haben.

Ich erkläre außerdem, dass die Dissertation weder in gleicher noch in ähnlicher Form bereits in einem anderen Prüfungsverfahren vorgelegen hat.

Ort, Datum

Unterschrift

Acknowledgements

At first, I express my sincere gratitude to my primary supervisor PD Dr Robert Blum. He provided constant support by helping with words and deeds at the bench. In addition, he was a good partner for important scientific discussions, as well as a seemingly endless source of new ideas. My sincere gratitude for guiding me all the way towards this PhD!

Robert Blum was also the one who received the grant BL567/3-1 from Deutsche Forschungsgemeinschaft. So, thanks to Robert and DFG for funding this/my work! It enabled an impressively smooth workflow.

Probably of equal importance were my dear colleagues! I thank all of you as a group because I find it impossible to pick out special ones! Every single one helped me in uncountable situations! I cannot recall a single person who never helped me! That`s great! So, obviously, my colleagues provided a very productive and fun working environment, which I am very grateful for!

I happily make an exception for Andrea Wetzel, who is officially Dr Andrea Wetzel now! I thank her for being a great colleague! Andrea was my fellow, same lab, same office PhD student for 2 years and continued to be a good friend!

Further, I thank my second and third supervisors, Prof Carsten Hoffmann and Prof Manfred Heckmann. Both contributed important experience and ideas to this study and both always found the time for our meetings!

Next, I thank the head of the institute, Prof Michael Sendtner! He manages a thriving institute full of interesting people with even more interesting minds and ideas. I am very glad I met and heard all of them. Equally important, Prof Sendtner provided the seminars that taught me state of the art, as well as basic, scientific methods, findings and opinions.

Furthermore, I thank the people constituting the graduate school of life sciences (GSLS) for providing additional classes and courses and an excellent platform to meet fellow students!

I also owe my family and friends a debt of gratitude! Thank you for the encouragement and your patience! I hope I will be able to give back at least some of all the support you bestowed on me so generously for such a long time!

With gratitude,

Samira Samtleben